TOPICS IN HIGH-ENERGY PHYSICS: THE STANDARD MODEL AND BEYOND

by

Andrew Eric Blechman

A dissertation submitted to The Johns Hopkins University in conformity with the requirements for the degree of Doctor of Philosophy.

Baltimore, Maryland

August, 2006

Abstract

This thesis is compiled from the various projects I completed as a graduate student at the Johns Hopkins University Physics Department.

The first project studied threshold effects in excited charmed baryon decays. The strong decays of the $\Lambda_c^+(2593)$ are sensitive to finite width effects. This distorts the shape of the invariant mass spectrum in $\Lambda_{c1}^+ \to \Lambda_c^+ \pi^+ \pi^-$ from a simple Breit-Wigner resonance, which has implications for the experimental extraction of the $\Lambda_c^+(2593)$ mass and couplings. A fit is performed to unpublished CLEO data which gives $M(\Lambda_c^+(2593)) - M(\Lambda_c^+) = 305.6 \pm 0.3$ MeV and $h_2^2 = 0.24^{+0.23}_{-0.11}$, with h_2 the $\Lambda_{c1} \to \Sigma_c \pi$ strong coupling in the chiral Lagrangian.

In the second project, by shining a hypermultiplet from one side of the bulk of a flat five-dimensional orbifold, supersymmetry is broken. The extra dimension is stabilized in a supersymmetric way, and supersymmetry breaking does not damage the radius stabilization mechanism. The low energy theory contains the radion and two complex scalars that are massless in the global supersymmetric limit and are stabilized by tree level supergravity effects. It is shown that radion mediation can play the dominant role in communicating supersymmetry breaking to the visible sector and contact terms are exponentially suppressed at tree level.

The third project studied lepton flavor violation in flavor anarchic Randall-Sundrum models. All Yukawa couplings and mixing matrices are generated at the TeV-scale by wavefunction overlaps in the five-dimensional Anti-deSitter geometry present in this theory, without introducing any additional structure. This leads to a TeV-scale solution to both the flavor and electroweak hierarchy problems. A thorough scan of the available parameter space is performed, including the effects

of allowing the Higgs boson to propagate in the full five-dimensional space-time. These models give constraints at the few TeV level throughout the natural range of parameters. Near-future experiments will definitively test this model.

Advisors: Adam F. Falk, David E. Kaplan

Acknowledgements

There are many people whom I am indebted to for all that they did for me during these last several years. First and foremost, I want to thank Professors Adam Falk and David Kaplan. Adam took me in the moment I arrived at Johns Hopkins, and encouraged me to strive high and dive deep into everything I did. When he stopped doing physics to become the dean, Dave took up the slack. His friendly and relaxed attitude was welcome, and his patience with me was boundless. Thanks guys, you're the best!

I have been very happy to have been in the High Energy Theory group at Johns Hopkins. Everyone has been very friendly to me, and I am grateful to all of them for their friendship as well as their help. I'm especially grateful to Dan Pirjol, Kaustubh Agashe, Frank Petriello, Roberto Contino, Gero von Gersdorff, Adam Lewandowski, Mike May, Chi Xiong, Jeff Tober, Tom Kramer, Ian Tolfree, Minho Son, E.J. Rhee and Yanyan Gao. The other professors in the group have also been very helpful and supportive to me, and I'm very grateful to them: Professors Raman Sundrum, Jon Bagger, Gabor Domokos and Susan Kovesi-Domokos. The secretaries and admininstrators have been invaluable to me from the beginning: Janet Krupsaw, Carm King, Pam Carmen, Norma Berry, Connie Fleigel, Phyllis Alban and Lonnie Clark.

Some of my friends here and abroad were instrumental in keeping me sane these past five years. Seth Jonas, Clayton Lapointe, Sonny Mantry, Chris Merchant, Rishiraj Pravahan, Divya Singh, Vivek Thampy, Brock Tweedie and Dori Witt – stay cool!

I also want to thank my family for all of their support over the years. Ilene

and Kevin for a place to stay while I looked for an appartment in Baltimore, and for many random dinners! And of course to my parents for all their help.

I owe everything to my best friend, both professionally and personally, Linda Carpenter. You keep me honest in everything I do. Thanks for being there.

Thank you all!

Contents

List of Figures

List of Tables

Chapter 1

Introduction

This thesis is a collection of work I have done as a graduate student. The introduction will review the Standard Model of Particle Physics and some of its extensions that are considered throughout the thesis, as well as introduce some important techniques that are used throughout my research. The remaining chapters contain the material previously published in [1, 2, 3].

1.1 The Standard Model and Its Flaws

The Standard Model of particle physics (SM) provides a wonderful and surprisingly accurate picture of the universe at the smallest scales. However, despite its successes, we know that it cannot be the entire story. Before going into details, let us review the SM, count the free parameters and isolate its most severe problems.

The SM is a chiral gauge theory that describes all of the known matter and interactions that we see in nature, except for neutrino masses. The gauge theory is $SU(3)_C \times SU(2)_L \times U(1)_Y$. The $SU(3)_C$ group is the strong interactions of Quantum Chromodynamics (QCD), and describes interactions with the strong force carriers called gluons. $SU(2) \times U(1)$ is the Electroweak interaction proposed by Glashow, Weinberg and Salam [4], which describe interactions with electroweak force carriers W^a (weak left isospin) and B (hypercharge Y). Each of these forces has a coupling constant (g_s, g, g'), giving three parameters.

QCD exibits asymtotic freedom [5]. This means that the strong coupling decreases as the energy scale of the interaction increases. To leading order, this is given by

$$\alpha_s(Q) = \frac{2\pi}{b_0 \log(Q/\Lambda)}$$

where $b_0 = 11 - 2n_f/3$, n_f is the number of flavors with mass less than Q, and $\Lambda \sim 200$ MeV. It is this property of QCD that is believed to enforce the phenomenon of "confinement", where all the color-charged particles can only live in bound states called hadrons.

QCD is special in that it also has an additional parameter called θ_{QCD}. This comes from the following operator:

$$\Delta\mathcal{L} = \frac{g_s^2 \theta_{QCD}}{64\pi^2} \epsilon^{\mu\nu\rho\sigma} G^a_{\mu\nu} G^a_{\rho\sigma} \tag{1.1}$$

where $G^a_{\mu\nu}$ is the gluon field strength. This operator is a total divergence, so it does not affect any perturbative result, but it is generated by non-perturbative effects and cannot be ignored due to the largness of g_s[1]. However, it violates CP symmetry and can give dangerous contributions to the neutron electric dipole moment, constraining $\theta_{\rm QCD} \leq 10^{-10}$. The reason for the smallness of $\theta_{\rm QCD}$ is still an open question and is called the "strong CP problem".

There must be something that breaks the electroweak symmetry to the weak force and E&M. This is accomplished in the standard model with the introduction of a new scalar field[2] $H = (\mathbf{1}, \mathbf{2})_{1/2}$ with mass m_H. This field develops a vacuum expectation value (vev)

$$\langle H \rangle = \frac{v}{\sqrt{2}} \begin{pmatrix} 0 \\ 1 \end{pmatrix}$$

which then breaks the EW symmetry, giving masses to the $W^\pm$ and Z gauge

[1] There are similar operators generated for the other gauge groups, but the non-perturbative effect goes as e^{-1/g^2}, so only the gluons can have any observable effect.

[2] The notation $(A, B)_C$ refers to how the field transforms under $SU(3), SU(2), U(1)$ respectively.

bosons, and leaving behind a massless photon[3]. This is called the Higgs Mechanism [6]. The nature of the Higgs field is still an open question in high energy physics, and will hopefully be better understood after the Large Hadron Collider (LHC) starts to collect data. The SM Higgs sector introduces two new parameters into the theory: m_H and v.

One of the biggest open questions of particle physics is the nature of electroweak symmetry breaking (EWSB). Scalar fields typically have quadratically divergent quantum mechanical mass corrections, so in the simplest model of the Higgs being a scalar field, we expect quantum corrections push the Higgs mass as high as it can go. The question of why the Higgs mass is so much lighter than the Planck scale is known as the "hierarchy problem". Most particle physicists are hopeful that we will get a better handle on the solution of this problem one way or another with the help of the LHC.

The SM fermions organize themselves into five multiplets under the gauge group:

$$\begin{aligned} Q^i &= (\mathbf{3},\mathbf{2})_{1/6} \\ \bar{U}^i &= (\bar{\mathbf{3}},\mathbf{1})_{-2/3} \\ \bar{D}^i &= (\bar{\mathbf{3}},\mathbf{1})_{1/3} \\ L^i &= (\mathbf{1},\mathbf{2})_{-1/2} \\ E^i &= (\mathbf{1},\mathbf{1})_{1} \end{aligned} \tag{1.2}$$

Each of these multiplets appears three times in what are called "generations" ($i = 1, 2, 3$). The first three multiplets are the quarks, matter particles that feel QCD and are therefore confined to hadrons. Q are the left handed quarks which form doubets under $SU(2)_L$. They are the up and down (u, d), charm and strange (c, s) and top and bottom (t, b). The first quark in each pair has electric charge $+2/3$ and the second quark has charge $-1/3$ in units of e. $\bar{U}, \bar{D}$ contain the right handed quarks that are singlets under $SU(2)_L$. $U^i = (u, c, t)$ and $D^i = (d, s, b)$.

[3]The Z boson is given by $\cos\theta_W W^3 - \sin\theta_W B$, and the photon is the orthogonal combination, where $\cos\theta_W \equiv \frac{g}{\sqrt{g^2+g'^2}}$.

The last two multiplets are the leptons, which do not feel QCD and are therefore free particles. L are the electron and its neutrino (e, ν_e), the muon and its neutrino (μ, ν_μ) and the tau and its neutrino (τ, ν_τ). The neutrinos are electrically neutral, while their partners all have charge -1. E are the corresponding right handed charged leptons (e, μ, τ); there are no ν_R in the SM.

The flavor structure of the standard model is very interesting: since there are three copies of five multiplets, there is an accidental flavor symmetry $U(3)^5$. This flavor structure is broken only in the Yukawa sector:

$$\mathcal{L}_{\text{Yukawa}} = -\Gamma_u^{ij} \bar{Q}_i \tilde{H} U_j - \Gamma_d^{ij} \bar{Q}_i H D_j - \Gamma_e^{ij} \bar{L}_i H E_j \tag{1.3}$$

where i, j are generation indices and $\tilde{H} = \epsilon H^*$. When the Higgs field is set to its vev, these terms become mass terms for the quarks and leptons. Each Yukawa matrix is a complex 3×3 matrix and therefore introduces 18 parameters each, but most of these are unphysical. We will discuss the quark and lepton sectors separately.

The two quark Yukawa matrices contribute 36 parameters in the quark sector; but some of these parameters can be rotated away by the quark flavor symmetry, which is $U(3)^3$. This looks like it has the freedom to rotate away 27 parameters, but the Yukawas still respect an overall baryon-number symmetry $U(1)_B$, so we can only remove 26 parameters; this leaves 10 parameters left. The Yukawa matrices are diagonalized by bi-unitary transformations:

$$\begin{aligned} \Gamma_u^{\text{diag}} &= S_{Q_u} \Gamma_u S_U^\dagger \\ \Gamma_d^{\text{diag}} &= S_{Q_d} \Gamma_u S_D^\dagger \end{aligned}$$

This transformation diagonalizes the Yukawa matrices, but it introduces a non-trivial flavor-violating coupling in the gauge sector:

$$\Delta\mathcal{L} = \bar{Q}_u^i S_{Q_u}^{\dagger ij} \gamma^\mu S_{Q_d}^{jk} Q_d^k W_\mu^+ + \text{h.c.}$$

So there is a new unitary (off-diagonal) matrix $V \equiv S_{Q_u}^\dagger S_{Q_d}$ called the Cabibbo-

Kobayashi-Maskawa (CKM) Matrix. It has three mixing angles and a phase[4]. In summary, we are left with six quark masses, and the four CKM matrix parameters.

The lepton sector is similar, but in that case there are more symmetries that survive. Electron-, muon-, and tau- numbers remain, leaving $U(3)^2 \to U(1)^3$. So we are free to rotate away 15 parameters in the lepton Yukawas. Since there is only one complex Yukawa matrix, this leaves 3 parameters left: the three lepton masses. Notice that in Equation (1.3), the neutrinos are massless. In a very real sense, neutrino masses are the first evidence of physics beyond the SM! But since I do not consider neutrino masses anywhere in this thesis, I will not go further into this very fascinating subject.

These 13 parameters are all hierarchical. We still do not have a good understanding of where this hierarchy comes from. This goes under the name of the flavor puzzle or the "flavor hierarchy problem".

In summary, the SM has 19 free parameters: the six quark masses and three lepton masses, the three CKM mixing angles and one CKM phase, three gauge couplings, the Higgs mass and vev, and θ_{QCD}. Neutrino masses add even more parameters to this list.

1.2 Effective Field Theory of the SM and QCD

One of the biggest practical challenges to computing predictions of the SM is the effects of QCD. To that end, some very powerful effective field theories (EFT) have been developed to handle these problems. Here I will briefly introduce some of the ones used throughout my research: chiral perturbation theory (ChPT) and heavy quark effective theory (HQET). Not only have these EFT been directly useful, but the techniques they imploy, such as spurion analysis and naive dimensional analysis, play a major role in most of what I do.

[4]In principle, a $U(3)$ matrix has six phases, but we can rotate five of these away by a phase redefinition of the six left handed quark fields. We cannot remove one phase because the overall phase of the quarks is redundant.

1.2.1 Chiral Perturbation Theory

Chiral symmetry is used in context with the "light" quarks (up, down and strange). If we put the quarks into a three-component column vector:

$$q_{L,R} = \begin{pmatrix} u_{L,R} \\ d_{L,R} \\ s_{L,R} \end{pmatrix}$$

the chiral symmetry reads:

$$\begin{aligned} q_L &\rightarrow L q_L \\ q_R &\rightarrow R q_R \end{aligned}$$

where L and R are 3×3 unitary matrices. Hence the chiral symmetry is $SU(3)_L \times SU(3)_R$. This symmetry is broken by a chiral condensate $\langle 0| \overline{q}_R q_L |0\rangle = v \neq 0$, since $v \rightarrow v L R^\dagger$. However, the symmetry is only partially broken; it is still invariant under the special transformation:

$$L = R = V$$

We write this explicitly as:

$$SU(3)_L \times SU(3)_R \rightarrow SU(3)_V \tag{1.4}$$

This symmetry breaking pattern leaves us with 8 Goldstone bosons. Sure enough, we have eight light pseudoscalar bosons at our disposal with the proper quantum numbers of isospin and strangeness: three pions, four kaons and an eta. ChPT will describe interactions between these eight particles at relatively low energies.

We parametrize the Goldstone bosons by the 3×3 matrix Σ:

$$\Sigma_{ab} \equiv \overline{q}_{Ra} q_{Lb} \tag{1.5}$$

so that $\langle 0| \overline{q}_{Ra} q_{Lb} |0\rangle = v \Sigma_{ab}$. It is clear from the transformation law of the quark fields that

$$\Sigma \to L\Sigma R^\dagger \tag{1.6}$$

To see how this field parametrizes the Goldstone bosons, we can write out Σ in terms of the exponential of a "pion matrix":

$$\Sigma = e^{\frac{2i\Pi}{f}} \tag{1.7}$$

$$\Pi = \begin{pmatrix} \frac{1}{\sqrt{2}}\pi^0 + \frac{1}{\sqrt{6}}\eta & \pi^+ & K^+ \\ \pi^- & -\frac{1}{\sqrt{2}}\pi^0 + \frac{1}{\sqrt{6}}\eta & K^0 \\ K^- & \overline{K}^0 & -\frac{2}{\sqrt{6}}\eta \end{pmatrix} \tag{1.8}$$

where f is called the pion decay constant. To write down the chiral theory, all we need to do is write down the most general operators that are products of the Σ and are invariant under the full $SU(3)_L \times SU(3)_R$ chiral symmetry. In addition, if this is to describe QCD, we need the terms to be parity and charge-conjugation even. The term of lowest dimension we can write down with all of these properties is:

$$\mathcal{L}_0 = \frac{f^2}{8} Tr[\partial_\mu \Sigma \partial^\mu \Sigma^\dagger] + \cdots \tag{1.9}$$

One can expand the Σ in powers of the pion matrix (or equivalently in inverse powers of f) and take the trace to get the all the interactions explicitly in terms of the Goldstone bosons. The coefficient out in front is to make sure that these terms are properly normalized.

There is another very convenient parametrization of the Goldstone bosons. Define:

$$\xi \equiv e^{\frac{i\Pi}{f}} = \sqrt{\Sigma} \tag{1.10}$$

Now under $SU(3)_L \times SU(3)_R$ transformations, $\xi \to L\xi U^\dagger(x) = U(x)\xi R^\dagger$ where $U(x)$ is a *nonlinear* transformation on ξ. Under this transformation we can define two currents called the *vector* and *axial* currents:

$$V^\mu = \frac{1}{2}(\xi^\dagger \partial^\mu \xi + \xi \partial^\mu \xi^\dagger) \quad \rightarrow \quad U V^\mu U^\dagger + U \partial^\mu U^\dagger \tag{1.11}$$

$$A^\mu = \frac{i}{2}(\xi^\dagger \partial^\mu \xi - \xi \partial^\mu \xi^\dagger) \quad \rightarrow \quad U A^\mu U^\dagger \tag{1.12}$$

Note that V^μ transforms like a gauge field while A^μ transforms like an adjoint. This will be useful later.

In Equation (1.9) the Goldstone bosons are massless. To include masses in the theory, we go back to full QCD and ask how the mass terms for the quarks transform:

$$\mathcal{L}_m = -\overline{q}_L M q_R - \overline{q}_R M q_L \tag{1.13}$$

where M is the quark mass matrix:

$$M = \begin{pmatrix} m_u & 0 & 0 \\ 0 & m_d & 0 \\ 0 & 0 & m_s \end{pmatrix} \tag{1.14}$$

The mass terms then transform under the full chiral symmetry as:

$$\mathcal{L}_m \rightarrow -\overline{q}_L L^\dagger M R q_R - \overline{q}_R R^\dagger M L q_L \tag{1.15}$$

$\mathcal{L}_m$ is not invariant under chiral symmetries. However, we can get around the problem by pretending that M is not a constant matrix, but rather a field that has transformation properties; to distinguish it from the constant matrix, I will put a tilde over it ($\tilde{M}$). This field is called a spurion. If we let

$$\tilde{M} \rightarrow L \tilde{M} R^\dagger$$

and write the second term in Equation (1.15) in terms of $\tilde{M}^\dagger$, we can make Equation (1.15) invariant. Armed with this knowledge, we can add terms to the chiral Lagrangian with masses:

$$\mathcal{L} = \frac{f^2}{8} Tr[\partial_\mu \Sigma \partial^\mu \Sigma^\dagger] + \mu Tr[\tilde{M}^\dagger \Sigma + \Sigma^\dagger \tilde{M}] + \cdots \tag{1.16}$$

where μ is some unknown coefficient with dimension of $(mass)^3$. Now that we have the form of the massive chiral Lagrangian, we can drop the spurion field and replace $\tilde{M}$ with the usual quark mass matrix in Equation (1.14). We can now read off the masses of the pions to lowest order:

$$\begin{aligned} m^2_{\pi^\pm} &= \frac{4\mu}{f^2}(m_u + m_d) \\ m^2_{K^0} &= \frac{4\mu}{f^2}(m_d + m_s) \\ m^2_{K^\pm} &= \frac{4\mu}{f^2}(m_u + m_s) \\ m^2_{\pi^0,\eta} &= \frac{4\mu}{f^2}\begin{pmatrix} (m_u + m_d) & \frac{1}{\sqrt{3}}(m_u - m_d) \\ \frac{1}{\sqrt{3}}(m_u - m_d) & \frac{1}{3}(m_u + m_d) + \frac{4}{3}m_s \end{pmatrix} \end{aligned}$$

These are precisely the Gell-Mann-Okubo relations in the quark model of hadron physics. Note that the quark masses are linear while the hadron masses are quadratic, and there is mixing between the π^0 and the η. These relations could be made better by including higher order terms in the theory.

To get a qualitative idea of how good chiral perturbation is, we must consider the size of the next to leading order effects, and hope that they are small compared to the lowest order results. Since this is a low-energy theory, we are expanding in powers of energy/momentum or equivalently in number of derivatives. Because the Lagrangian is a Lorentz scalar, we must always have an even number of derivatives (to contract every index). The leading higher order terms in the chiral Lagrangian have dimension 4; for example:

$$\mathcal{L}_4 = c_1 Tr[\partial^\mu \partial^\nu \Sigma^\dagger \partial_\mu \partial_\nu \Sigma] + c_2 Tr[\partial_\mu \Sigma^\dagger \partial^\mu \Sigma \Sigma^\dagger \frac{\mu}{f^2} M] + c_3 Tr[\Sigma^\dagger \frac{\mu}{f^2} M \Sigma \frac{\mu}{f^2} M] + \cdots \tag{1.17}$$

By dimensional analysis, we can guess that the coefficients c_i corresponding to terms with $2n$ derivatives and m factors of[5] $(\frac{\mu}{f^2})M$ have the form:

[5]This quantity has dimensions $(mass)^2$ and is the relevant quantity that appears in the mass equations.

$$c_i \sim \frac{f^2}{\Lambda_\chi^{2(n+m-1)}} \tag{1.18}$$

where Λ_χ is the chiral symmetry breaking scale. The more derivatives or mass terms, the larger the exponent of this parameter. Therefore, if we can make this parameter large, then we can honestly say that the higher dimension operators are less important.

Unfortunately, we cannot justify making Λ_χ arbitrarily large. The reason is that the radiative corrections diverge, requiring renormalization. But this renormalization will end up shifting Λ_χ by large amounts if we make it arbitrarily large. It is therefore not "natural" to assume such a large value, as it will get thrown back to a smaller value by quantum effects.

The solution is to apply a technique called naive dimensional analysis (NDA). In this procedure, we ask what is the "natural" size of the radiative corrections, and then chose Λ_χ to be of the same size. We do this by calculating higher order processes coming from Equations (1.16-1.17) and making sure that the radiative corrections do not exceed the results from the lowest order calculation. For example, we can look at $\pi - \pi$ scattering and ask how quantum effects change our answer. This interaction is described by a quartic operator $A\pi^4$, where A is given schematically at next-to-leading order by:

$$A \sim \frac{p^2}{f^2}\left[1 + \frac{1}{16\pi^2}\left(\frac{\Lambda^2}{f^2} + \frac{p^2}{f^2}\log(\Lambda/\mu)\right) + \frac{p^2}{f^2}c_1\right] + \mathcal{O}(f^{-6})$$

Λ is a cutoff regulator and μ is the renormalization scale. The quadratically divergent piece is just a constant up to the overall tree-level factor p^2/f^2, and so it can be absorbed into the overall normalization of f. The logarithmically divergent contribution is quartic in momentum, so it has the same form as the first term in Equation (1.17); it renormalizes the coupling $c_1 \sim f^2/\Lambda_\chi^2$. If we make an $\mathcal{O}(1)$ change in μ we will generate a change in A:

$$\delta A \sim \frac{1}{16\pi^2}\frac{p^4}{f^4}$$

This is compensated for by shifting c_1:

$$c_1 \sim \frac{f^2}{\Lambda_\chi^2}\left(1 + \frac{\Lambda_\chi^2}{16\pi^2 f^2}\right) \tag{1.19}$$

If we don't want this higher order contribution to dominate the leading term, we cannot take $\frac{\Lambda_\chi^2}{f^2} >> 16\pi^2$. The most "natural" choice for the symmetry breaking scale would be when the quantum correction is the same order as the lowest order term, so we will choose:

$$\Lambda_\chi \sim 4\pi f \sim 1\text{GeV} \tag{1.20}$$

Sure enough, this is the scale at which QCD becomes perturbative and we must abandon ChPT in favor of the full theory of quarks and gluons.

The moral of all of this is that we expect chiral perturbation theory to hold as long as we're at energies noticeably less than 1 GeV. Chiral perturbation theory has told us not only the masses and low-energy interactions of the mesons, but it has even told us precisely where to start looking for new physics! This shows how powerful effective theories can be.

1.2.2 Heavy Quark Effective Theory

Chiral perturbation theory discussed the hadrons with light quarks. What if you have a hadron with a heavy quark? In this discussion, "heavy quark" refers to either a charm or bottom quark; top quarks do not form hadrons because of their short lifetime.

To get a feeling for this "heavy quark effective theory" (HQET), consider dribbling a basketball on the ground. Conservation of energy and momentum insists that each time the ball hits the floor, the floor must recoil slightly. Therefore the Earth is recoiling against the force of the basketball bounce. Needless to say, the Earth's recoil will be negligible, and it is a perfectly valid approximation to say that the ball bounces back with all its energy intact (ignoring friction, etc.).

The analogy goes over quite well for heavy hadrons. In these particles, we have one heavy quark Q along with one (for mesons) or two (for baryons) quarks that are light (u, d or s). The light quarks together with any QCD fuzz that occurs inside

the hadron are often rather off-handedly called the "light brown muck". In truth, this brown muck interacts with the heavy quark through non-perturbative QCD interactions, but because the heavy quark is so much heavier than everything else, it is safe to assume that to leading order it decouples from the interactions, just like the Earth interacting with the basketball. Therefore, to a leading approximation, we can say that the heavy quark just sits there in the hadron with no special dynamics, while the light degrees of freedom interact in a mush elastically with the heavy quark.

Because the light brown muck decouples from the heavy quark, we can write down new conserved quantum numbers, specifically the quantum numbers of the light degrees of freedom. These are often denoted by an "l" for light. For example, the total angular momentum of the light brown muck (spin plus orbital) is written "J_l", and we can construct hadrons with angular momentum $J_l \otimes \frac{1}{2}$ when including the heavy quark. This is a bad approximation in general, as QCD generally prohibits you from specifying the individual quantum numbers of the quarks. However, thanks to the heavy quark approximation, this becomes a good description of heavy hadrons.

More quantum numbers means we can get a handle on the hadron spectrum as well as understand allowed decays by insisting that the HQET Lagrangian respect the light quantum numbers. Since this is only an effective theory, we know that the results that follow will not be exactly what we see, but like any effective theory we should be able to decide precisely how good these approximations are, as well as roughly what corrections appear to make the picture even more accurate. In our case, HQET can be derived from full QCD in the limit that the heavy quark mass m_Q becomes infinite. Corrections to any results should therefore go like $\frac{1}{m_Q}$.

A quark is described by a Dirac spinor Q and a Lagrangian:

$$\mathcal{L} = \overline{Q}(i\not{D} - m_Q)Q \tag{1.21}$$

We can take the heavy quark limit by defining:

$$Q = e^{-im_Q v\cdot x}(h_v + \chi_v) \tag{1.22}$$

where

$$\not{v} h_v = h_v \qquad \not{v} \chi_v = -\chi_v \tag{1.23}$$

h_v represents the heavy quark while χ_v represents the off-shell degrees of freedom[6]; v^μ is the four-velocity of the heavy quark. The heavy quark is nearly on shell, so we can drop the χ_v term to lowest order. After plugging Equation (1.22) into Equation (1.21) and using Equation (1.23) we can write down the Lagrangian that describes the heavy quark to lowest order:

$$\mathcal{L}_0 = \overline{h}_v i v \cdot D h_v \tag{1.24}$$

h_v now describes a heavy quark with four-momentum

$$p_Q^\mu = m_Q v^\mu + k^\mu \tag{1.25}$$

where k is called the "residual momentum" and represents how much the quark is off shell. Since we're dropping χ_v we require that $|k| << m_Q$ in order for the theory to be consistent.

At this point, we are able to construct the operators that describe hadrons with a heavy quark. The heavy quark decouples from the light brown muck, so if we parameterize the light degrees of freedom by some operator A_j, the hadron in question looks like

$$X = A_j h_v$$

The operator X written this way contains two states corresponding to hadrons with total angular momenta $j \pm \frac{1}{2}$ respectively.

As an example, consider $\overline{q}_a h_v$ mesons ($a = u, d, s$)[7]. This state has brown muck quantum numbers[8] $j_l^{P_l} = \frac{1}{2}^-$. These quantum numbers correspond to the

[6]Because this is quantum mechanics, a particle that decays can have the "wrong mass" due to its finite lifetime and the uncertainty principle ($\Delta E \Delta t \sim \hbar$). Particles with the wrong mass are said to be "off shell" while particles with their proper masses are said to be "on shell".

[7]Here I consider mesons for definiteness, but realize that the theory works just as well for baryons.

[8]$j_l^{P_l}$ stands for spin-parity quantum numbers of the light brown muck.

pseudoscalar (P_a) and vector ($P_a^{*\mu}$) mesons with spin 0 and 1 respectively. These mesons can be combined into a larger 4×4 matrix called a superfield:

$$H_a \equiv \left(\frac{1+ \not{v}}{2}\right) \left[\gamma_\mu P_a^{*\mu} - P_a \gamma_5\right]$$

Similarly, the superfield for heavy mesons with $j_l^{P_l} = \frac{1}{2}^+$:

$$S_a \equiv \left(\frac{1+ \not{v}}{2}\right) \left[\gamma_\mu \gamma_5 P_a^{\prime\mu} - P_a^*\right]$$

Note that due to the heavy quark spin symmetry, the fields inside each superfield have the same mass.

It is convenient to work with superfields in HQET because they have very nice transformation laws. For example, under heavy quark spin transformations parameterized by the operator S_Q, $H_a \to S_Q H_a$. This is easy to see from knowing $h_v \to S_Q h_v$ and the fact that A_j does not transform under heavy quark spin transformations. Now it is straightforward to write down the Lagrangian for these mesons:

$$\mathcal{L}_0 = Tr\left[\overline{H} iv \cdot D H\right] + Tr\left[\overline{S}(iv \cdot D - \Delta_S) S\right] \tag{1.26}$$

where $\Delta_S \equiv M_S - M_H$.

We wish to write down interactions among these mesons. The trick behind this is to combine HQET with ChPT. We designed our superfields so that $H \to HU^\dagger$, where U is the nonlinear chiral transformation discussed below Equation (1.10). Using the axial vector current A^μ from Equation (1.12), we can write down interactions by insisting on preserving all the symmetries, including Lorentz invariance and heavy quark spin/flavor symmetry. For example:

$$\mathcal{L}_{int} = gTr\left[\overline{H} S \gamma^\mu \gamma^5 A_\mu\right] + \cdots \tag{1.27}$$

where g is a coupling constant that can be measured by matching to either the full QCD or to experiment.

Corrections to this picture should go as $\frac{1}{m_Q}$, and will thus automatically violate the heavy quark flavor symmetry. To see this explicitly, we go back to Equation

(1.22) and do *not* drop the χ_v term. Plugging this into the equations of motion gives us:

$$\chi_v = \frac{1}{2m_Q} i\not{D} h_v + \mathcal{O}(m_Q^{-2}) \tag{1.28}$$

Notice that each covariant derivative brings down a factor of $-ik_\mu$, and we expect this residual momentum to be on the order of Λ_{QCD}, since this is the typical energy scale of quarks in hadrons. Therefore, these new terms are order Λ_{QCD}/m_Q. Higher-order corrections correspond to higher powers of this ratio. We can plug this back into our original Lagrangian in Equation (1.21) and simplify using the equations of motion to get:

$$\mathcal{L} = \overline{h}_v iv \cdot D h_v + \frac{1}{2m_Q} \overline{h}_v \left[(iD)^2 - g_s \sigma_{\mu\nu} G^{\mu\nu} \right] h_v \tag{1.29}$$

where $\sigma^{\mu\nu} \equiv \frac{i}{2}[\gamma^\mu, \gamma^\nu]$. There is also a term corresponding to the operator $\bar{h}_v (v \cdot D)^2 h_v$, however this term vanishes from the field equations for h_v to this order.

Let us take a closer look at the new terms in Equation (1.29). The first term goes like D^2 and has no gamma matrices. This means that it does not affect the spin of the heavy quark and preserves the spin symmetries of the lowest-order theory, although it does break the heavy flavor symmetry due to its dependence on m_Q. However, the second term does contain gamma matrices in the $\sigma^{\mu\nu}$, and therefore this term explicitly violates the heavy quark spin symmetry. This is just like the mass term in the Chiral Lagrangian. Following our intuition from before, we can calculate the effects on the theory by introducing a spurion field $\Phi^{\mu\nu} = \frac{1}{2m_Q}\sigma^{\mu\nu}$ [7]. Looking at Equation (1.29), the spurion must transform under heavy quark symmetry as $\Phi^{\mu\nu} \to S_Q \Phi^{\mu\nu} S_Q^\dagger$. We can now write down operators using this spurion. For example:

$$\Delta\mathcal{L} = \lambda_H Tr\left[\overline{H}\Phi^{\mu\nu} H \sigma_{\mu\nu}\right] + \lambda_S Tr\left[\overline{S}\Phi^{\mu\nu} S \sigma_{\mu\nu}\right] + \cdots \tag{1.30}$$

where the λs are coefficients that can be fit from experiment. These terms are responsible for the mass shift among the mesons in the superfields $(m_{P^*} - m_P)$ and

are therefore noticeable and important. From experiment, we find that $\lambda \sim \Lambda_{QCD}$ which should not be surprising.

To summarize, heavy quark effective theory is an extremely powerful tool because it introduces new symmetries (heavy quark spin/flavor symmetry) that tell you how to write down interactions for the different hadrons. In the spirit of any effective theory, HQET also tells you where the theory breaks down, and how you can fix it by introducing new terms through a spurion analysis.

1.3 Supersymmetry

Usually, radiative corrections are controlled by symmetries: fermion masses are controlled by chiral symmetry, gauge boson masses are controlled by gauge symmetries. So the natural question to ask is if there is a symmetry that can control the Higgs mass and thus solve the hierarchy problem. One possible answer (although certainly not the only one) is supersymmetry.

In supersymmetric theories, every fermion is paired up with a boson of identical mass and quantum numbers. The minimal extension of the SM is called the minimal supersymmetric standard model (MSSM) [8]. Each quark and lepton has corresponding spin-0 bosons called squarks and sleptons; each gauge boson has a spin-1/2 fermion called a gaugino; and the Higgs boson has a corresponding spin-1/2 fermionic partner called the Higgsino (actually, there are two Higgs doublets in the MSSM). Because fermions and bosons in loops contribute with opposite signs, the quadratic divergence cancells in the Higgs mass correction, and the hierarchy problem is solved.

There is a problem, however: the universe is not supersymmetric. We have never seen any signs of squarks, sleptons or gauginos. The explanation for this is that supersymmetry is spontaneously broken at some scale. This then makes the squarks, sleptons and gauginos heavy. Model builders have spent the last several years coming up with ways to explain how this works. There are two steps to consider: how do you break supersymmetry? And how do you communicate that breaking to the supersymmetric particles? This second step is called the mediation

mechanism.

There are a few questions that these models must address:

- *Generating soft terms:* Mediation mechanisms generate SUSY breaking terms in the action. It is known that in order for SUSY to continue to solve the hierarchy problem after it is broken, only "soft" terms can appear. These are mass terms for the supersymmetric particles and the Higgs bosons and trilinear couplings between the scalars. Any mediation mechanism must be sure to not generate any other interactions that might spoil the hierarchy solution.

- *Constraining Parameter Space:* Even with the restriction above, there are over 100 new parameters, including mixings and phases that can generate dangerous flavor changing neutral currents (FCNC) and CP-violation. Any viable mediation mechanism must constrain these new terms.

- *Radiative EWSB and Fine Tuning*: In the MSSM, EWSB and SUSY breaking are related. In order for this balance to work, the MSSM is fine-tuned. For example, the lightest Higgs mass is constrained at treel level to be less than M_Z, but loop corrections from top-stop loops push this bound up logarithmically as $\sim \log(m_{\tilde{t}_1} m_{\tilde{t}_2}/m_t^2)$. So in order to have a Higgs mass that is not too light (and thefore violates the LEP2 bound of 114 GeV [9]), we need the stop to be much heavier than the top. A good mediation mechanism must somehow explain this fine tuning.

- μ *Problem:* The μ term is a supersymmetric mass for the Higgs. However, in order to facilitate radiative EWSB, μ must be the same order of magnitude as the SUSY-breaking terms. Since these terms are totally independent of each other there is no good reason to assume that this is the case. A good mediation mechanism must explain this relationship.

1.4 Extra Dimensions, The Randall-Sundrum Model and the Flavor Puzzle

The hierarchy problem can also be solved by the introduction of extra spacial dimensions. Such models usually involve a fifth (or more) dimensions that are hidden from us, but in which gravity can still affect. In d space dimensions, Gauss's Law gives us the form of the gravitational potential per unit mass:

$$\Phi(r) = \frac{M^{1-d}}{r^{d-2}}$$

where M represents the scale where gravity becomes strong (for d=3, it is just the Planck mass M_P and I use the relation $G_N = M_P^{-2}$)[9]. But if only three of the dimensions are infinite in extent, and the rest are compacitified somehow into a finite volume V_{d-3}, this changes to

$$\Phi(r) = \frac{M'^{1-d}}{rV_{d-3}}$$

This formula is valid for distances much larger than the size of the extra dimensions. This solves the hierarchy problem [10] because now we have the relation

$$M^{-2} = \frac{M'^{1-d}}{V_{d-3}} \tag{1.31}$$

So even if $M' \sim$ TeV, we can still get the scale of $M \sim M_P$ by making an appropriate choice of V_{d-3}. So the hierarchy is no longer a mysterious relationship, but a simple consequence of the geometry of the universe.

The most immediate consequence of extra dimensions that can be tested in a paricle physics experiment is the existence of an infinite tower of new particles for each SM field that lives in the extra dimension. This is just a consequence of the famous "particle-in-a-box" setup of ordinary quantum mechanics. When the particle has a wavefunction that is constrained to live in a finite volume, there is a tower of states with higher energy (mass). This tower is called the Kaluza-Klein (KK) tower, named after the first people who suggested extra dimensions [11]. The

[9]Throughout this thesis I will use "natural units" where $\hbar = c = 1$.

details of this tower depend on the specific geometry of a given model; but if a model exists where the KK mass can be as low as a few TeV, there is a very good chance that the LHC will discover it!

A very specific and beautiful model of extra dimensions was proposed by Randall and Sundrum (RSI) [12]. They propopsed the existence of an extra dimension compactified on an orbifold $0 \leq \phi \leq \pi$ that is a slice of $5D$ Anti-deSitter space (AdS):

$$ds^2 = e^{-2kr_c\phi}\eta_{\mu\nu}dx^\mu dx^\nu - r_c^2 d\phi^2 \tag{1.32}$$

3-Branes are placed at the orbifold fixed points. The brane at $\phi = 0$ is called the Planck (UV) brane, and the brane at $\phi = \pi$ is called the TeV (IR) brane. In the original model, Randall and Sundrum proposed confining all the particles in the SM on the TeV brane. Then if the fundamental $5D$ scale is given by the Planck scale (M_P), the $4D$ scale depends on your location in the extra dimension as $M_4(\phi) = M_P e^{-kr_c\phi}$. In particular, the energy scale generated on the IR brane is $M_P e^{-k\pi r_c}$; thus by choosing $kr_c \sim \mathcal{O}(10)$, we can generate $M_4(\pi) \sim$ TeV, solving the gauge hierarchy problem. This is the origin of the names "Planck brane" and "TeV brane".

It would be sad if the above model were the whole story. With all the SM fields in one place, we are still left with another hierarchy in the flavor sector. Specifically, we know that all of the Yukawa couplings (except the top) are small and hierarchical. The above model offers no solution to this additional hierarchy problem. Not only that, it turns out that the flavor sector in the RSI model is UV sensitive, and requiring consistency with electroweak precision forces us to chose a cutoff roughly $\mathcal{O}(10^3\text{TeV})$ to avoid dangerous FCNC as well as contributions to the S and T parameters. But this presents a problem, since the only cutoff available to us is the electroweak scale.

There is a way out of these problems. The only requirement to solve the gauge hierarchy problem is that the Higgs boson should live near the TeV brane. Therefore, we can consider the case where the other SM fields live in the bulk. This immediately solves the flavor hierarchy problem since the strength of the

couplings to the Higgs (a.k.a. Yukawa couplings) is then a function of how much of the wavefunction is peaked near the TeV brane. Hense by localizing the fermions throughout the bulk and keeping the Higgs near the TeV brane, we can generate a 4D hierarchy in the Yukawa sector, even with anarchic $\mathcal{O}(1)$ Yukawa couplings. These "anarchic RS models" allow us to set all of the Yukawa couplings, including the off-diagonal elements, nearly equal and all $\mathcal{O}(1)$; then all of the 4D structure comes from the warped geometry. In addition, this automatically raises the scale of higher-dimension operators living near the Planck brane, relieving the tension with electroweak precision constraints.

1.5 Outline

This thesis is a collection of papers that have been written while I was a graduate student at Johns Hopkins.

Chapter 2 analyzes the decay of a strong isosinglet baryon with a charm quark and no strange quark:

$$\Lambda_{c1}^{+} \to \Lambda_{c}^{+}\pi\pi$$

Although this is a three-body decay, it is the most likely channel after eliminating all others by parity, isospin and spin symmetries. Since the Λ_c baryon has charge $+1$, there are two channels corresponding the $\pi^+\pi^-$ and $\pi^0\pi^0$. This process likes to go through a resonance:

$$\Lambda_{c1} \to \Sigma_c\pi \to [\Lambda_c\pi]\pi$$

where the brackets are to emphasize that these are the daughter particles of the resonant Σ_c. This particle comes in charges $+2, +1, 0$; the $+2, 0$ charged resonances are for the charged pion channel, while the $+1$ resonance is for the neutral pion channel. However, there is a subtlety in the charged pion channel: the invariant mass of the $\Sigma_c\pi^{\pm}$ is very close to (or even slightly greater than) the mass of the Λ_{c1}; more precisely, the difference in mass between the initial and final states is smaller than the "width" of the Λ_{c1}. Naively, therefore, the Σ_c resonance cannot form in the charged pion channel and the decay has to proceed through a non-resonant

mode. However, even if there is a mass deficit, it can still be that the resonant decay occurs if the Σ_c is off mass shell. However, it is also possible that the original Λ_{c1} itself was off mass shell before it decayed. Such effects could noticeably alter the results, as the usual Breit-Wigner decay amplitude will no longer be appropriate.

In this analysis, my collaborators and I have recomputed the decay amplitude directly from the HQET Lagrangian, considering only the dominant decay mode. From the HQET+ChPT Lagrangian we generate an energy distribution for the resonant decay of the Λ_{c1} in both the charged and neutral pion channels. We find that the neutral pion channel resembles a Breit-Wigner distribution while the distribution for the charged pion channel is distorted, precisely as expected. Fitting charged pion data to a usual Breit-Wigner would bias the results toward higher values for the mass. We fit our model to data taken at CLEO and find that the expected mass changes from $\Delta_{\Lambda_{c1}} = (308.9 \pm 0.6)$ MeV to $\Delta_{\Lambda_{c1}} = (305.6 \pm 0.3)$ MeV. For comparison, the neutral pion channel has been fit to the usual Breit-Wigner and measured at $\Delta = (306.3 \pm 0.7)$ MeV. Therefore, we find that our calculation predicts a closer mass to the measured results of the neutral pion channel. This result was recently included in the Particle Data Book [13].

In Chapter 3, the mechanism of "shining" is used to break supersymmetry by means of boundary conditions in an extra dimension. The model has a single flat extra dimension compactified on an orbifold. In the extra dimension lives two supersymmetric hypermultiplets[10], and on each brane lives sources for these fields. The first hypermultiplet feels sources on both branes that give the scalar fields an exponential profile. The only way to satisfy the boundary conditions and minimize the energy is to force the size of the extra dimension to a unique value. This then stabilizes the extra dimension and gives mass to the radion, the component of the $5D$ graviton that describes the shape of the extra dimension. The second hypermultiplet is also used in a similar way, but with different boundary conditions. The tension between these incompatible boundary conditions breaks supersymmetry. Upon integrating out the fifth dimension, we then expect the $4D$

[10] A hypermultiplet is a collection of two complex scalars and one Dirac fermion that form a closed set of fields that transform among each other under $5D$ SUSY transformations.

effective theory to have a spontaneously broken SUSY spectrum.

Models like this lend themselves to a gravity-based mediation mechanism called radion mediated supersymmetry breaking (RMSB), where the radion superfield aquires a SUSY-breaking vev. This mechanism was developed previously [14] and is liked because its spectrum closely resembles that of gaugino mediated SUSY breaking (gMSB), where SUSY breaking is communicated through gaugino loops that make contact with a new singlet field with a SUSY-breaking vev; this does a very good job solving several of the problems previously mentioned [15]. Unlike gaugino mediation, however, RMSB does not need any new singlets, since the radion plays that role. However, it is very hard to make RMSB the dominant contribution to the spectrum compared to other mechanisms; the only model that people knew of that had dominant RMSB was the no-scale model, which is unstable to radiative corrections. Previous work has been done to try and make RMSB dominant by modifying the no-scale model so that it was stable but still allowed for large RMSB contributions [16]. This shining scenario is the first model that is different from no-scale and still has dominant radion mediation, dispelling the idea that only no-scale-type models can behave this way.

Chapter 4 considers some phenomenology in the lepton sector of anarchic RS models that can be tested in upcoming experiments. Because gauge theories in extra dimensions generate new interactions with the KK gauge bosons, there is no longer enough symmetry to diagonalize all of the operators, and we expect flavor violation to occur. We look at this violation in the lepton sector, where current experiments are probing deeply into rare lepton number violating decays. Neutrinoless trilepton decays of the μ and τ as well as $l \to l^{'}\gamma$ are considered. These two types of decays turn out to be sensitive to Yukawa parameters in conflicting ways, so that between the two constraints we can pin down the allowed parameter space.

It turns out that the current bounds on these decays are very strong, and for the naive point in parameter space representing "anarchic RS", the bounds on M_{KK}, the mass of the Kaluza-Klein particles becomes $\mathcal{O}(10)$ TeV. This is starting to become fine tuned, and is a bad sign for the model. We can lower the

bound naturally down to ~ 5 TeV, but it is hard to get any lower. This means that the LHC may still see these new particles, if they exist. Smaller, upcoming experiments will be putting even stronger bounds on the branching fractions for these rare decays, so it might also be that if M_{KK} is low enough we may even observe these rare decays. We just have to wait and see!

Chapter 2

Threshold Effects in Excited Charmed Baryon Decays

The charmed baryon system is a convenient testing ground for the ideas and predictions of heavy quark symmetry[1]. This is due to the rich mass spectrum and the relatively narrow widths of the resonances. The properties of these states are the subject of active experimental study at both fixed target experiments (FOCUS, SELEX, E-791) and e^+e^- machines (CLEO, BaBar, Belle). For a recent review of the experimental situation, see Ref. [17].

In addition to the usual quantum numbers (I, J^P), the charmed baryon states can be labelled also by the spin-parity of the light degrees of freedom $j_\ell^{\pi_\ell}$, which are good quantum numbers in the limit of an infinitely heavy charm quark. This property leads to nontrivial selection rules for the strong couplings of these states to light hadrons [18]. These predictions are automatically built into an effective Lagrangian describing the couplings of the heavy baryon states to Goldstone bosons [19].

The lowest lying charmed baryons are $L = 0$ states and live in $\bar{\mathbf{3}}$ and $\mathbf{6}$ representations of flavor SU(3). It is convenient to group them together into superfields defined as in Ref. [20], a vector $T_i = \frac{1+\not{v}}{2}(\Xi_c^0\,, -\Xi_c^+\,, \Lambda_c^+)_i$ for the $\bar{\mathbf{3}}$, and a tensor $S_\mu^{ij} = \frac{1}{\sqrt{3}}(\gamma_\mu + v_\mu)\gamma_5 B^{ij} + B_\mu^{*ij}$ for the $\mathbf{6}$. These superfields satisfy the constraints

[1] This work was originally published in [1].

from heavy quark symmetry $\not{v}T = T$, $\not{v}S_\mu = S_\mu$ and the condition $\frac{1+\not{v}}{2}\gamma^\mu S_\mu = 0$, which can be used to restrict the form of their Lagrangian interactions [21]. The strong couplings of the lowest lying heavy baryons are described by the effective Lagrangian containing two couplings $g_{1,2}$ [20] (we use here the normalization of Ref. [27] for these couplings)

$$\mathcal{L}_{\rm int} = \frac{3}{2} i g_1 \varepsilon_{\mu\nu\sigma\lambda} (\bar{S}^\mu_{ik} v^\nu A^\sigma_{ij} S^\lambda_{jk}) - \sqrt{3} g_2 \epsilon_{ijk} (\bar{T}^i A^{jl}_\mu S^\mu_{kl}) \,, \tag{2.1}$$

where $A_\mu = \frac{i}{2}(\xi^\dagger \partial_\mu \xi - \xi \partial_\mu \xi^\dagger) = -\frac{1}{f_\pi}\partial_\mu \Pi + \cdots$ is the usual nonlinear axial current of the Goldstone bosons, defined in terms of $\xi = \exp(i\Pi/f_\pi)$ with $f_\pi = 132$ MeV.

In this paper we focus on the negative parity $L = 1$ orbitally excited charmed baryons. Combining the quark spins with the $L = 1$ orbital momentum gives 7 Λ-type and 7 Σ-type states without strangeness [25, 26] (see Table 2). In the constituent quark model, these states fall into two distinct groups, corresponding to the symmetric and antisymmetric irreducible representations of S_2. The symmetric (antisymmetric) states are denoted in Table 2 with unprimed (primed) symbols. Quark model estimates for the masses of these states [25, 26] suggest that symmetric states are lighter than the antisymmetric ones. Although the permutation symmetry S_2 is not a true symmetry of QCD beyond the quark model, we will continue to refer to the higher mass charm baryon states as 'antisymmetric', as opposed to the lower 'symmetric' states. The properties of these states were studied in the quark model in Refs. [25, 26, 27, 34] and using large N_c methods in [29, 30, 31].

The CLEO, ARGUS and E687 Collaborations [22] observed two negative parity charm baryons, $\Lambda_c^+(2593)$ and $\Lambda_c^+(2625)$. In accordance with the expectations from the constituent quark model, these states were identified with the $\Lambda_{c1}(\frac{1}{2}, \frac{3}{2})$ states in Table 2. Their average masses and widths are [23]

$$\begin{aligned} M(\Lambda_c^+(2593)) - M(\Lambda_c^+) &= 308.9 \pm 0.6 \text{ MeV}\,, \qquad \Gamma(\Lambda_c^+(2593)) = 3.6^{+2.0}_{-1.3} \text{ MeV} \\ M(\Lambda_c^+(2625)) - M(\Lambda_c^+) &= 341.7 \pm 0.6 \text{ MeV}\,, \qquad \Gamma(\Lambda_c^+(2625)) < 1.9 \text{ MeV} \end{aligned} \tag{2.2}$$

State	(I,J)	$j_\ell^{\pi_\ell}$
$\Lambda_{c1}(\frac{1}{2},\frac{3}{2})$	$(0,\frac{1}{2}),(0,\frac{3}{2})$	1^-
$\Sigma_{c0}(\frac{1}{2})$	$(1,\frac{1}{2})$	0^-
$\Sigma_{c1}(\frac{1}{2},\frac{3}{2})$	$(1,\frac{1}{2}),(1,\frac{3}{2})$	1^-
$\Sigma_{c2}(\frac{3}{2},\frac{5}{2})$	$(1,\frac{3}{2}),(1,\frac{5}{2})$	2^-
$\Sigma'_{c1}(\frac{1}{2},\frac{3}{2})$	$(1,\frac{1}{2}),(1,\frac{3}{2})$	1^-
$\Lambda'_{c0}(\frac{1}{2})$	$(0,\frac{1}{2})$	0^-
$\Lambda'_{c1}(\frac{1}{2},\frac{3}{2})$	$(0,\frac{1}{2}),(0,\frac{3}{2})$	1^-
$\Lambda'_{c2}(\frac{3}{2},\frac{5}{2})$	$(0,\frac{3}{2}),(0,\frac{5}{2})$	2^-

Table 2.1: The quantum numbers of the expected p-wave strangeless charmed baryons. The corresponding states with strange quarks can be constructed by completing the SU(3) multiplets to which the above states belong.

where the bound on $\Gamma(\Lambda_c^+(2625))$ is quoted to 90% CL.

Motivated by these data, the lowest lying states $\Lambda_{c1}(\frac{1}{2},\frac{3}{2})$ were studied in a chiral Lagrangian approach in Ref. [24], where their couplings to Goldstone bosons were first derived. These states can be grouped together into a superfield $R_\mu^i = \frac{1}{\sqrt{3}}(\gamma_\mu + v_\mu)\gamma_5 R^i + R_\mu^{(*)i}$ with $R_i^{(*)} = (\Xi_{c1}^0\,, -\Xi_{c1}^+\,, \Lambda_{c1}^+)_i$, subject to the same constraints as the superfield S_μ.

At leading order in the heavy quark expansion, the pion couplings of these states to the sextet ground state baryons S_μ are given by two terms, corresponding to $S-$ and $D-$wave pion emission, respectively

$$\begin{aligned}\mathcal{L}_{\rm int} &= h_2\epsilon_{ijk}\bar{S}_\mu^{kl} v_\nu A_{lj}^\nu R_\mu^i \\ &\quad + ih_8\epsilon_{ijk}\bar{S}_\mu^{kl}\left(\mathcal{D}^\mu A^\nu + \mathcal{D}^\nu A^\mu + \frac{2}{3}g^{\mu\nu}(v\cdot\mathcal{D})(v\cdot A)\right)_{lj} R_\nu^i + \text{h.c.} \quad (2.3)\end{aligned}$$

with the covariant derivative $\mathcal{D}_\mu A_\nu = \partial_\mu A_\nu + [V_\mu\,, A_\nu]$ and $V_\mu = \frac{1}{2}(\xi^\dagger\partial_\mu\xi + \xi\partial_\mu\xi^\dagger)$. This formalism was extended to the other $p-$wave charmed baryons in Table 2 in Refs. [27, 28], where prospects were given for their discovery. A total of 6 $S-$wave and 8 D-wave couplings are required for a complete description of the strong couplings of the states in Table 2.

Knowledge of the pion couplings h_2, h_8 of the lowest orbital excitations $\Lambda_{c1}(\frac{1}{2},\frac{3}{2})$ will provide information about the other excited baryons, and could thus help guide

the search for the missing states. For example, assuming SU(3) symmetry, the widths of the orbitally excited charm baryons containing strange quarks $\Xi'_{c1}(\frac{1}{2},\frac{3}{2})$ can be predicted [28, 27], with results in good agreement with the CLEO data on $\Xi'_{c1}(\frac{1}{2})$ [32] and $\Xi'_{c1}(\frac{3}{2})$ [33]. Furthermore, in the constituent quark model, the couplings of all unprimed states in Table 2 can be shown to be related to h_2, h_8 [27, 34]. Assuming that the masses of these states are known, these relations can be therefore used to predict the decay modes and widths of all these states. Finally, once determined in the charm system, the same couplings would also give the properties of the excited bottom baryons. Clearly, a precise determination of the two couplings h_2, h_8 is of great interest.

There are a few issues which complicate such a determination, following from the peculiarities of the actual mass spectrum. The states $\Lambda_{c1}(\frac{1}{2},\frac{3}{2})$ are observed through their 3-body decays in the $\Lambda_c^+\pi^+\pi^-$ channel. These are resonant decays, proceeding through intermediate $\Sigma_c^{(*)}\pi$ states. The masses, and recently the widths of the Σ_c baryons have been measured by the FOCUS [36] and CLEO [37] Collaborations. The average results of these measurements are [23]

$$\begin{aligned} M(\Sigma_c^{++}) - M(\Lambda_c^+) &= 167.67 \pm 0.15 \text{ MeV}\,, & \Gamma(\Sigma_c^{++}) &= (2.05^{+0.41}_{-0.38} \pm 0.38) \text{ MeV} \\ M(\Sigma_c^{+}) - M(\Lambda_c^+) &= 166.4 \pm 0.4 \text{ MeV}\,, & \Gamma(\Sigma_c^{+}) &\leq 4.6 \text{ MeV}(90\% \text{ CL}) \\ M(\Sigma_c^{0}) - M(\Lambda_c^+) &= 167.32 \pm 0.15 \text{ MeV}\,, & \Gamma(\Sigma_c^{0}) &= (1.55^{+0.41}_{-0.37} \pm 0.38) \text{ MeV} \end{aligned} \tag{2.4}$$

In the heavy quark limit, the only allowed resonant channels are $\Lambda_{c1}(\frac{1}{2}) \to [\Sigma_c\pi]_S$, $[\Sigma_c^*\pi]_D$, and $\Lambda_{c1}(\frac{3}{2}) \to [\Sigma_c\pi]_D, [\Sigma_c^*\pi]_{S,D}$, where the subscript denotes the orbital angular momentum. From (2.2) and (2.4) it follows that the dominant $S-$wave decays of the $\Lambda_{c1}(2593)$ proceed very close to threshold. Furthermore, the available energy in the decay is comparable or less than the width of the decaying state

$$\Lambda_{c1}(2593) - \left[\begin{array}{c} (\Sigma_c^0(2455) + \pi^+) \\ (\Sigma_c^{++}(2455) + \pi^-) \end{array} \right] \sim \left(\begin{array}{c} 2 \text{ MeV} \\ 1.7 \text{ MeV} \end{array} \right) \leq \Gamma(\Lambda_{c1}^+(2593)) \tag{2.5}$$

On the other hand, the decay into the $\Sigma^+\pi^0$ channel takes place ~ 7.5 MeV above threshold, such that it turns out to dominate the width of the $\Lambda_{c1}(2593)$.

The situation with the spin-$\frac{3}{2}$ state $\Lambda_c(2625)$ is somewhat different. For this case, the decay is dominated by the $D-$wave channel $[\Sigma_c\pi]_D$, which is well above threshold (~ 45 MeV), while the $S-$wave accessible modes $[\Sigma_c^*\pi]_S$ lie about 30 MeV below threshold and are thus nonresonant.

This suggests that finite width effects are important in the $\Lambda_c(2593)$ decays. The situation is somewhat similar to $e^+e^- \to t\bar{t}$ production close to threshold, which is mediated by a very broad toponium resonance. The net effect is a distortion of the shape of the invariant mass spectrum in $\Lambda_{c1}(2593) \to \Lambda_c^+\pi^+\pi^-$ from a simple Breit-Wigner shape. The resulting line shape depends both on the unknown couplings $h_{2,8}$ and on the masses and widths of the intermediate Σ_c states. This should be taken into account for the extraction of the mass and width of the $\Lambda_{c1}(2593)$. The purpose of this paper is to present a detailed calculation of these effects.

Consider the amplitude for producing the Λ_{c1} resonance, followed by its decay to a 3-body state $\Lambda_{c1}^+ \to \Lambda_c^+\pi\pi$, of total momentum $p_\mu = M_{\Lambda_c^+}v_\mu + k_\mu$ and invariant mass $M(\Lambda_c^+\pi\pi) = \sqrt{p^2(\Lambda_c\pi\pi)}$. This is written in the factorized form

$$A(i \to \Lambda_{c1}X \to \Lambda_c^+\pi\pi X) = \frac{i}{\Delta - \Delta_{\Lambda_{c1}} + i\Gamma_{\Lambda_{c1}}(\Delta)/2}[\bar{U}(\Delta)\frac{1+\not{v}}{2}V(\Delta, X)]\,, \quad (2.6)$$

where $\Delta = v\cdot k = M(\Lambda_c^+\pi\pi) - M(\Lambda_c^+)$ is the residual energy of the propagating resonance $\Lambda_c(2593)$ and $\Delta_{\Lambda_{c1}} = M(\Lambda_{c1}) - M(\Lambda_c^+)$. $U_\alpha(\Delta)$ and $V_\alpha(\Delta, X)$ are spinor amplitudes parameterizing the decay $\Lambda_{c1}^+ \to \Lambda_c^+\pi\pi$ and its production, respectively. $U_\alpha(\Delta)$ depends on the momenta and spins of the $\Lambda_c\pi\pi$ state, and is calculable in heavy hadron chiral perturbation theory for values of the residual energy $\Delta \ll 1$ GeV. On the other hand, not much is known about the production spinor $V_\alpha(\Delta, X)$, which depends on all the details of the production process.

Squaring the amplitude (2.6), adding the phase space factors and summing over the unobserved states X, one finds the following expression for the $\Lambda_c^+\pi\pi$ production cross-section as a function of the invariant mass Δ:

$$\frac{d\sigma(\Delta)}{d\Delta} \sim \frac{1}{(\Delta - \Delta_{\Lambda_{c1}})^2 + \Gamma_{\Lambda_{c1}}(\Delta)^2/4} \left[\bar{U}(\Delta) \frac{1+\not{v}}{2} \omega(\Delta) \frac{1+\not{v}}{2} U(\Delta) \right] \times \mathrm{dLips}(\Lambda_{c1} \to \Lambda_c^+ \pi\pi) \qquad (2.7)$$

We have introduced here the density matrix $\omega_{\alpha\beta}(\Delta)$ parameterizing the production of a Λ_{c1} resonance in the process $i \to \Lambda_{c1} X$

$$\omega_{\alpha\beta}(\Delta) \equiv \sum_X \int d\mu(X) V_\alpha(\Delta, X) \bar{V}_\beta(\Delta, X) (2\pi)^4 \delta(p_i - p_X - p_{\Lambda_{c1}}) \qquad (2.8)$$

The matrix ω depends on the resonance momentum $p_{\Lambda_{c1}}$ and details of the experimental setup such as the total beam momentum and polarization. Fortunately, the spin structure of the matrix ω is not required if one sums over the spins and momenta of the final decay products in $\Lambda_{c1}^+ \to \Lambda_c^+ \pi\pi$. If this is done, the amplitudes in Eq. (2.7) can be written as

$$\sum_{s_{\Lambda_c}} \int \mathrm{dLips}(\Lambda_{c1} \to \Lambda_c^+ \pi^+ \pi^-) U_\alpha(\Delta) \bar{U}_\beta(\Delta) = \left(\frac{1+\not{v}}{2} \right)_{\alpha\beta} \Gamma(\Lambda_{c1}^+ \to \Lambda_c^+ \pi^+ \pi^-) \qquad (2.9)$$

Inserting this into (2.7) one finds that the production cross section as a function of invariant mass takes the factorized form

$$\frac{d\sigma(\Delta)}{d\Delta} \sim \mathrm{Tr} \left[\frac{1+\not{v}}{2} \omega(\Delta) \right] \frac{\Gamma(\Lambda_{c1}^+ \to \Lambda_c^+ \pi^+ \pi^-)}{(\Delta - \Delta_{\Lambda_{c1}})^2 + \Gamma_{\Lambda_{c1}}^2(\Delta)/4} \qquad (2.10)$$

The dependence on Δ introduced by the production factor $\mathrm{Tr}\,[\frac{1+\not{v}}{2}\omega(\Delta)]$ is unknown, and it can be expected to introduce a slow variation with a characteristic scale $\sim \Lambda_{QCD}$. This can be neglected when compared with the much faster variation of the denominator. The width $\Gamma(\Delta)$ in the numerator is equal to the spin-averaged partial width of a Λ_{c1} resonance of mass $\Delta + M(\Lambda_c^+)$ into a specific channel, e.g. $\Lambda_c^+ \pi^+ \pi^-$, while the width in the denominator $\Gamma_{\Lambda_{c1}}(\Delta)$ sums over all allowed channels. These decay widths are given explicitly by [27]

$$\Gamma_{+-} \equiv \Gamma(\Lambda_{c1}^+ \to \Lambda_c^+ \pi^+ \pi^-) = \frac{g_2^2}{16\pi^3 f_\pi^4} M_{\Lambda_c^+} \int dE_1 dE_2 \left\{ \vec{p}_2{}^2 |A(E_1,E_2)|^2 + \vec{p}_1{}^2 |B(E_1,E_2)|^2 + 2\vec{p}_1 \cdot \vec{p}_2 \mathrm{Re}\left[A(E_1,E_2) B^*(E_1,E_2)\right] \right\} \tag{2.11}$$

where E_1, E_2 are the pion energies in the rest frame of the Λ_{c1} resonance and we have defined

$$A(E_1,E_2) = \frac{h_2 E_1}{\Delta - \Delta_{\Sigma_c^0} - E_1 + i\Gamma_{\Sigma_c^0}/2} + h_8 \left(-\frac{\frac{2}{3}\vec{p}_1{}^2}{\Delta - \Delta_{\Sigma_c^{*0}} - E_1 + i\Gamma_{\Sigma_c^{*0}}/2} + \frac{2\vec{p}_1 \cdot \vec{p}_2}{\Delta - \Delta_{\Sigma_c^{*++}} - E_2 + i\Gamma_{\Sigma_c^{*++}}/2} \right) \tag{2.12}$$

$$B(E_1,E_2;\Delta_{\Sigma_c^{(*)0}}, \Delta_{\Sigma_c^{(*)++}}) = A(E_2,E_1;\Delta_{\Sigma_c^{(*)++}}, \Delta_{\Sigma_c^{(*)0}}) \tag{2.13}$$

The decay rate $\Gamma(\Lambda_{c1}^+ \to \Lambda_c^+ \pi^0 \pi^0)$ is given by a similar relation, with an additional factor of $1/2$ to account for the identical pions in the final state, and with the replacements $\Delta_{\Sigma_c^{(*)++}}, \Delta_{\Sigma_c^{(*)0}} \to \Delta_{\Sigma_c^{(*)+}}$.

In these expressions we work at leading order in the $1/m_c$ expansion in matrix elements, but use the exact 3-body phase space. This procedure includes formally subleading contributions in the $1/m_c$ expansion, which are however enhanced by kinematics and are required for reproducing the data in other similar situations [35]. We neglect the radiative decay channel $\Lambda_{c1}^+ \to \Lambda_c^+ \gamma$, which is expected to contribute about 20 keV to the total width [29].

After integration over the Dalitz plot, the decay width (2.11) can be written as

$$\Gamma_{+-}(\Delta) = g_2^2 \left\{ h_2^2 a_{+-}(\Delta) + h_8^2 b_{+-}(\Delta) + 2h_2 h_8 c_{+-}(\Delta) \right\} . \tag{2.14}$$

A similar result is obtained for the rate into $\Lambda_c^+ \pi^0 \pi^0$ with coefficients a_{00}, b_{00}, c_{00}. The coupling g_2 appears here both explicitly, and implicitly through the $\Sigma_c^{(*)}$ widths in the denominators of $A(E_1,E_2)$ and $B(E_1,E_2)$. These are given by

$$\Gamma(\Sigma_c^{(*)}) = \frac{g_2^2}{2\pi f_\pi^2} \frac{M_{\Lambda_c}}{M_{\Sigma_c^{(*)}}} |\vec{p}_\pi|^3 . \tag{2.15}$$

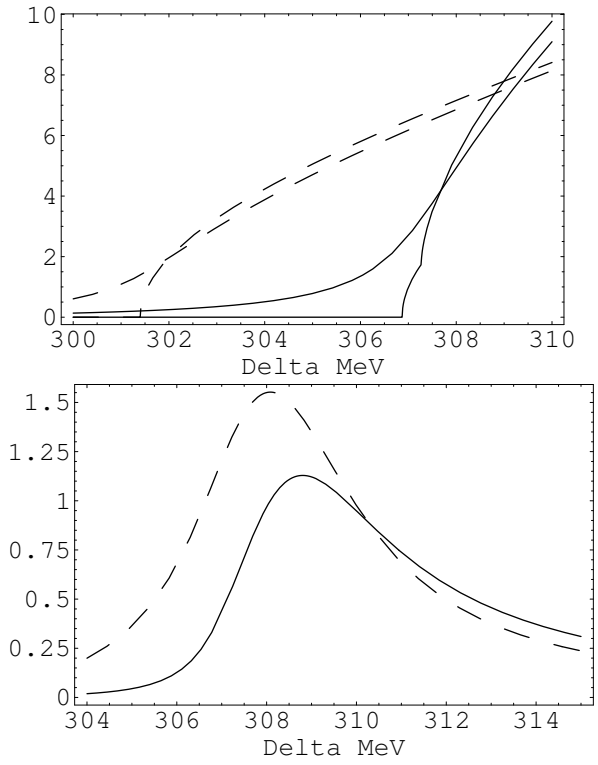

(a) (b)

Figure 2.1: (a) The partial mass-dependent width of the $\Lambda_c(2593)$ in the $\Lambda_c^+\pi^+\pi^-$ channel ($g_2^2 a_{+-}(\Delta)$ - solid line) and in the $\Lambda_c^+\pi^0\pi^0$ channel ($g_2^2 a_{00}(\Delta)$ - dashed line), as a function of $\Delta = M(\Lambda_c^+\pi\pi) - M(\Lambda_c^+)$, with $g_2^2 = 0.34$; the curves with sharp thresholds are computed in the narrow width approximation (Eqs. (2.16), (2.17)) and are independent on g_2; (b) The $\Lambda_c^+(2593)$ resonance shape as seen in the $\Lambda_c^+\pi^+\pi^-$ channel (solid curve) and in the $\Lambda_c^+\pi^0\pi^0$ channel (dashed curve). The results in (b) correspond to $\Delta_{\Lambda_{c1}} = 309$ MeV and $h_2^2 = 0.3$.

Using the observed masses this gives $\Gamma(\Sigma_c^{++,+,0}) = \{6.15\,, 7.06\,, 6.01\}g_2^2$ MeV, and $\Gamma(\Sigma_c^{++*,+*,0*}) = \{47.9\,, 47.4\,, 46.3\}g_2^2$ MeV. The extracted values for g_2 from the Σ_c and Σ_c^* experimental widths are somewhat different: $\langle g_2^2\rangle_{\Sigma_c} = 0.25 \pm 0.17$, and $\langle g_2^2\rangle_{\Sigma_c^*} = 0.33 \pm 0.15$, which can be attributed to an $1/m_c$ effect. Although the uncertainty in this coupling is rather large, $g_2^2 = 0.29 \pm 0.23$, the resulting effect on our predictions (2.14) is very small, because they are very close to the narrow-width case for the Σ_c (see the discussion around Eqs. (2.16), (2.17)).

Our main interest here is in the functional dependence of $a_{+-,00}(\Delta)$, which

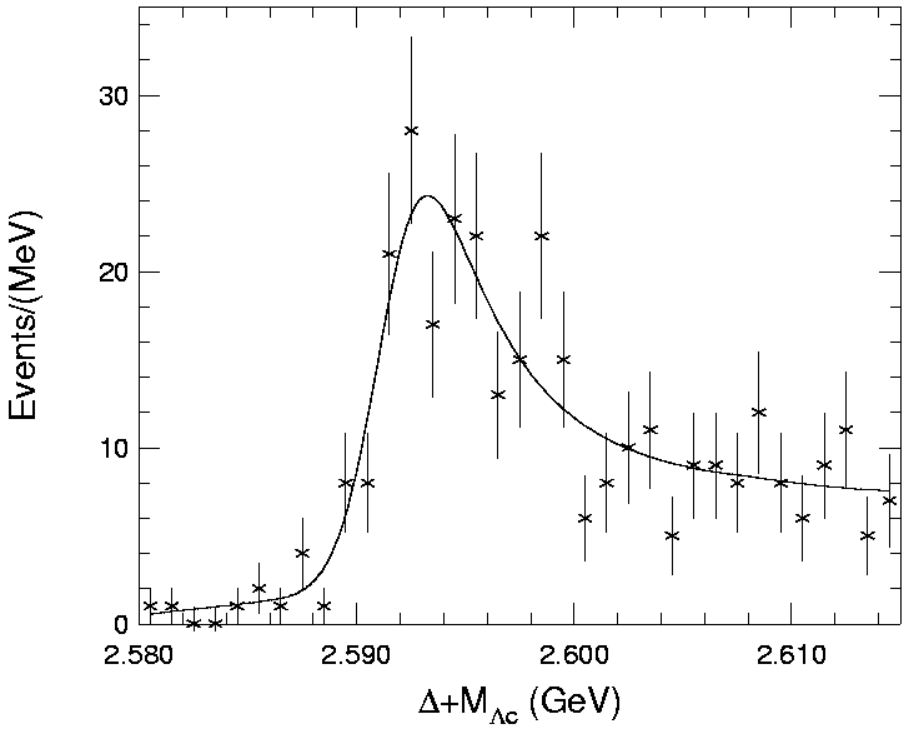

Figure 2.2: Fit to the invariant mass spectrum in $\Lambda_c^+(2593) \to \Lambda_c^+\pi^+\pi^-$ as explained in the text.

dominate numerically the rates $\Gamma_{+-,00}$. These coefficients are plotted in Fig. 1(a) as functions of Δ; the qualitative features of these curves can be understood without a detailed computation, as follows. The coefficients $a(\Delta)$ give the partial widths into the $[\Sigma_c\pi]_S$ channel, which start at threshold $\Delta = 2M(\pi^+)$, and rise slowly up to the threshold for production of $[\Sigma_c^0\pi^+]_S$ and $[\Sigma_c^{++}\pi^-]_S$ at $\Delta = 306.9$ MeV and $\Delta = 307.2$ MeV, respectively. Above this threshold, the rate rises much faster, which explains the 'kink' seen in Fig. 1(a) in the $\pi^+\pi^-$ channel. On the other hand, the threshold in the neutral pion channel lies lower, at $\Delta = 301.4$ MeV, corresponding to the opening of the $[\Sigma_c^+\pi^0]_S$ channel. Since the central value of the Λ_{c1} mass lies around 307 MeV, the rapid variation of $a_{+-}(\Delta)$ in this region will likely affect the extraction of $\Delta_{\Lambda_{c1}}$.

It is instructive to compare these results with those obtained in the narrow

width approximation, where the mass-dependent partial widths in (2.11) are approximated with 2-body widths [28]

$$\begin{aligned}\Gamma_{\rm NW}(\Lambda_{c1}^+ \to \Lambda_c^+\pi^+\pi^-) &= \Gamma(\Lambda_{c1}^+ \to \Sigma_c^0\pi^+) + \Gamma(\Lambda_{c1}^+ \to \Sigma_c^{++}\pi^-) \\ &= a(\pi^\pm)|\vec{p}_\pi\,| \qquad (2.16)\\ \Gamma_{\rm NW}(\Lambda_{c1}^+ \to \Lambda_c^+\pi^0\pi^0) &= \Gamma(\Lambda_{c1}^+ \to \Sigma_c^+\pi^0) = a(\pi^0)|\vec{p}_\pi\,| \qquad (2.17)\end{aligned}$$

where $\vec{p}_\pi$ is the pion momentum in $\Lambda_{c1} \to \Sigma_c\pi$ decays. Neglecting isospin violation in the Σ_c masses, the $a(\pi)$ parameters are given in the heavy quark limit by

$$a(\pi^\pm) = \frac{h_2^2}{\pi f_\pi^2}\frac{M_{\Sigma_c}}{M_{\Lambda_{c1}}}E_\pi^2\,, \qquad a(\pi^0) = \frac{1}{2}a(\pi^\pm)\,. \qquad (2.18)$$

In the limit $g_2 \to 0$, the exact result (2.11) reduces to the narrow width approximation in Eqs. (2.16) and (2.17), that is $\Gamma \to \Gamma_{\rm NW}$. As one can see from Fig. 1(a), the narrow width results give a good approximation to the exact widths (computed with $g_2^2 = 0.34$), for Δ not too close to threshold.

In Fig. 1(b) we show invariant mass distributions $\Delta = M(\Lambda_c^+\pi\pi) - M(\Lambda_c^+)$ in $\Lambda_c^+(2593)$ decays, in both charged and neutral pions channels. The shape of the invariant mass distribution in the charged pions channel $\Lambda_c^+\pi^+\pi^-$ is distorted towards larger values of Δ compared to a simple Breit-Wigner curve. In particular, extractions of the $\Lambda_c^+(2593)$ parameters from the charged pions channel alone could overestimate the mass of this resonance by a few MeV, which is larger than the present 1σ uncertainty (2.2) on this parameter. These effects are not present in the neutral pions channel, for which the shape of the mass spectrum comes closer to a pure Breit-Wigner resonance.

The first observation of the $\Lambda_c^+\pi^0\pi^0$ mode has been presented in unpublished CLEO data [38], where the corresponding invariant mass distribution was used to extract the mass of the $\Lambda_c^+(2593)$. The result is lower than that obtained from the $\Lambda_c^+\pi^+\pi^-$ channel (2.2), in agreement with our expectations,

$$[M(\Lambda_c^+(2593)) - M(\Lambda_c^+)]_{\Lambda_c\pi^0\pi^0} = 306.3 \pm 0.7 \text{ MeV}\,. \qquad (2.19)$$

Experimental difficulties connected with the low π^0 detection efficiency could limit the precision of such a determination. We propose therefore that the shape of the $\Lambda_c^+\pi^+\pi^-$ invariant mass spectrum be fit to the distribution (2.10) with parameters $(\Delta_{\Lambda_{c1}}, h_2)$ (instead of a Breit-Wigner curve with parameters $(\Delta_{\Lambda_{c1}}, \Gamma)$).

In Fig. 2 we show the results of such a fit, performed using the CLEO data presented in [38] (see Fig. 5.5 in this reference), including detector resolution effects. The parameters of the $\Lambda_c(2593)$ resonance extracted from this fit are [2]

$$M(\Lambda_c^+(2593)) - M(\Lambda_c^+) = 305.6 \pm 0.3 \text{ MeV}\,, \qquad h_2^2 = 0.24^{+0.23}_{-0.11}\,, \tag{2.20}$$

and correspond to a resonance mass in reasonably good agreement with (2.19). A conventional fit of this same data using a Breit-Wigner function, yields a mass difference of around 308 MeV, in agreement with the published measurements [22]. Note that the threshold effects effectively lower the resonance mass (2.20) compared with the previous determinations (2.2). Our treatment also leads to a reduction in the uncertainties connected with the poorly measured Σ_c widths. The result for the coupling h_2^2 is somewhat lower than previous determinations of this coupling [28] ($h_2^2 = 0.30^{+0.21}_{-0.14}$) and [27] ($h_2^2 = 0.33^{+0.20}_{-0.13}$).

In conclusion, we have discussed in this paper the impact of threshold effects on the determination of the $\Lambda_c^+(2593)$ parameters from its strong decays into $\Lambda_c^+\pi\pi$, and we have presented theory motivated fits of the mass and couplings of this state. Our results suggest that the excitation energy of the $\Lambda_c^+(2593)$ is about 2-3 MeV lower than obtained in previous determinations.

[2] The data shown in Fig. 2 was obtained in Ref. [38] by adding the measured mass difference to a fixed Λ_c^+ mass of 2286.7 MeV. Thus, for consistency, we subtracted this value from our fitted mass to obtain the result (2.20).

Chapter 3

Shining on an Orbifold

Supersymmetry (SUSY) and extra dimensions are some of the most active areas of research in high energy physics today[1]. In addition to their mathematically aesthetic value, they might be able to solve the hierarchy problems of particle physics, and both are motivated by string theory. However, the world we live in is four dimensional and not supersymmetric. Therefore if SUSY exists it must be broken, probably spontaneously. And if extra dimensions exist they must be compactified or in some way hidden. These two constraints provide a wealth of possible phenomenology.

Extra dimensions have another problem. If you naively try to compactify them, they are inherently unstable due to Casimir forces. Therefore any self-consistent model with extra dimensions must include a way to stabilize the dimensions against these quantum fluctuations.

One method of doing just that is known as the Goldberger-Wise (GW) mechanism [40]. This was originally designed to stabilize the extra dimension of the RS1 Model [12]. Goldberger and Wise proposed including a scalar field that lived in the bulk but that had independent potentials localized on branes at the two orbifold fixed points. These independent potentials generate a profile for the scalar, and matching boundary conditions enforces a stabilized extra dimension.

A similar idea that involves supersymmetry was considered in [41]. In this

[1]This work was originally published in [2].

paper, the extra dimension is a circle and a hypermultiplet has a source term on a brane located at $y = 0$. This hypermultiplet has an exponential profile in the bulk. Then a "probe brane" is included that interacts with the hypermultiplet. The F-flatness conditions conspire to stabilize the radius of the extra dimension by fitting boundary conditions. This method can also be used to break supersymmetry by fixing the model so that it is impossible to satisfy the F-flatness conditions and the boundary conditions at the same time. Breaking SUSY in this way is generally called "shining" [41, 42].

This paper extends this idea to a flat orbifold. A single hypermultiplet lives in the bulk, and it has sources on branes located at both orbifold fixed points. Fitting boundary conditions overconstrains the problem and forces the radius to be stabilized. A very nice side effect of this model is that supersymmetry need not be broken in order to stabilize the radius. Once we stabilize the radius of the extra dimension we can break supersymmetry using the same technique. We shine another hypermultiplet from the brane at $y = 0$ and find that we cannot match boundary conditions and preserve supersymmetry at the same time. We show that that this SUSY breaking does not have any sizeable effect on the radius stabilization mechanism. This method is improved from [41] since the orbifold geometry means that we do not need any chiral superfields living on one of the branes.

Our model is similar to one proposed previously by Maru and Okada, but they consider the warped case [43]. However, they claim that there is no viable flat space limit. We show why this is not correct. We will also correct a claim about the zero modes of the 4D effective theory.

In the next section we will present the model and show how the shining mechanism can be used to both stabilize the radius and break supersymmetry. In the following section we will consider the four-dimensional effective theory that reproduces the low energy physics. We will also discuss how supergravity effects help stabilize the flat directions, and how radion [14] and anomaly [44] mediated supersymmetry breaking can occur.

3.1 The Model

In this section we will present the model in terms of $N = 1$ superfields in five dimensions. We work with a single extra dimension compactified on a flat orbifold $S^1/\mathbb{Z}_2$:

$$ds^2 = \eta_{\mu\nu} dx^\mu dx^\nu - R^2 dy^2 \tag{3.1}$$

where we are using a mostly minus metric throughout this paper. R is the radius modulus field, or "radion", which parameterizes the size of the extra dimension, and $y \in [0, \pi]$ is an angular variable. The orbifold parity defines a symmetry under the transformation $y \to -y$. The five-dimensional fields in the theory will be either even or odd under this parity.

This model consists of two hypermultiplets (Φ, Φ^c) and (Ψ, Ψ^c) that are shined across the bulk from a brane located at $y = 0$. One of these hypermultiplets will be used to stabilize the extra dimension while the other one will be used to break supersymmetry. In the convention that we use, the conjugate superfields are even under the orbifold parity while the other chiral superfields are odd.

The five-dimensional action for our model is given by [45, 46]:

$$\begin{aligned} S &= \int d^4x\, dy \int d^4\theta\, \varphi^\dagger \varphi\, \frac{T + T^\dagger}{2} \left\{ -3M_5^3 + \Phi^\dagger \Phi + \Phi^{c\dagger} \Phi^c + \Psi^\dagger \Psi + \Psi^{c\dagger} \Psi^c \right\} \\ &\quad + \int d^4x\, dy \int d^2\theta\, \varphi^3 \left\{ \Phi^c (\partial_y + mT) \Phi + \Psi^c (\partial_y + \mu T) \Psi \right\} + \text{h.c.} \\ &\quad + \int d^4x\, dy \int d^2\theta\, \varphi^3 \left\{ \Phi^c [J\delta(y) - J'\delta(y - \pi)] + \Psi^c K \delta(y) + \alpha \delta(y) \right\} + \text{h.c.} \end{aligned} \tag{3.2}$$

where φ is the conformal compensator and T is the radion superfield[2] (see Appendix A). α is a constant superpotential living on the $y = 0$ brane that will be used to cancel the cosmological constant after SUSY breaking. Notice that this action

[2]Notice the T dependence in the bulk mass term for the hypermultiplet. This dependence was not included in Equations 11-14 of [45]. However their later inclusion of F_T in the action was correct, so this does not change any of their results. Therefore we assume that this is simply a typo in their paper.

has a $U(1)_R$ symmetry in the bulk and the $y = \pi$ brane with $R(\Psi^c) = R(\Phi^c) = +2$ and all other superfields neutral. This symmetry is explicitly broken on the $y = 0$ brane by the α term. This will be important later. Also notice that if we extend our domain in y to the covering space $y \in [-\pi, \pi]$ the mass terms contain a sign function. We leave this out to avoid the cumbersome notation, but it is very important when going to the four dimensional effective theory.

This model is virtually identical to the model of Maru and Okada [43]. In that paper the authors stabilized the extra dimension in the case of a warped background using a hypermultiplet with delta-function sources on both branes. However they claim that the only way this can be done is in warped space and that if you take the flat space limit you get a runaway potential for the radion. This is not the case if you take the appropriate flat space limit. Specifically, they parameterized their bulk masses in terms of a c-parameter: $m = (\frac{3}{2} + c)k$ where k is the curvature in the warp factor. Then if you naively take the limit $k \to 0$ the bulk masses would vanish and the radion would no longer be stabilized. The appropriate thing to do is to take the limit as $k \to 0$ while holding the bulk mass fixed. It is easy to take this limit in their paper and we get the same results presented here for the radion potential.

As a first step in analyzing the model we ignore supergravity contributions, so $T = R$ and $\varphi = 1$; in other words, $F_T = F_\varphi = 0$. We will come back to this in a later section. With these conditions the remaining F-term equations of motion are:

$$
\begin{aligned}
RF^c_\Phi &= (mR + \partial_y)\phi + \Big[J\delta(y) - J'\delta(y - \pi)\Big] && (3.3)\\
RF^c_\Psi &= (\mu R + \partial_y)\psi + K\delta(y) && (3.4)\\
RF_\Phi &= (mR - \partial_y)\phi^c && (3.5)\\
RF_\Psi &= (\mu R - \partial_y)\psi^c && (3.6)
\end{aligned}
$$

Supersymmetry is maintained if we can find (y-dependent) vevs of the scalar fields so that all of the above F-terms vanish. Let us first consider the F-flatness condition $F^c_\Phi = 0$. The first delta function gives the boundary condition $\phi(0) = -\frac{J}{2}$

so there is a unique solution:

$$\phi(y) = -\frac{J}{2}\Theta(y)e^{-mR|y|} \tag{3.7}$$

where $\Theta(y)$ is the Heaviside step function with the convention $\Theta(0\pm) = \Theta(\pi\mp) = \pm 1$. The boundary condition at $y = \pi$ then overconstrains the problem and fixes the radius:

$$R = \frac{1}{m\pi}\log\left(\frac{J}{J'}\right) \tag{3.8}$$

Hence this model stabilizes the size of the extra dimension as long as $|J| > |J'|$ and they each have the same sign.

The Ψ sector breaks supersymmetry through the shining mechanism [41]. To understand how this works notice that if we set $F^c_\Psi = 0$ we can write down the solution:

$$\psi(y) = -\frac{K}{2}\Theta(y)e^{-\mu R|y|} \tag{3.9}$$

The coefficient is set by the delta function source on the $y = 0$ brane. Notice however that there is no source on the $y = \pi$ brane; combined with the fact that $\psi(y)$ is an odd field the boundary condition is $\psi(\pi) = 0$. This boundary condition is inconsistent with Equation (3.9), and therefore supersymmetry is broken on the boundary at $y = \pi$.

Finally let us consider the last two F-terms. Setting these equations to zero gives the general results:

$$\phi^c = Be^{mR|y|} \tag{3.10}$$

$$\psi^c = Ce^{\mu R|y|} \tag{3.11}$$

The coefficients B and C are arbitrary and represent an indetermination of the four-dimensional zero modes of these scalars. Hence, upon integrating out the fifth dimension these fields correspond to flat directions.

That there are two flat directions in our theory should come as no surprise [47]. ψ^c is the scalar field in the multiplet that breaks supersymmetry ($F^c_\Psi \neq 0$), so it is expected to be flat at tree level. That ϕ^c is also a flat direction should not surprise us either. It is due to the fact that the condition $F^c_\Phi = 0$ was used to stabilize the extra dimension, i.e.: give the radion a mass. This leaves over an extra degree of freedom corresponding to the massless ϕ^c. This interpretation of the flat directions differs from [43]; this difference will be clarified when we discuss the 4D effective theory.

3.2 4D Spectrum

Now we will consider the four-dimensional effective theory generated by the action in Equation (3.2). In the first section we will derive the effective potential for the radion and SUSY breaking by setting all the hyper-scalars to their vevs from the previous section. In the next section we will consider the contributions coming from the hyper-scalars and write down an effective superpotential and Kahler potential that captures these effects. In the third section we will consider the lowest order effects of supergravity (turning F_φ and F_T back on). In the final section we will look at how other fields are affected by the shining field. We consider the specific examples of putting matter on one of the branes, and of putting a gauge field in the bulk.

3.2.1 Radion Potential

We now wish to construct an effective potential for the radion. In the process we will also be able to parameterize the size of supersymmetry breaking. In order to do this we need to compute the four-dimensional effective potential. Ignoring any contributions from supergravity this potential is given by:

$$V = \int_0^\pi dy R \left[|F_\Psi|^2 + |F^c_\Psi|^2 + |F_\Phi|^2 + |F^c_\Phi|^2 \right] \tag{3.12}$$

There is a very nice way to understand Equation (3.12) that was presented in

[41]: think of the extra dimension coordinate y as a (continuous) index for the chiral superfields. Then the potential is nothing more than the sum of all of the magnitude-squared F-terms, which is precisely what Equation (3.12) is. F_Ψ and F_Φ are proportional to the flat directions so they will not contribute to the effective potential at tree level. We will see how the zero modes of the even scalars contribute to the effective potential in a later section. This leaves two terms to calculate.

Supersymmetry is explicitly broken in the F_Ψ^c term. To isolate that result we must consider the full equations of motion for the scalar field upon integrating out the auxiliary fields. Rather than do that explicitly, we employ the following trick, which is equivalent. We insist that the boundary conditions on the fields are sacred; therefore $\psi(\pi) = 0$ must be enforced. We have already seen that this condition cannot be satisfied for $F_\Psi^c = 0$ but we can get as close as possible if we make the following ansatz:

$$\psi(y) = -\frac{K}{2}\Theta(y)\left[e^{-\mu R|y|} - e^{-\mu R\pi}f(y)\right] \tag{3.13}$$

where $f(y)$ is some function that satisfies the boundary conditions $f(0) = 0$, $f(\pi) = 1$. This will enforce the boundary condition but at the cost of introducing a term into the potential:

$$\Delta V = \int_0^\pi dy \frac{K^2}{4R} e^{-2\mu R\pi}|\partial f - \mu R f|^2 \tag{3.14}$$

Now we can chose this function to minimize the potential. Performing this minimization using variational methods and using the boundary conditions gives:

$$f(y) = \frac{\sinh(\mu R y)}{\sinh(\mu R \pi)} \tag{3.15}$$

We can plug this result back into Equation (3.14) and integrate over y to get:

$$\Delta V = \frac{1}{2}\frac{\mu K^2}{e^{2\mu\pi R} - 1} \tag{3.16}$$

F_Φ^c vanishes only when $R = r_0$, the stabilized radius defined in Equation (3.8). For an arbitrary radius, $F_\Phi^c \neq 0$ and we can repeat the above steps exactly for $\phi(y)$

appearing in F_Φ^c. We try the ansatz:

$$\phi(y) = -\frac{J}{2}\Theta(y)\left[e^{-mR|y|} - \left(\frac{J'}{J} - e^{-mR\pi}\right)g(y)\right] \tag{3.17}$$

where $g(y)$ has the same boundary conditions as $f(y)$. Indeed, upon minimizing the potential we find that $g(y)$ has the same form as $f(y)$ with μ replaced by m. Plugging it back into Equation (3.12) and integrating over y we find:

$$V(R) = \frac{1}{2}\frac{m(J - J'e^{m\pi R})^2}{e^{2m\pi R} - 1} + \Delta V \tag{3.18}$$

This potential is minimized for the radius given in Equation (3.8). Near this stabilized radius $\Delta V \sim \mu K^2 (J/J')^{-2\mu/m}$ does not give a significant correction relative to the first term due to the exponential suppression for even moderate values of the parameters. For concreteness, we chose the parameters: $J = K = M_5^{3/2}/10$, $J' = M_5^{3/2}/100$, $\mu = M_5/10$ and $m = M_5/75$. Then we find $R \sim 55 l_5$ where l_5 is the 5D Planck length. This generates a compactification scale $M_c \sim 0.02 M_5$. Using the well-known relation $M_P^2 = M_5^3/M_c$, we estimate $M_5 \sim 10^{17}$ GeV. We estimate the vacuum energy at this radius to be $M_{SUSY} = 3 \times 10^{-5} M_5 \sim 10^{12}$ GeV.

We can take the second derivative of this potential to find the mass of the radion. After taking into account the normalization of the radion (see Appendix A) we find $m_r \sim 10^{-3} M_P \sim 10^{15}$ GeV for the above values of the parameters.

3.2.2 Higher Modes and the Effective Superpotential

To get the effective scalar potential in four dimensions we must do a KK expansion of the fields. The details of this are reviewed in Appendix B. Here we quote the results:

$$\phi(x,y) = -\frac{J}{2}\Theta(y)e^{-mR|y|} + \sqrt{\frac{2}{\pi}}\sum_n \phi_n(x)\sin(ny) \tag{3.19}$$

$$\phi^c(x,y) = -B(x)e^{+mR|y|} + \sqrt{\frac{2}{\pi}}\sum_n \phi_n^c(x)\sin\left[ny + \tan^{-1}\left(\frac{n}{mR}\right)\right] \tag{3.20}$$

and similarly for (ψ, ψ^c) with $(B, m, J) \to (C, \mu, K)$. The KK masses are given by the simple relation: $M_n^2 = m^2 + n^2/R^2$ $(n > 0)$ for both ϕ and ϕ^c (ψ and ψ^c) and $M_B = M_C = 0$. The minus sign in front of $B(x)$ is inserted for later convenience. The first term in Equation (3.19) is a y-dependent vev. There is no zero mode for the odd field, as explained in Appendix B. This is another correction to [43], who suggest that the zero mode of the odd field corresponds to the flat direction. This role is played by the even zero mode $B(x)$, as explained earlier.

To get the 4D effective theory we insert this result into the full five-dimensional Lagrangian and integrate over y. Since the KK modes all have masses at the compactification scale or higher they should not seriously affect the low energy physics; we will see that they decouple below. We also have the (y-dependent) vev of the odd field; that just gives us the potential previously calculated in Equation (3.18). We are left with the zero mode for the even field:

$$\mathcal{L}_4 = \int_0^\pi dy\, e^{2mRy} |\partial B|^2 = \frac{1}{2m}(e^{2mR\pi} - 1)|\partial B|^2 + \mathcal{O}(\partial R) \tag{3.21}$$

Now define $R = r_0 + r$. We can canonically normalize the field $B(x)$ by making the field redefinition: $B \to B\left(\frac{2m}{e^{2m\pi r_0}-1}\right)^{1/2}$ and we finally have (after including the ψ-sector):

$$\begin{aligned} \mathcal{L}_4 &= |\partial B|^2 + \lambda |\partial B|^2 \left[2\pi m r + 2\pi^2 m^2 r^2 + \cdots\right] \\ &\quad + |\partial C|^2 + \tilde{\lambda} |\partial C|^2 \left[2\pi \mu r + 2\pi^2 \mu^2 r^2 + \cdots\right] + \mathcal{O}(\partial r) \\ &\quad - V(r_0 + r) \end{aligned} \tag{3.22}$$

where $V(r_0 + r)$ is the potential in Equation (3.18) and the terms in brackets come from expanding $2e^{\pi m r}\sinh(\pi m r)$. Using Equation (3.8):

$$\lambda = \frac{1}{1 - e^{-2m\pi r_0}} = \frac{1}{1 - (J'/J)^2} \tag{3.23}$$

$$\tilde{\lambda} = \frac{1}{1 - e^{-2\mu\pi r_0}} = \frac{1}{1 - (J'/J)^{2\mu/m}} \tag{3.24}$$

Equation (3.22) is the four-dimensional effective Lagrangian for the canonically normalized scalar field zero modes and their lowest order couplings to the radion.

In addition to Equation (3.22), there are also terms that involve the derivative of R. These terms are already quadratic in the B field, so they represent other higher order effects that do not interest us here.

The higher KK modes do not have any problem or ambiguity in their coupling to the radion, which comes from the KK mass term:

$$\Delta\mathcal{L} = -\sum_n \phi_n^{c\dagger}\left\{\partial^2 + \left[m^2 + \frac{n^2}{r_0^2}\left(1+\frac{r}{r_0}\right)^{-2}\right]\right\}\phi_n^c$$

Now we would like to write down the four-dimensional Lagrangian in terms of superfields. The only relevant fields that appear in the low energy theory are the B, C scalars and the radion. The kinetic terms and the interaction terms can be derived from a Kahler potential[3]:

$$K_4 = \mathcal{B}^\dagger\mathcal{B}\left(e^{m\pi(T+T^\dagger)} - 1\right) + \mathcal{C}^\dagger\mathcal{C}\left(e^{\mu\pi(T+T^\dagger)} - 1\right) \tag{3.25}$$

where $\mathcal{B}$ and $\mathcal{C}$ are the four dimensional chiral superfields containing B and C respectively. We also need to write down a superpotential that gives us Equation (3.18):

$$W_4 = -\sqrt{\frac{m}{2}}\left(J - J' e^{m\pi T}\right)\mathcal{B} - \sqrt{\frac{\mu}{2}}K\mathcal{C} \tag{3.26}$$

This choice for the Kahler potential and superpotential will, after the appropriate canonical rescaling, reproduce Equation (3.22).

3.2.3 Effects from Supergravity

We are now in a position to incorporate effects from supergravity. We start with the effective four-dimensional Lagrangian:

$$\mathcal{L}_4 = \int d^4\theta\, \varphi^\dagger\varphi\left\{-\frac{3}{2}M_5^3(T+T^\dagger) + K_4\right\} + \int d^2\theta\, \varphi^3\,(W_4 + \alpha) + \text{h.c.} \tag{3.27}$$

[3]There is a subtlety here. When writing down the Kahler and superpotential we must match to the component Lagrangian before rescaling the fields. So Equations (3.25) and (3.26) are actually found from matching to Equation (3.21) after a field redefinition $B \to \sqrt{2m}B$, $C \to \sqrt{2\mu}C$ to get the dimensions right.

where the first term is the supergravity contribution derived in [48] and K_4 and W_4 are given in Equation (3.25) and (3.26) respectively. The constant α is required to cancel the cosmological constant in order to properly normalize the gravitino mass [49]. The details of deriving Equation (3.27) from the full 5D theory can be found in [50]. The superpotential for $\mathcal{C}$ is reminiscent of the Polonyi model [51]. In Polonyi models, the vev of the scalar field is pushed up to the Planck scale. This will happen here as well, but it does not do any damage to our results [52].

First we integrate out the auxiliary fields to get a scalar potential. After rescaling the fields so they have canonical kinetic terms as in Equation (3.22), we get:

$$V_4(B,C,R) = V(R) + \frac{2R}{3M_5^3}\left\{X_{\tilde{B}}[\tilde{B} - \langle\tilde{B}\rangle]^2 + X_{\tilde{C}}[\tilde{C} - \langle\tilde{C}\rangle]^2\right\} - U_0 + \mathcal{O}(M_5^{-6}) \tag{3.28}$$

where $V(R)$ is the potential given in Equation (3.18), $U_0 = \frac{2R}{3M_5^3}(X_{\tilde{B}}\langle\tilde{B}\rangle^2 + X_{\tilde{C}}\langle\tilde{C}\rangle^2)$, and

$$\tilde{B} \equiv \frac{1}{\sqrt{1+\epsilon^2}}(B + \epsilon C) \tag{3.29}$$

$$\tilde{C} \equiv \frac{1}{\sqrt{1+\epsilon^2}}(C - \epsilon B) \tag{3.30}$$

So we find that the B and C fields mix, but they can be redefined to have definite masses and vevs. These quantities along with the mixing parameter ϵ are given in Appendix C. If we remove the C field (no supersymmetry breaking[4]) but there is still a cosmological constant (so $\alpha \neq 0$) then we find that $\langle B\rangle = \sqrt{\frac{m}{2}}\frac{3\alpha}{m^2\pi r_0 J'}$. This is exactly as we expect from [50].

All of the above masses and vevs depend on the radius, but we have fixed $R = r_0$, the radius fixed by the Φ-sector given in Equation (3.8). There is also mixing with the radion, and supergravity will give additional contributions to the radion mass; this is not very important since $V(R)$ generates a radion mass just below the compactification scale while supergravity effects are all suppressed by

[4]This can be thought of as the limit $K \to 0$ since in that case the Ψ sector would have no odd profile in the bulk.

powers of the Planck scale. So it is sufficient to fix the radion at r_0 since any radion mixing with the scalars will be very small. This means that there are actually two sources of supersymmetry breaking: one source comes from the C field directly ($F_C \neq 0$), and another source from the fact that $R = r_0$ is not the true minimum of the potential in Equation (3.18). We claim that the second source of supersymmetry breaking is negligible compared to the first. This can be seen by letting $R_{\text{truevac}} = r_0 + \delta$, where δ is small from the argument following Equation (3.18). In fact, a numerical analysis shows that for the values of parameters given, $\delta \sim 0$ to a very good approximation. Therefore we need not worry about these additional contributions.

The masses of the scalars can be computed for the values of the parameters mentioned below Equation (3.18). We find $m_{\tilde{B}} \sim 10^{12}$ GeV, and $m_{\tilde{C}} \sim 10^7$ GeV. Both of these masses are well below the compactification scale and m_r as promised.

Finally, we demand that the cosmological constant be tuned to zero. Fixing the radion to its classical value and the scalar fields to their vevs gives $V(r_0) - U_0 = 0$. This can easily be solved for α; see Appendix C.

We can now use the formula to compute $\langle F_\phi \rangle$ and $\langle F_T \rangle$. We find[5]:

$$\langle F_\phi^\dagger \rangle = \frac{\alpha}{M_5^3 r_0} - \frac{\sqrt{2\mu} K (J'/J)^{\mu/m} \langle C \rangle}{3 M_5^3 r_0} - \frac{\langle F_T^\dagger \rangle}{2 r_0} \tag{3.31}$$

$$\frac{\langle F_T^\dagger \rangle}{2 r_0} = \frac{\frac{3\alpha}{2 r_0} - \sqrt{\frac{\mu}{2}} \frac{K}{r_0} \left(1 + \mu \pi \tilde{\lambda} r_0\right) (J'/J)^{\mu/m} \langle C \rangle - \sqrt{\frac{m}{2}} m \pi J' \langle B \rangle}{2 r_0 (1-\lambda) m^2 \pi^2 \langle B \rangle^2 + 2 r_0 (1 - \tilde{\lambda}) \mu^2 \pi^2 \langle C \rangle^2 + \frac{3}{2} M_5^3} \tag{3.32}$$

The first term in Equation (3.31) cancels the cosmological constant; the second term comes from the SUSY-breaking F-term (F_C); the final term is the radion-mediated contribution given in Equation (3.32). For the given parameters this generates $\frac{|\langle F_T \rangle|}{2 r_0} \sim 10^6$ GeV and $m_{3/2} = \langle F_\varphi \rangle \sim 10^6$ GeV. These quantities are the same order of magnitude due to the large Polonyi vev $\langle C \rangle$ which can cancel the

[5]Notice that $\langle B \rangle, \langle C \rangle$ are vevs of the original fields before mixing. They can be computed by inverting Equations (3.29-3.30).

cosmological constant term in Equation (3.31). Notice that in the limit considered earlier where $C \equiv 0$ but there is still a cosmological constant, we find to this order after plugging in our result for $\langle B \rangle$ given below Equation (3.30) that $\langle F_T^\dagger \rangle = 0$ and $\langle F_\varphi^\dagger \rangle = \frac{\alpha}{M_5^3 r_0}$, again in agreement with [50].

3.2.4 Soft Masses from the Shining Sector

We now ask what happens to the MSSM in our model of SUSY breaking. In the full 5D theory, supersymmetry is broken near the brane at $y = \pi$. Thus, we can place the MSSM on the brane at $y = 0$ and ask if this will generate any contact interactions in the 4D effective theory. Such terms would look like:

$$\mathcal{L}_c = \int_0^\pi dy \delta(y) \int d^4\theta \frac{Q^\dagger Q \Psi^{c\dagger} \Psi^c}{M_5^3} \tag{3.33}$$

where Q is a chiral superfield in the MSSM.

Now it is sufficient to only consider the zero mode of the hyper-scalar since all of the KK modes have masses of order the compactification scale or higher, and these will generate Planck and Yukawa suppressed interactions. In this case:

$$\Psi^c(x, y) = \sqrt{\frac{2\mu}{e^{2\mu\pi R} - 1}} \mathcal{C}(x) e^{\mu R|y|} \tag{3.34}$$

is the canonically normalized mode. This will generate contact terms of the form:

$$\mathcal{L}_c = \int d^4\theta \frac{\mu}{M_5^3} Q^\dagger Q \mathcal{C}^\dagger \mathcal{C} e^{-2\mu\pi r_0} \tag{3.35}$$

and this gives a contribution to the masses of the MSSM scalars:

$$\Delta m_{\tilde{q}}^2 = \frac{\mu |F_C|^2}{M_5^3} e^{-2\mu\pi r_0} \sim \frac{\mu M_{SUSY}^4}{M_5^3} \left(\frac{J}{J'} \right)^{-2\mu/m} \tag{3.36}$$

So these contact interactions will be exponentially suppressed at tree level. One could have guessed that this would be the case, since the wavefunction of the zero mode of the even field is an exponentially increasing function of y. Thus the bulk scalar likes to spend all of its time far away from the visible brane at $y = 0$.

However, we generally expect that radiative corrections might spoil this result and must be checked in models that incorporate this shining mechanism.

Now consider putting a gauge field in the bulk (for simplicity, let it be a $U(1)$ gauge field, but it does not have to be). This would give an extra contribution to the action:

$$\Delta\mathcal{L}_4 = \int d^2\theta \frac{T}{4g_5^2}\mathcal{W}_\alpha\mathcal{W}^\alpha + \text{h.c.} \tag{3.37}$$

This term generates a contribution to the gaugino mass through radion mediation [14]:

$$\Delta m_{1/2}^{(RMSB)} = \frac{\langle F_T\rangle}{2r_0} \sim m_{3/2} \tag{3.38}$$

Anomaly mediation also gives a contribution to the gaugino masses. This formula is complicated somewhat by the fact that the Polonyi model has a Planck-scale vev [53], but the important point is that $\Delta m_{1/2}^{(AMSB)} \ll \Delta m_{1/2}^{(RMSB)}$ due to a loop factor. So radion mediation is the dominant contribution to $m_{1/2}$ coming from supergravity.

We can also have contact interactions between the gauge field and the shining field:

$$\Delta\mathcal{L} = \int_0^\pi dy\,[\delta(y) + \delta(y-\pi)] \int d^2\theta \frac{\Psi^c\mathcal{W}_\alpha\mathcal{W}^\alpha}{M_5^{3/2}} \tag{3.39}$$

We must have the delta functions because $\mathcal{N} = 2$ SUSY forbids such contact interactions in the bulk. This will introduce a new contribution to the gaugino mass. The $y = \pi$ contribution is roughly:

$$\Delta m_{1/2}^{(C)} = \frac{|F^C|}{M_5} \sim \frac{M_{SUSY}^2}{M_5} \tag{3.40}$$

Thus this contact term gives a contribution to the gaugino mass $\Delta m_{1/2}^{(C)} \sim 10^7$ GeV, which is comparable to $\Delta m_{1/2}^{(RMSB)}$ at tree level.

We can suppress this contribution to the gaugino mass by making use of the $U(1)_R$ symmetry mentioned below Equation (3.2). From Equation (3.37) we see

that $R(\mathcal{W}_\alpha) = +1$ so that the contact term in Equation (3.39) breaks the R symmetry by 2 units. Thus it can only be generated on the $y = 0$ brane where the α term has already broken the R-symmetry. Thus the generated contact term in Equation (3.39) only has the delta function at $y = 0$. Plugging in Equation (3.34) for Ψ^c and integrating over y will now generate an exponentially suppressed contribution to the mass in analogy with Equation (3.36):

$$m_{1/2}^{(C)} \sim \frac{M_{SUSY}^2}{M_5} \left(\frac{J}{J'}\right)^{-\mu/m} \ll \Delta m_{1/2}^{(RMSB)}$$

So we find that it is possible for the RMSB contribution to dominate the gaugino mass.

3.3 Discussion

This paper has extended the shining mechanism of supersymmetry breaking to the geometry of flat orbifolds. This is a very nice way to break supersymmetry via a hidden sector in extra dimensions. It avoids the need for extra superfields living on the boundary branes as in [41]. It can easily be extended to other interesting situations such as matter or gauge fields in the bulk, where radion mediation can play an important role.

This paper has also clarified some of the issues raised in [43]. In particular, contrary to their claim, it *is* possible to fit their model to the flat case and there is nothing special about the warped geometry. We have also clarified the role of the zero modes in the low energy theory.

In addition we have shown how supergravity plays the usual role of radiative corrections in stabilizing the flat scalars. This is because our model is actually a Polonyi model in disguise, which is a free field theory in the limit $M_5 \to \infty$.

This model of supersymmetry breaking only introduces exponentially suppressed contact terms at tree level when the MSSM is put on the brane at $y = 0$. So it might be possible to generate realistic soft masses for the squarks and sleptons. In addition, radion mediated SUSY breaking might play an important part if the bulk contact terms can be suppressed. Here, this was accomplished by imposing

an R-symmetry that originally appeared as an accidental symmetry in the bulk and is broken on the brane at $y = 0$.

The classic example of a model with radion mediation as the dominant mechanism of SUSY breaking is the "no-scale model" [54], where $F_\varphi \equiv 0$ [45]. This model is known to be unstable after radiative corrections are included. Recently, it has been improved by including a general stabilization mechanism and a constraint was derived to keep the model "almost no-scale" [16]:

$$\langle K_{T^\dagger T} \rangle \ll \frac{M_5^3}{2\pi r_0}$$

where K is a radius-stabilizing Kahler potential. This constraint corresponds to making sure that F_φ remains small relative to F_T/r_0. The model considered here violates this constraint: both sides of the innequality are the same order of magnitude. This is because our model has $F_\varphi \sim F_T/r_0$. Anomaly mediation is then suppressed by a loop factor, not a small F_φ. This is what leads to dominant radion mediation.

Finally, notice that this model, although in flat space, has a Kahler potential that depends on the exponential of the radion. This is reminiscent of warped space, and there might be a corresponding reinterpretation of the effective four-dimensional theory. This could lead to interesting consequences for AdS/CFT, warped supergravity, etc, and is left for future research.

Chapter 4

Probing the Randall-Sundrum Geometric Origin of Flavor with Lepton Flavor Violation

4.1 Introduction

The Standard Model (SM) of particle physics is a remarkably successful description of nature[1]. However, it contains several unsatisfactory features. In particular, there are many hierarchies built into the model that have no *à priori* explanation. The most famous of these is the huge separation between the electroweak and Planck scales. There have been many proposed solutions to this problem. One possibility is the Randall-Sundrum scenario (RS) [12]. In this model, our four-dimensional space-time is embedded into a five-dimensional anti de-Sitter space. The extra "warped" fifth dimension is compactified on an orbifold. This space-time is described by the metric

$$ds^2 = e^{-2kr_c\phi}\eta_{\mu\nu}dx^\mu dx^\nu - r_c^2 d\phi^2, \tag{4.1}$$

where $-\pi \leq \phi \leq \pi$. Three-branes are placed at the orbifold fixed points $\phi = 0$ and $\phi = \pi$ (and its reflection at $\phi = -\pi$). The brane at $\phi = 0$ is called the

[1]This work was originally published in [3].

Planck or ultraviolet (UV) brane, while the brane at $\phi = \pi$ is called the TeV or infrared (IR) brane. For sizes of the fifth dimension $kr_c \sim 11 - 12$, the TeV scale is obtained from the fundamental Planck scale via an exponential warping induced by the anti de-Sitter geometry: $M_{\rm TeV} = M_{\rm pl} e^{-k\pi r_c}$. It was shown that this setup can be naturally stabilized [59]. The original model placed all SM fields on the IR brane.

This scenario does not explain all unnatural parameters in the SM. The fermion Yukawa couplings, except for the top quark coupling, are small and hierarchical. The minimal RS model offers no solution to this flavor hierarchy problem. In addition, the flavor sector in the RS model is sensitive to ultraviolet physics, and requires a cut-off of roughly 10^3 TeV to avoid dangerous flavor-changing neutral currents. This is problematic, as the only cut-off available is the electroweak scale.

One solution to this problem is to permit some or all of the SM fields to propagate in the full $5D$ space [60, 61, 62]. The only requirement for solving the gauge hierarchy problem is to have the Higgs field localized near the IR brane. This immediately presents a solution to the flavor hierarchy problem [61, 62], since the Yukawa couplings of the Higgs field to the fermions become dependent on the position of the fermion fields relative to the IR brane. By placing fermions at different positions in the $5D$ bulk, a hierarchy in the effective $4D$ Yukawa couplings can be generated even with anarchic $\mathcal{O}(1)$ $5D$ couplings. These "anarchic" RS models set all diagonal and off-diagonal Yukawa couplings to $\mathcal{O}(1)$. In addition, allowing fermions to propagate in the bulk suppresses the operators leading to dangerous flavor changing neutral currents [62, 63]. Some collider [64] and flavor physics [65, 66, 67, 68, 69] phenomenology of these models has been considered previously.

Additional work is needed to make this scenario fully realistic. It was shown that the simplest formulation leads to large violations of the custodial symmetry in the SM [70]. There are two known solutions to this problem. The first extends the bulk gauge symmetry to $SU(2)_L \times SU(2)_R$; when broken by boundary conditions, a bulk custodial $SU(2)$ symmetry is preserved [71]. The second model introduces large brane kinetic terms to suppress precision electroweak constraints [72]. Both

solutions allow for the masses of the first Kaluza-Klein (KK) excitations to be as low as 3 TeV, generating interesting phenomenology which may be observable at the upcoming Large Hadron Collider (LHC).

In this paper we probe the anarchic RS scenario by examining its effects on lepton flavor-violating observables. We study here a minimalistic model; we assume the SM gauge group, KK masses of a few TeV or larger, and an anarchic $5D$ Yukawa structure. We allow the Higgs boson to propagate in the full $5D$ space, which encompasses features found in several recent models [73, 74]. Specific theories such as those mentioned above with a left-right symmetric bulk or large brane kinetic terms will predict slightly different effects than we find here, but we believe that our analysis captures the most important effects. We note that the flavor violation we study here is completely independent of neutrino physics parameters. We subject the anarchic RS picture to a complete set of experimental constraints: the rare μ decays $\mu \to e\gamma$ and $\mu^{\pm} \to e^{+}e^{-}e^{\pm}$, the rare τ decays $\tau \to \{e, \mu\}\gamma$ and tri-lepton decay modes, and $\mu - e$ conversion in the presence of nuclei. We find constraints on the KK scale of a few TeV throughout parameter space. Interestingly, there is a "tension" between dipole operator decays such as $l \to l^{'}\gamma$ and the remaining processes. They have different dependences on the $5D$ Yukawa parameters, leading to strong constraints throughout parameter space. We also find that when the Higgs field is localized on the TeV brane, the dipole decays $l \to l^{'}\gamma$ are UV sensitive and uncalculable in the RS theory. This does not occur when the Higgs boson can propagate in the full $5D$ space-time. We emphasize the important role played by several future experiments: MEG [75], which will improve the constraints on $\mu \to e\gamma$ by two orders of magnitude; PRIME [76], which will strengthen the bounds on $\mu - e$ conversion by several orders of magnitude; super-B factories, which will improve the bounds on rare τ decays by an order of magnitude. Measurements from these three experiments will definitively test the anarchic RS picture.

We briefly compare our work to previous papers on lepton flavor violation in the RS framework. Reference [77] studied lepton flavor violation in a scenario where only a right-handed neutrino propagates in the full $5D$ spacetime. The studies in [65, 69] allowed all SM fermions and gauge bosons to propagate in the bulk.

Reference [65] did not incorporate custodial isospin, and therefore considered KK masses of 10 TeV, while the paper [69] considered a model with structure in the $5D$ masses and Yukawa couplings. None of these studies considered a bulk Higgs field. They also did not address the UV sensitivity of dipole decays in the brane Higgs field scenario, nor did they discuss the tension between tree-level and loop-induced processes. We also present a more detailed study of future experimental prospects than previous analyses.

This paper is organized as follows. In Section 2 we present our notation and describe the model. We discuss in Section 3 the $\mu - e$ conversion and tri-lepton decay processes, which are mediated by tree-level gauge boson mixing. We discuss the loop-induced decays $l \to l^{'}\gamma$ in Section 4. In Section 5 we present our Monte Carlo scan over the anarchic RS parameter space. We summarize and conclude in Section 6.

4.2 Notation and Conventions

In this section we present our notation and describe the model we consider. The basic action is

$$S = \int d^4x d\phi \sqrt{G}[\mathcal{L}_{\text{gauge}} + \mathcal{L}_{\text{fermion}} + \mathcal{L}_{\text{Higgs}}]. \tag{4.2}$$

The Lagrangian for gauge fields in the bulk, $\mathcal{L}_{\text{gauge}}$, has been studied in [60]. $\mathcal{L}_{\text{fermion}}$ was presented in [61, 62, 64] using an IR brane Higgs boson; we will review the relevant formulae and discuss the transition to a bulk Higgs below. Our setup of the bulk Higgs field will follow the discussion in [74].

4.2.1 Brane Higgs field

We begin by considering the case of the Higgs field localized on the IR brane. The Lagrangian in this case is

$$\mathcal{L}_{\text{Higgs}} = \left[D_\mu H (D^\mu H)^\dagger - V(H) - \mathcal{L}_{\text{Yukawa}}\right] \Big[\delta(\phi - \pi) + \delta(\phi + \pi)\Big], \tag{4.3}$$

where D_μ is the covariant derivative. $\mathcal{L}_{\text{Yukawa}}$ describes the Yukawa interactions with the fermions. The Lagrangian for bulk fermions was derived in [61, 62, 64]; it takes the form

$$\mathcal{L}_{\text{fermion}} = i\bar{\Psi}E_A^M\Gamma^A D_M\Psi - \text{sgn}(\phi)kc_\Psi\bar{\Psi}\Psi. \tag{4.4}$$

where E_A^M is the inverse vielbein. This Lagrangian admits zero-mode solutions. The c_Ψ parameters indicate where in the fifth dimension the zero-mode fermions are localized: either near the TeV brane ($c < 1/2$) or near the Planck brane ($c > 1/2$). The $4D$ Yukawa couplings of these fermions are exponentially sensitive to the c_Ψ parameters. We perform the KK decomposition of the fermion field by splitting it into chiral components, $\Psi = \Psi_L + \Psi_R$, yielding

$$\Psi_{L,R}(x,\phi) = \sum_n \frac{e^{2kr_c|\phi|}}{\sqrt{r_c}}\psi_{L,R}^{(n)}(x)f_{L,R}^{(n)}(\phi;c). \tag{4.5}$$

The c dependence becomes part of the KK wavefunction $f_{L,R}^{(n)}(\phi;c)$; explicit formulas for these wavefunctions can be found in [61, 62, 64].

The SM contains two types of fermions, corresponding to singlets (S) and doublets (D) under $SU(2)_L$. In the SM, we require that the S fermions are right-handed while the D fermions are left-handed. However, in five dimensions we must have both chiralities. To get a chiral zero-mode sector we use the orbifold parity of RS models. In particular, we choose (S_R, D_L) to be even under the orbifold parity (Neuman boundary conditions) and (S_L, D_R) to be odd (Dirichlet boundary conditions). The odd fields will not have zero modes, and the even zero modes will correspond to the SM fermions. We now group these fermions and their first KK modes into the vectors

$$\begin{aligned} \Psi_L^I &= (D_L^{i(0)}, D_L^{i(1)}, S_L^{i(1)}), \\ \Psi_R^I &= (S_R^{i(0)}, S_R^{i(1)}, D_R^{i(1)}), \end{aligned} \tag{4.6}$$

where i is a flavor index ($i = e, \mu, \tau$) and $I = 1...9$. We will show in a later section that higher KK modes have a negligible effect on our results.

The fundamental $5D$ Yukawa interaction is

$$\mathcal{L}_{\text{Yukawa}} = \frac{\lambda_{5D}^{ij}}{k}\bar{D}_L^i H S_R^j. \tag{4.7}$$

Using the vectors in Eq. 4.6 and substituting in the KK expansion of Eq. 4.5 yields

$$\mathcal{L}_{\text{Yukawa}} = \frac{\Lambda_{IJ}}{k}\bar{\Psi}_L^I H \Psi_R^J + \text{h.c.}, \tag{4.8}$$

where

$$\Lambda = \begin{pmatrix} \lambda_{4D} & \lambda_{4D}F_R & 0 \\ F_L\lambda_{4D} & F_L\lambda_{4D}F_R & 0 \\ 0 & 0 & 0 \end{pmatrix}. \tag{4.9}$$

Each internal block is a 3×3 matrix, with

$$F_{L,R} \equiv \begin{pmatrix} f^{(1)}_{e_{L,R}}/f^{(0)}_{e_{L,R}} & 0 & 0 \\ 0 & f^{(1)}_{\mu_{L,R}}/f^{(0)}_{\mu_{L,R}} & 0 \\ 0 & 0 & f^{(1)}_{\tau_{L,R}}/f^{(0)}_{\tau_{L,R}} \end{pmatrix} \tag{4.10}$$

These should be evaluated on the TeV brane, since that is where the Higgs is localized. We find

$$\lambda^{ij}_{4D} = \frac{\epsilon}{kr_c} f^{(0)}_i f^{(0)}_j \lambda^{ij}_{5D} = \sqrt{\frac{(1-2c_i)(1-2c_j)}{(\epsilon^{1-2c_i}-1)(\epsilon^{1-2c_j}-1)}}\epsilon^{1-(c_i+c_j)} \times \lambda^{ij}_{5D}, \tag{4.11}$$

where $\epsilon = e^{\pi k r_c}$ and there is no sum over i, j. It is straightforward to write down the mass matrix for the fermions:

$$\mathcal{M} = \begin{pmatrix} M_0 & M_0F_R & 0 \\ F_LM_0 & F_LM_0F_R & M_{KK} \\ 0 & M_{KK} & 0 \end{pmatrix}, \tag{4.12}$$

where $M_0^{ij} = \frac{v}{\sqrt{2}}\lambda^{ij}_{4D}$ is the zero mode mass matrix. M_{KK} is a diagonal matrix that contains the KK masses. M_0 is not diagonal. We can diagonalize this zero mode mass matrix in the usual way, by constructing a biunitary transformation (U_L, U_R) so that $M_D = U_L M_0 U_R^\dagger$ is diagonal. We can embed this rotation into the full matrix above by multiplying on the left by $\text{diag}(U_L, 1, 1)$ and on the right by $\text{diag}(U_R^\dagger, 1, 1)$. This gives

$$\mathcal{M} = \begin{pmatrix} M_D & \frac{v}{\sqrt{2}}\Delta_R & 0 \\ \frac{v}{\sqrt{2}}\Delta_L & \Delta_1 & M_{KK} \\ 0 & M_{KK} & 0 \end{pmatrix}. \tag{4.13}$$

We have set $\frac{v}{\sqrt{2}}\Delta_R = U_L M_0 F_R = M_D U_R F_R$ and $\frac{v}{\sqrt{2}}\Delta_L = F_L M_0 U_R^\dagger = F_L U_L^\dagger M_D$. A factor of $\frac{v}{\sqrt{2}}$ was extracted to make it easier to match to the Yukawa matrix. Notice that the middle entry can also be written in terms of the diagonal zero-mode matrix: $\Delta_1 = F_L M_0 F_R = F_L U_L^\dagger M_D U_R F_R$. From now on, we will use this expression. To find the Yukawa matrix Λ in this basis, we just divide Eq. 4.13 by $\frac{v}{\sqrt{2}}$ and set $M_{KK} = 0$. We note that this implies we are considering the exchange of a complex Higgs boson, which is equivalent to the exchange of the physical Higgs boson and the longitudinal component of the Z. The diagonalization of this mass matrix is discussed in the Appendix.

4.2.2 Bulk Higgs field

We now discuss the changes that occur when we allow the Higgs to propagate in the full $5D$ space. A new coupling of the Higgs boson to the fermion KK states exists: $H\bar{S}_L^{(1)} D_R^{(1)}$+h.c. This is not present in the brane Higgs case because the S_L and D_R wavefunctions vanish identically on the TeV brane due to the Dirichlet boundary conditions. The fermion mass matrix becomes

$$\mathcal{M} = \begin{pmatrix} M_D & \frac{v}{\sqrt{2}}\Delta_R & 0 \\ \frac{v}{\sqrt{2}}\Delta_L & \Delta_1 & M_{KK} \\ 0 & M_{KK} & \Delta_2 \end{pmatrix}. \tag{4.14}$$

$\Delta_{L,R,1}$ are not the same as in the brane case; they now include overlap integrals of the KK and zero-mode fermion wavefunctions with the Higgs wavefunction. Δ_2 represents the wavefunction overlaps between the first KK modes of the right-handed doublet and left-handed singlet leptons; the explicit expressions as well as the details of diagonalizing $\mathcal{M}$ can be found in the Appendix. We note that all of the Δ are proportional to the $4D$ Yukawa couplings.

Our discussion of the bulk Higgs field will follow the presentation in [74]. The $5D$ profile for the Higgs vev is

$$\chi_H(\phi) = N_H e^{2\sigma} J_\nu\left(i x_T e^{k r_c(\phi-\pi)}\right). \tag{4.15}$$

Here, x_T is the solution of a root equation giving the tachyonic mass, N_H is a normalization factor, $\sigma = k r_c \phi$, and ν is the index of the solution. We will simplify

this further for our discussion by using the asymptotic expansion of the Bessel function for large index, $J_\nu(z) \sim z^\nu$. Using this expansion gives the following normalized profile:

$$\chi_H(\phi) = \sqrt{\frac{kr_c(1+\nu)}{e^{2(1+\nu)kr\pi}-1}} e^{(2+\nu)\sigma}. \tag{4.16}$$

This satisfies the constraint

$$1 = 2\int_0^\pi d\phi e^{-2\sigma}\chi_H^2(\phi), \tag{4.17}$$

where the factor of 2 comes from the $[-\pi, 0]$ integration. In our analysis we will vary the index ν, without worrying about its dependence on the model parameters in [74]. This also makes a connection with the A_5 composite Higgs models in [73], which is approximately realized in this framework as $\nu = 0$. We can also make a direct comparison to the TeV brane Higgs scenario, which is realized by $\nu \to \infty$.

We will now study the effect of the bulk Higgs field on the gauge boson sector. We begin with the action

$$S_{gauge} = \int d^5x\sqrt{-G}\, G^{MN}\, (D_M H)^\dagger\, D_N H. \tag{4.18}$$

Performing a standard KK decomposition, and expanding $H = v\chi_H/\sqrt{2r_c}$, we arrive at the mass matrix

$$\frac{m_0^2}{2}\sum_{m,n=0} a_{mn} A_\mu^{(m)} A^{\mu(n)}, \tag{4.19}$$

with

$$a_{mn} = 4\pi\int_0^\pi d\phi\, e^{-2\sigma}\chi_H^2\chi^{(m)}\chi^{(n)}. \tag{4.20}$$

The $\chi^{(n)}$ are the usual gauge wave-functions, which can be found in [60]. We note that $\chi^{(0)} = 1/\sqrt{2\pi}$. We show in Fig. 4.1 the elements $f_i = a_{0i}$ of this mixing matrix. The expectation is that as $\nu \to \infty$, these should approach the brane Higgs values of $(-1)^{i+1}\sqrt{2\pi kr_c} \approx \pm 8.42$, assuming the value $kr_c = 11.27$; this is indeed what occurs.

We must now study the fermion sector, particularly what form the $4D$ Yukawa couplings take in terms of the $5D$ values. We begin with the action

$$S_{ffH} = \frac{\lambda_{5D}\sqrt{1+\nu}}{\sqrt{k}}\int d^5x\,\sqrt{-G} H^\dagger \psi_D \psi_S^c. \tag{4.21}$$

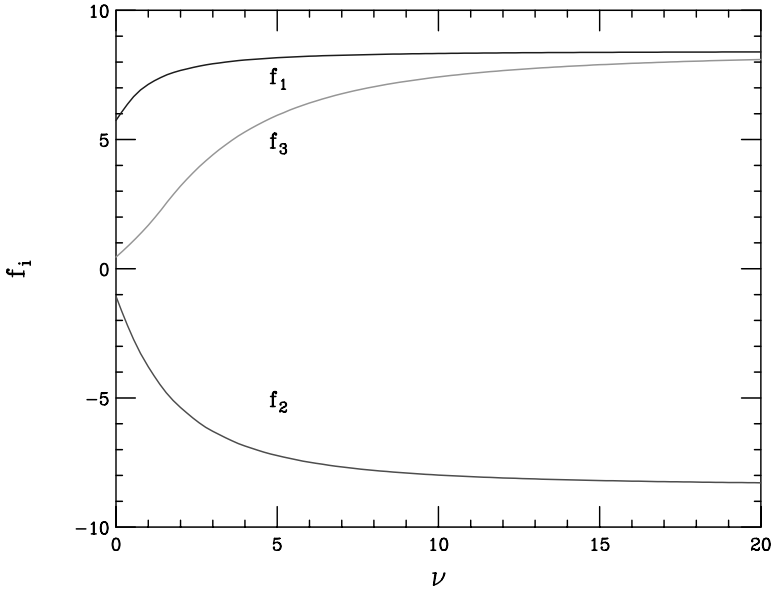

Figure 4.1: f_i, the off-diagonal elements of the gauge boson mass matrix that describe the mixing of the zero-mode with the i-th KK-mode.

where the ν-dependent prefactor is included to reproduce the correct $4D$ Yukawa coupling as $\nu \to \infty$. The zero-mode fermion wave-function is $e^{2\sigma} f^{(0)}/\sqrt{r_c}$, where

$$f^{(0)} = \sqrt{\frac{kr_c(1-2c)}{2\left(e^{(1-2c)kr_c\pi}-1\right)}} e^{-c\sigma}. \tag{4.22}$$

Inserting this into the action, and expanding H as before, we find the following expression for the 4D Yukawa:

$$\begin{aligned} \lambda_{4D} &= \frac{\lambda_{5D}\,(1-2c)}{e^{(1-2c)kr_c\pi}-1}\left[\sqrt{kr_c(1+\nu)}\int_0^\pi d\phi\,\chi_H e^{-2c\sigma}\right] \\ &= \frac{\lambda_{5D}\,(1-2c)}{e^{(1-2c)kr_c\pi}-1}\left[\frac{1+\nu}{\sqrt{e^{2(1+\nu)kr_c\pi}-1}}\,\frac{e^{(2+\nu-2c)kr_c\pi}-1}{2+\nu-2c}\right]. \end{aligned} \tag{4.23}$$

For simplicity, we have only presented the diagonal Yukawa coupling. To reproduce the brane Higgs diagonal Yukawa coupling in Eq. 4.11, the bracketed integral should reduce to $e^{(1-2c)kr_c\pi}$ as $\nu \to \infty$. It is simple to check that this occurs.

4.2.3 The anarchic RS parameters

We discuss here the parameters of the anarchic RS model and give their natural values. We first note that Eq. 4.11 relates the diagonal $5D$ Yukawa couplings to

the fermion c parameters through the measured fermion masses. The off-diagonal entries are removed after diagonalization with $U_{L,R}$. The preferred size of the Yukawa couplings can be determined by demanding consistency with $Z \to b\bar{b}$ measurements and by the size of the top quark mass; this yields $\lambda_{5D} \approx 2$ [71]. We assume three couplings (Y_e, Y_μ, Y_τ) of this approximate magnitude. The size of these couplings implies $c > 1/2$ for all three leptons, indicating that they are localized near the Planck brane. For simplicity, we take $c_L = c_R$. We note that this range of c is the appropriate one for first and second generation quarks also; for the third generation, $c_{b_L} = c_{t_L} \sim 0.45$, while $c_{b_R} \sim 0.5$ and $c_{t_R} \sim 0$ [71].

We can also estimate the natural sizes of the $U_{L,R}$ matrix elements. For illustration, we consider here a two-family scenario; it is straightforward to extend this example to three families. Assuming an anarchic RS scenario, so that all of the $\lambda_{5D}^{ij} \sim \mathcal{O}(1)$, we can use Eq. 4.11 to write the $4D$ Yukawa matrix as

$$\lambda_{5D} = \begin{pmatrix} Y_{11} & Y_{12} \\ Y_{12} & Y_{22} \end{pmatrix} \Rightarrow \lambda_{4D} \sim \begin{pmatrix} Y_{11} f_e^{(0)2} & Y_{12} f_e^{(0)} f_\mu^{(0)} \\ Y_{12} f_e^{(0)} f_\mu^{(0)} & Y_{22} f_\mu^{(0)2} \end{pmatrix}, \tag{4.24}$$

where we have assumed for simplicity a symmetric $5D$ Yukawa matrix. Assuming $\mathcal{O}(1)$ Yukawa couplings, the functional dependences of the fermion masses on the wave-functions are

$$m_e \sim f_e^{(0)2}, \;\; m_\mu \sim f_\mu^{(0)2}, \tag{4.25}$$

while the mixing matrices take the form

$$U \sim \begin{pmatrix} 1 & -\sqrt{\frac{m_e}{m_\mu}} \\ \sqrt{\frac{m_e}{m_\mu}} & 1 \end{pmatrix}. \tag{4.26}$$

We therefore find that $|U_{12}| \sim \sqrt{\frac{m_e}{m_\mu}}$. Including the τ then gives $|U_{13}| \sim \sqrt{\frac{m_e}{m_\tau}}$ and $|U_{23}| \sim \sqrt{\frac{m_\mu}{m_\tau}}$. The diagonal entries $|U_{ii}| \sim 1$. We will assume mixing matrix elements of these approximate magnitudes in our analysis.

4.2.4 Operator Matching

We discuss in this subsection the formalism we will use to compare the RS predictions to the experimental measurements. Our presentation closely follows

the discussion in [78]. Tri-lepton decays of the form $l \to l_1 \bar{l}_2 l_3$ and $\mu - e$ conversion are mediated by tree-level mixing with heavy gauge bosons and generate four-fermion interactions, while $l \to l^{'}\gamma$ occurs via a loop-induced dipole operator. We can parameterize these effects in the following effective Lagrangian:

$$\begin{aligned} -\mathcal{L}_{\text{eff}} &= C_R(q^2)\frac{1}{2m_\mu}\bar{e}_R\sigma^{\mu\nu}F_{\mu\nu}\mu_L + C_L(q^2)\frac{1}{2m_\mu}\bar{e}_L\sigma^{\mu\nu}F_{\mu\nu}\mu_R \\ &+\frac{4G_F}{\sqrt{2}}\left[g_3(\bar{e}_R\gamma^\mu\mu_R)(\bar{e}_R\gamma_\mu e_R) + g_4(\bar{e}_L\gamma^\mu\mu_L)(\bar{e}_L\gamma_\mu e_L)\right. \\ &\left. + g_5(\bar{e}_R\gamma^\mu\mu_R)(\bar{e}_L\gamma_\mu e_L) + g_6(\bar{e}_L\gamma^\mu\mu_L)(\bar{e}_R\gamma_\mu e_R)\right] + \text{h.c.} \end{aligned} \tag{4.27}$$

The form factors[2] $C_{L,R}(q^2)$ and the couplings g_i are then computed in a straightforward matching procedure. We will discuss this computation in detail in the following two sections.

4.3 Tri-lepton decays and $\mu - e$ conversion

In this section and the next we study the predictions that the minimal RS model makes for lepton flavor violation. We focus on processes in the muon sector, such as $\mu^- \to e^+e^-e^-$ and $\mu - e$ conversion in the presence of nuclei, and rare tau decays of the form $\tau \to l_1\bar{l}_2 l_3$ currently being studied at BABAR and BELLE. The dipole-mediated decays will be discussed in the next section.

The dominant effects arise from flavor non-diagonal couplings of the zero-mode Z-boson. Contributions from exchange of the Higgs boson are suppressed by small fermion masses, and we will show later that those coming from direct KK exchange are suppressed by a large fermion wave-function factor. There are also contributions to these processes from the dipole exchanges denoted by $C_{L,R}$ in Eq. 4.27, but these are loop-suppressed and small in the parameter space of interest. We also find that KK-fermion mixing effects are sub-dominant in the parameter space of interest. We derive here the relevant couplings. We denote the physical basis by Z_0, Z_1, and the gauge basis by $Z^{(0)}, Z^{(1)}$. For simplicity, we restrict our discussion here to the first KK level; in our analysis we include the first several modes. After

[2]Note that these form factors are normalized differently than the $A_{L,R}$ in [78]: $C = -\frac{8G_F m_\mu^2}{\sqrt{2}}A$.

diagonalizing the gauge boson mass matrix, we find that these are related via

$$Z^{(0)} = Z_0 + f\frac{m_Z^2}{M_{KK}^2}Z_1, \quad Z^{(1)} = Z_1 - f\frac{m_Z^2}{M_{KK}^2}Z_0. \tag{4.28}$$

f parameterizes the mixing between the zero and first KK level. With a brane Higgs field, $f = \sqrt{2k\pi r_c} \sim \mathcal{O}(10)$. A plot of f for a bulk Higgs field is shown in Fig. 4.1. The couplings between the zero-mode fermions and $Z^{(1)}$ are determined by the appropriate overlap integral. We define the ratio of these couplings to the SM couplings as α_e, α_μ, and α_τ, where $g^{(1)} = \alpha g^{SM}$; the α_i are then given by

$$\alpha_i = 2\sqrt{2\pi}\int_0^\pi d\phi\, e^\sigma \chi^{(1)}[f_i^{(0)}]^2. \tag{4.29}$$

Since the fermion wave-functions are localized at different points in the bulk, the α_i differ, but they are all roughly $\mathcal{O}(0.1)$ in magnitude. We present a plot of the α_i in Fig. 4.3. In the fermion flavor basis, the matrix which describes the $Z^{(1)}$ couplings takes the form

$$g^{SM}\,(\bar{e}_F, \bar{\mu}_F, \bar{\tau}_F)\;\not{Z}^{(1)} \begin{pmatrix} \alpha_e & 0 & 0 \\ 0 & \alpha_\mu & 0 \\ 0 & 0 & \alpha_\tau \end{pmatrix} \begin{pmatrix} e_F \\ \mu_F \\ \tau_F \end{pmatrix}. \tag{4.30}$$

We must first rotate the fermions to the mass basis. As was explained in the last section, we introduce unitary matrices U_L, U_R, so that $L_M = U_L L_F$, $R_M = U_R R_F$, where L_F denotes the left-handed flavor basis-vector, L_M the left-handed mass basis-vector, etc. The flavor-basis coupling matrices $C_{L,R}^F = g_{L,R}\,\mathrm{diag}(\alpha_e, \alpha_\mu, \alpha_\tau)$ are rotated to $C_{L,R} = U_{L,R}\, C_{L,R}^F\, U_{L,R}^\dagger$. The flavor-violating couplings are the off-diagonal entries of $C_{L,R}$; we find

$$\begin{aligned} g_{L,R}^{(1)\mu e} &= g_{L,R}\left(U_{11}^{L,R}U_{21}^{L,R*}\alpha_e + U_{12}^{L,R}U_{22}^{L,R*}\alpha_\mu + U_{13}^{L,R}U_{23}^{L,R*}\alpha_\tau\right), \\ g_{L,R}^{(1)\tau\mu} &= g_{L,R}\left(U_{21}^{L,R}U_{31}^{L,R*}\alpha_e + U_{22}^{L,R}U_{32}^{L,R*}\alpha_\mu + U_{23}^{L,R}U_{33}^{L,R*}\alpha_\tau\right), \\ g_{L,R}^{(1)\tau e} &= g_{L,R}\left(U_{11}^{L,R}U_{31}^{L,R*}\alpha_e + U_{12}^{L,R}U_{32}^{L,R*}\alpha_\mu + U_{13}^{L,R}U_{33}^{L,R*}\alpha_\tau\right), \end{aligned} \tag{4.31}$$

where $g_{L,R}$ are the usual SM couplings. We can use the unitarity of $U_{L,R}$ to rewrite

these as

$$\begin{aligned} g_{L,R}^{(1)\mu e} &= g_{L,R}\left[U_{12}^{L,R}U_{22}^{L,R*}(\alpha_\mu-\alpha_e)+U_{13}^{L,R}U_{23}^{L,R*}(\alpha_\tau-\alpha_e)\right], \\ g_{L,R}^{(1)\tau\mu} &= g_{L,R}\left[U_{21}^{L,R}U_{31}^{L,R*}(\alpha_e-\alpha_\mu)+U_{23}^{L,R}U_{33}^{L,R*}(\alpha_\tau-\alpha_\mu)\right], \\ g_{L,R}^{(1)\tau e} &= g_{L,R}\left[U_{12}^{L,R}U_{32}^{L,R*}(\alpha_\mu-\alpha_e)+U_{13}^{L,R}U_{33}^{L,R*}(\alpha_\tau-\alpha_e)\right]. \end{aligned} \tag{4.32}$$

Using Eq. 4.28, the couplings to Z_0 are obtained via multiplication by $-fm_Z^2/M_{KK}^2$: $g_{L,R}^{\mu e} = -fm_Z^2/M_{KK}^2 g_{L,R}^{(1)\mu e}$, etc. The couplings to Z_1 are identical to those in Eq. 4.32, to leading order in the gauge boson mixing.

We now use these to derive the flavor-violating couplings g_{3-6} of Eq. 4.27:

$$\begin{aligned} g_3^{\mu e} &= 2g_R\left[g_R^{\mu e}+\alpha_e g_R^{(1)\mu e}\frac{m_Z^2}{M_{KK}^2}\right], \\ g_4^{\mu e} &= 2g_L\left[g_L^{\mu e}+\alpha_e g_L^{(1)\mu e}\frac{m_Z^2}{M_{KK}^2}\right], \\ g_5^{\mu e} &= 2g_L\left[g_R^{\mu e}+\alpha_e g_R^{(1)\mu e}\frac{m_Z^2}{M_{KK}^2}\right], \\ g_6^{\mu e} &= 2g_R\left[g_L^{\mu e}+\alpha_e g_L^{(1)\mu e}\frac{m_Z^2}{M_{KK}^2}\right]. \end{aligned} \tag{4.33}$$

These are for $\mu - e$ flavor violation; similar expressions hold for $\tau - \mu$ and $\tau - e$. The first term on each line is from the Z_0 coupling, while the second is from direct Z_1 exchange. Substituting in the expressions from Eq. 4.32, we find

$$g_3^{\mu e} = -2g_R^2\frac{m_Z^2}{M_{KK}^2}(f-\alpha_e)\left[U_{12}^R U_{22}^{R*}(\alpha_\mu-\alpha_e)+U_{13}^R U_{23}^{R*}(\alpha_\tau-\alpha_e)\right], \tag{4.34}$$

and similar expressions for the other couplings. Since $f \gg |\alpha_e|$, we can neglect the direct KK exchange effect.

We will study the decays $\mu^- \to e^-e^+e^-$, $\tau^- \to \mu^-\mu^+\mu^-$, $\tau^- \to e^-e^+e^-$, $\tau \to \mu^-e^+e^-$, and $\tau \to e^-\mu^+\mu^-$. The remaining rare τ decays studied at BABAR and BELLE, $\tau \to e^-\mu^+e^-$ and $\tau \to \mu^-e^+\mu^-$, require an additional flavor-violating coupling than those above, and are therefore highly suppressed. The relevant

branching fractions from [78] are

$$\begin{aligned} BR(\mu \to 3e) &= 2\left(|g_3^{\mu e}|^2 + |g_4^{\mu e}|^2\right) + |g_5^{\mu e}|^2 + |g_6^{\mu e}|^2, \\ BR(\tau \to 3\mu) &= 2\left(|g_3^{\tau\mu}|^2 + |g_4^{\tau\mu}|^2\right) + |g_5^{\tau\mu}|^2 + |g_6^{\tau\mu}|^2, \\ BR(\tau \to 3e) &= 2\left(|g_3^{\tau e}|^2 + |g_4^{\tau e}|^2\right) + |g_5^{\tau e}|^2 + |g_6^{\tau e}|^2, \\ BR(\tau \to \mu ee) &= |g_3^{\tau\mu}|^2 + |g_4^{\tau\mu}|^2 + |g_5^{\tau\mu}|^2 + |g_6^{\tau\mu}|^2, \\ BR(\tau \to e\mu\mu) &= |g_3^{\tau e}|^2 + |g_4^{\tau e}|^2 + |g_5^{\tau e}|^2 + |g_6^{\tau e}|^2. \end{aligned} \tag{4.35}$$

The $\mu - e$ conversion rate is given by [79]

$$B_{conv} = \frac{2 p_e E_e G_F^2 m_\mu^3 \alpha^3 Z_{eff}^4 Q_N^2}{\pi^2 Z \Gamma_{capt}} \left[|g_R^{\mu e}|^2 + |g_L^{\mu e}|^2\right], \tag{4.36}$$

where G_F is the Fermi constant, α is the QED coupling strength, and the remaining terms are atomic physics constants defined in [79]. Numerical values for titanium, for which the most sensitive limits have been obtained [80], can be found in [78].

We will present a detailed scan of the anarchic RS parameter space in a later section. For now, to provide some guidance as to what scales these rare decays can probe, we perform a few simple estimates. We set the 5-D fermion Yukawas to the values suggested by 5-D Yukawa anarchy, $Y_e = Y_\mu = Y_\tau = 2$. We also use the intuition described in the previous section to set the mixing matrix entries to the values

$$U_{11}^{L,R} = 1,\ U_{12}^{L,R} = \sqrt{\frac{m_e}{m_\mu}},\ U_{13}^{L,R} = \sqrt{\frac{m_e}{m_\tau}}, \tag{4.37}$$

and similarly for the remaining rows of $U_{L,R}$; for this estimate, we set the phases of these elements to zero. We choose a value of $kr_c = 11.27$. We include the first 3 KK modes in this estimate, and we have checked that adding more does not affect our results. Employing these approximations, we check what limits can be obtained on M_{KK} from each process. We impose the following bounds: $BR(\mu \to 3e) < 10^{-12}$, which is the current PDG limit [13]; $B_{conv} < 6.1 \times 10^{-13}$, which is the strongest constraint obtained by the experiment SINDRUM II [80]. For the rare tau decays, we employ the strongest constraints from either BABAR or BELLE, which are $BR(\tau \to l_1 \bar{l}_2 l_3) < 2 \times 10^{-7}$ for each mode [81]. We present the bounds on M_{KK} for both the brane Higgs model and the bulk Higgs scenario

	Brane Higgs	$\nu = 0$
$BR(\mu \to 3e)$	2.5 TeV	2.0 TeV
B_{conv}	5.9	4.7
$BR(\tau \to 3\mu)$	0.62	0.51
$BR(\tau \to \mu ee)$	0.55	0.46
$BR(\tau \to 3e)$	0.16	0.13
$BR(\tau \to e\mu\mu)$	0.14	0.12

Table 4.1: Constraints on the first KK mode mass, M_{KK}, coming from various measurements for both a brane Higgs field and for the bulk Higgs case with $\nu = 0$. The bounds on M_{KK} are in TeV.

with $\nu = 0$ in Table 4.1. The limits from $BR(\mu \to 3e)$ and B_{conv} already probe the multi-TeV region, similar to that possible at the LHC. Although the limits from rare τ-decays are lower, they probe different model parameters which describe the third generation. These bounds will also improve as the B-factories acquire more data. We will show that these bounds are generic throughout the entire parameter space in a later section.

4.4 Dipole operator mediated decays

We now compute the decays of the form $l \to l'\gamma$, which are induced at the loop level by the diagram shown in Fig. 4.2. For simplicity, we discuss the decay $\mu \to e\gamma$. It is simple to translate our expressions into results for τ decays. The dominant contributions to these amplitudes come from exchange of a Higgs boson and KK fermions. This is because these diagrams contain terms proportional to the fourth power of the fermion wave-function ratio $f_{e,\mu} = f^{(1)}_{e,\mu}/f^{(0)}_{e,\mu}$. For $c = 1/2$, this ratio is $f_{e,\mu} = 2\pi kr_c \approx 70$; it grows rapidly for $c > 1/2$, the values relevant for the muon and the electron. This strong dependence on the fermion wave-function was first noted in [82]. There are also contributions coming from loops of KK Z bosons and KK fermions. However, as argued in reference [68] for the case of the KK gluon contribution to radiative quark decays, the flavor structure of this diagram is approximately aligned with the $4D$ Yukawa matrix and hence gives a

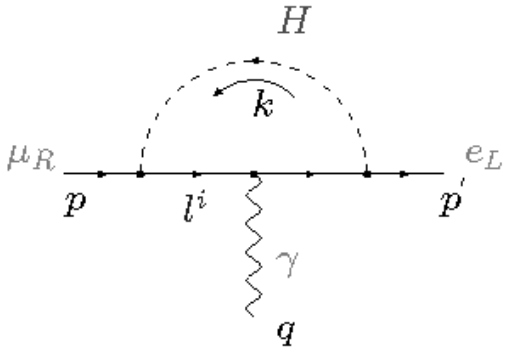

Figure 4.2: The Feynman diagram generating the dipole operator which mediates $l \to l'\gamma$ decays. l^i are the physical KK leptons. We have specialized to $\mu \to e\gamma$ in the figure. There is a similar diagram with $L \leftrightarrow R$.

suppressed contribution. The KK fermion-Higgs diagrams have a different flavor structure than the $4D$ Yukawa matrix.

The amplitude for the diagram in Fig. 4.2 is

$$\begin{aligned} A(\mu \to e\gamma) = & \\ & \textstyle\sum_i \int \frac{d^4k}{(2\pi)^4} \overline{u}(p')(i\Lambda_{e^0 i}) \frac{i(\hat{p}'+M^{(i)}_{KK})}{\hat{p}'^2 - M^{(i),2}_{KK}} (ie\gamma^\mu A_\mu) \frac{i(\hat{p}+M^{(i)}_{KK})}{\hat{p}^2 - M^{(i),2}_{KK}} (i\Lambda_{i\mu^0}) u(p) \cdot \frac{i}{k^2 - m_H^2} \\ = & \quad \overline{u}(p') \left[-eA_\mu \textstyle\sum_i \Lambda_{e^0 i} \int \frac{d^4k}{(2\pi)^4} \frac{(\hat{p}'+M^{(i)}_{KK})\gamma^\mu(\hat{p}+M^{(i)}_{KK})}{(\hat{p}'^2 - M^{(i),2}_{KK})(\hat{p}^2 - M^{(i),2}_{KK})(k^2 - m_H^2)} \Lambda_{i\mu^0} \right] u(p) \end{aligned} \tag{4.38}$$

where $\hat{p}^{(\prime)} = p^{(\prime)} + k$ and Λ_{ij} are the Yukawa matrices. We will assume the external lines are massless, which is valid up to subleading corrections in $1/f_{e,\mu}$. We have denoted the KK fermion masses by $M^{(i)}_{KK}$. At each KK level, there are two vector-like fermion pairs for each flavor with masses $M^{(1)}_{KK}$ and $M^{(2)}_{KK}$, as is clear from Eq. 4.6. The splitting of these masses through mixing will be important in evaluating this contribution. It is straightforward to evaluate this integral to find

$$A(\mu \to e\gamma; q^2) = \frac{1}{2m_\mu} \overline{u}(p') \sigma^{\mu\nu} F_{\mu\nu} u(p) \times (-i) C(q^2), \tag{4.39}$$

where

$$-iC(q^2) = \frac{iem_\mu}{16\pi^2}\sum_i \Lambda_{e^0 i} \times \left\{ \int_0^1 dz \int_0^{1-z} dy \frac{M_{KK}^{(i)}(1-z)}{q^2 y(1-y-z) - (1-z)M_{KK}^{(i),2} - zm_H^2} \right\} \Lambda_{i\mu^0} \tag{4.40}$$

We now set $q^2 = 0$ to derive

$$C(q^2 = 0) = \frac{em_\mu}{32\pi^2}\sum_i \Lambda_{e^0 i} \frac{I(m_H^2/M_{KK}^{(i),2})}{M_{KK}^{(i)}} \Lambda_{i\mu^0}, \tag{4.41}$$

where $I(x) = 1 - x + \mathcal{O}(x^2)$. The branching fraction becomes [78]

$$B(\mu \to e\gamma) = \frac{12\pi^2}{(G_F m_\mu^2)^2}\left[|C_L(0)|^2 + |C_R(0)|^2\right], \tag{4.42}$$

where we have inserted the helicity labels L, R on C. These helicity labels dictate which elements of the Yukawa matrix Λ should be used; we will make this explicit in the following discussion. We now consider separately the brane and bulk Higgs field cases. We will find that the brane Higgs prediction for $l \to l'\gamma$ is not calculable because it is sensitive to cut-off scale physics, while for the bulk Higgs case we can use our $5D$ effective field theory to make robust predictions.

4.4.1 UV sensitivity for the case of brane Higgs field

The leading contribution in Eq. 4.41, with $m_H = 0$ and $I(x) = 1$, vanishes up to factors suppressed by $1/f^2$ for a brane Higgs field because of the Yukawa matrix structure. With $m_H = 0$, we are only considering contributions proportional to $1/M_{KK}^{(1,2)}$. This mass splitting is cancelled by shifts in the Yukawa couplings to all orders in v/M_{KK}. The leading result therefore comes from $1/(M_{KK}^{(1,2)})^3$ contributions, and we must consider the m_H^2 terms to obtain these. The diagonalization of the fermion mass matrix in Eq. 4.14 is discussed in the detail in the Appendix. The result of this analysis is the following mass splitting:

$$\frac{1}{(M_{KK}^{(1)})^3} - \frac{1}{(M_{KK}^{(2)})^3} = -\frac{3\Delta_1}{M_{KK}^4}. \tag{4.43}$$

This yields the following coefficients of the dipole operator:

$$\begin{aligned} C_L(0) &= \frac{e m_\mu m_H^2}{32\pi^2 M_{KK}^4} \left[\Delta_R \Delta_1 \Delta_L\right]_{e\mu}, \\ C_R(0) &= \frac{e m_\mu m_H^2}{32\pi^2 M_{KK}^4} \left[\Delta_R \Delta_1 \Delta_L\right]^\dagger_{e\mu}. \end{aligned} \tag{4.44}$$

The Yukawa structures entering C_L and C_R differ by a hermitian conjugate.

However, it turns out that this result is masked by cut-off effects. A similar ultraviolet sensitivity of Higgs-fermion KK loops was also noted in [68]. The expected one-loop contribution from a given set of KK modes is finite with size

$$\frac{C_{L,R}^{KK}}{m_\mu^2} \sim \frac{\lambda_{5D}^2}{16\pi^2} \frac{1}{M_{KK}^2}. \tag{4.45}$$

For simplicity, we have not included the relevant mixing matrix elements in this estimate. Although the actual one-loop result for a brane Higgs field vanishes for $m_H = 0$, we cannot find a symmetry that requires this, and we expect it to be an accident of the one-loop result. The sum over two independent KK modes would have given a logarithmic divergence at one-loop:

$$\frac{C_{L,R}^{KK}}{m_\mu^2} \propto \log N_{KK} \sim \log\left(\Lambda_{5D}/k\right) \sim \log\left(\tilde{\Lambda}_{5D}/M_{KK}\right). \tag{4.46}$$

Here, N_{KK} is the total number of KK modes in the $5D$ effective theory, Λ_{5D} is the $5D$ cut-off of order 10^{19} GeV, and $\tilde{\Lambda}_{5D}$ is the warped-down $5D$ cut-off of order TeV. Similarly, M_{KK} is roughly the warped-down curvature scale k. To obtain this logarithmic divergence, it is crucial that KK fermion-Higgs couplings in the sum are independent of the KK index. We expect that higher-loop contributions are strongly power divergent because of the increasing number of sums over KK modes, and are as important as the one-loop result provided the cut-off scale physics is strongly coupled.

This divergence structure can be more easily seen using power-counting in the $5D$ theory. Since the $5D$ Yukawa coupling has mass dimension $[\lambda_{5D}/k] = [-1]$, the loop expansion for $\mu \to e\gamma$ has the form

$$\frac{C_{L,R}^{KK}}{m_\mu^2} \sim \frac{1}{16\pi^2}\left(\frac{\lambda_{5D}}{M_{KK}}\right)^2 \Big[\log\left(\frac{\Lambda_{5D}}{k}\right) + \frac{1}{16\pi^2}\frac{\lambda_{5D}^2}{k^2}\Lambda_{5D}^2 + ...\Big]. \tag{4.47}$$

In this expression, we have replaced the scale $k \sim 10^{18}$ GeV by its warped-down value M_{KK} in the overall coefficient. By simple dimensional analysis, the one-loop contribution can be log-divergent and the two-loop contribution is quadratically divergent; in KK language, the power divergence at two loops can be seen from the independent sums over 4 KK modes. The two-loop result is comparable to the one-loop prediction if the cut-off physics is strongly-coupled: $\Lambda_{5D}^2/k^2 \times \lambda_{5D}^2/\left(16\pi^2\right) \sim 1$. Therefore, the KK loop contribution is not calculable in this case.

Based on the above discussion, we also expect the higher-dimensional operators in the $5D$ theory coming from physics at the cut-off scale to be important. The relation between the warped-down $5D$ cut-off in the Yukawa sector and the KK scale for a brane Higgs field is $\tilde{\Lambda}_{5D} \sim M_{KK}/\left(4\pi/\lambda_{5D}\right)$, based on power counting of the $5D$ loop factor. To obtain the cut-off operator, we replace M_{KK} in Eq. 4.45 by the cut-off scale $\tilde{\Lambda}_{5D}$, and the loop factor by ~ 1, since the cut-off effect has no loop suppression. This shows that $\mu \to e\gamma$ is an UV sensitive observable for a Higgs field on the TeV brane. We can only parameterize the contribution as:

$$C_{L,R}^{total} = a\frac{m_\mu^2}{\tilde{\Lambda}_{5D}^2} \times U_{12}^{L,R}, \tag{4.48}$$

where a is an unknown, $O(1)$ coefficient, and we have included the appropriate mixing matrix element.

We now show that we can reliably calculate dipole induced decays for a bulk Higgs field. The Yukawa coupling in this case has mass dimension $[\lambda_{5D}/\sqrt{k}] = [-1/2]$, so the loop expansion is instead

$$\begin{aligned}\frac{C_{L,R}^{KK}}{m_\mu^2} \;\sim\; & \frac{1}{16\pi^2}\left(\frac{\lambda_{5D}}{\sqrt{M_{KK}}}\right)^2\Big[\frac{1}{M_{KK}} + \frac{1}{16\pi^2}\frac{\lambda_{5D}^2}{M_{KK}}\log\left(\frac{\Lambda_{5D}}{k}\right) \\ & + \left(\frac{1}{16\pi^2}\right)^2\frac{\lambda_{5D}^4}{M_{KK}^2}\tilde{\Lambda}_{5D} + ...\Big].\end{aligned}$$

From this $5D$ power-counting, we see that the one-loop KK contribution is finite. The two-loop result is logarithmically divergent, but is smaller than the one-loop prediction by ~ 0.1 provided $\lambda_{5D} \lesssim 4$. Three-loop and higher contributions are power-divergent and comparable to the two-loop result, but are again smaller than the one-loop effect.

Thus, in the bulk Higgs case, the KK effect is calculable. The effects from cut-off scale operators are suppressed, and we can reliably make a prediction using the RS theory. In our numerical analysis, we will include dipole decays for the bulk Higgs field case. For the brane Higgs scenario we will simply neglect them, since we cannot make a reliable prediction.

4.4.2 Contributions from a bulk Higgs field

We now consider the scenario when the Higgs boson is allowed to propagate in the bulk. In this case, the KK mode result is not overwhelmed by cut-off scale operators. The $m_H = 0$ limit does not vanish for a bulk Higgs. We make this approximation in our discussion, since the corrections are $\mathcal{O}(m_H^2/M_{KK}^2)$. We first work out the Yukawa structure appearing in Eq. 4.41. Using the results in the Appendix for the two KK fermions appearing in the diagram of Fig. 4.2, we find

$$\begin{aligned}
(\overline{e}_L^0 l_R^1)(\overline{l}_L^1 \mu_R^0) &= \left[\Delta_R \left[1 + \left(\frac{X}{4} - \frac{\Delta_2}{M_{KK}}\right)\right]\right]_{el} \left(\frac{1}{M_{KK}^{(1)}}\right) \\
&\quad \times \left[\left[1 + \left(\frac{X}{4} - \frac{\Delta_2}{M_{KK}}\right)\right] \Delta_L\right]_{l\mu} \\
(\overline{e}_L^0 l_R^2)(\overline{l}_L^2 \mu_R^0) &= \left[\Delta_R \left[1 - \left(\frac{X}{4} - \frac{\Delta_2}{M_{KK}}\right)\right]\right]_{el} \left(-\frac{1}{M_{KK}^{(2)}}\right) \\
&\quad \times \left[\left[1 - \left(\frac{X}{4} - \frac{\Delta_2}{M_{KK}}\right)\right] \Delta_L\right]_{l\mu}
\end{aligned} \tag{4.49}$$

In this expression we must sum over $l = e, \mu, \tau$. To simplify this we use the splitting between the KK fermion masses derived in the Appendix:

$$\frac{1}{M_{KK}^{(1)}} - \frac{1}{M_{KK}^{(2)}} = -\frac{\Delta_1 + \Delta_2}{M_{kk}^2} + \mathcal{O}\left(\frac{v^3}{M_{kk}^4}\right). \tag{4.50}$$

We find the following results for the dipole operator coefficients:

$$\begin{aligned}
C_L(0) &= \frac{3 e m_\mu}{32\pi^2 M_{KK}^2} \left[\Delta_R \Delta_2 \Delta_L\right]_{e\mu} \\
C_R(0) &= \frac{3 e m_\mu}{32\pi^2 M_{KK}^2} \left[\Delta_R \Delta_2 \Delta_L\right]_{e\mu}^\dagger
\end{aligned} \tag{4.51}$$

We note that in the limit of the Higgs boson being localized on the TeV brane, $\Delta_2 \to 0$; the result vanishes in this limit, as required.

An identical analysis can be performed for $\tau \to \mu\gamma$ and $\tau \to e\gamma$. We simply replace $m_\mu \to m_\tau$ and change the indices of the Yukawa structure appropriately in Eq. 4.51. We now perform an estimate of the bounds similar to that performed in the brane Higgs case. We set $Y_e = Y_\mu = Y_\tau = 2$, and set the mixing matrix elements to their canonical values as described before. We also set $\nu = 0$. We impose the following bounds on each of the three dipole decays: $BR(\mu \to e\gamma) < 1.2 \times 10^{-11}$, as obtained from [13]; $BR(\tau \to \mu\gamma) < 9 \times 10^{-8}$, the stronger of the bounds coming from BABAR and BELLE [83]; $BR(\tau \to e\gamma) < 1.1 \times 10^{-7}$, again the stronger of the bounds coming from BABAR and BELLE [84]. We find the following constraints for the canonical parameters:

$$\begin{aligned} BR(\mu \to e\gamma) &: M_{KK} > 15.8\,\text{TeV}; \\ BR(\tau \to e\gamma) &: M_{KK} > 1.4\,\text{TeV}; \\ BR(\tau \to \mu\gamma) &: M_{KK} > 2.4\,\text{TeV}. \end{aligned} \tag{4.52}$$

The constraints, particularly from $BR(\mu \to e\gamma)$, are quite strong. This arises in part from the large value of the Yukawa coupling, $Y = 2$, as we now discuss.

4.4.3 Tension between tree-level and loop-induced processes

We now discuss a tension between processes caused by tree-level gauge boson mixing such as $\mu - e$ conversion and $l \to l_1 \bar{l}_2 l_3$, and dipole operator decays. These have opposite dependences on the $5D$ Yukawa couplings, leading to strong constraints for all parameter choices. We first give a very simple scaling argument to motivate this, and then present numerical proof.

Our scaling argument uses the dependence of each process on the zero-mode fermion wave-function $f_l^{(0)}$ evaluated at the TeV brane. We will work for simplicity in the large ν limit, which mimics a brane-localized Higgs field. From Eqs. 4.22 and 4.23, we find that the wave-function scales roughly as $f_l^{(0)} \sim 1/\sqrt{\lambda_{5D}}$. The wave-function has weak c-dependent factors which we will ignore in this argument.

The quantity that governs the flavor violation in gauge boson mixing is the difference between α_l's, as is clear from Eq. 4.34. In the definition of α_l in Eq. 4.29, we can divide the overlap integral into two regions, one near the Planck brane and the other near the TeV brane, to show that the former is c-independent and that the latter carries the c-dependence and must be $\alpha_l|_{non-universal} \sim [f_l^{(0)}]|^2_{TeVbrane} \sim 1/\lambda_{5D}$. We therefore expect the non-universal part of α_l, and hence the flavor violation, to decrease for larger Yukawa couplings, which is indeed what we observe in Fig. 4.3. For the dipole mediated decays, recall that in Section 4.4 we claimed that the operator coefficients $C_{L,R}$ scaled as $C_{L,R} \sim 1/[f_l^{(0)}]^4 \sim \lambda_{5D}^2$; this can be verified using Eq. 4.51 and the results in the Appendix. The constraints coming from $l \to l'\gamma$ decays will increase with larger Yukawa couplings, the opposite dependence of the tree-level processes.

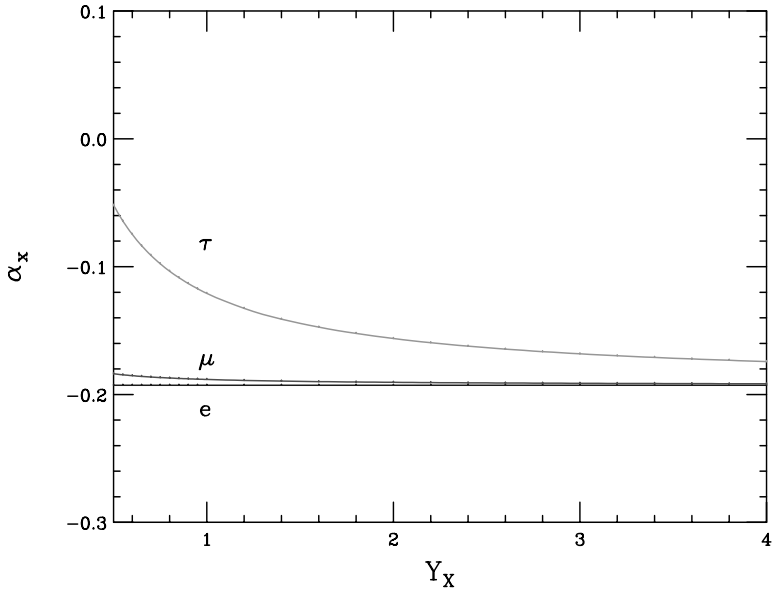

Figure 4.3: The ratios of the zero-mode fermion couplings to $Z^{(1)}$ over their SM values, for $x = e, \mu, \tau$, as functions of the Yukawa couplings Y_x.

To exhibit this behavior we present in Table 4.2 the bounds on the first KK mode mass for canonical mixing angles, $\nu = 0$, and for the two choices of Yukawa strength $Y_e = Y_\mu = Y_\tau = 1, 2$. We show the two most constraining processes, $\mu - e$ conversion and $BR(\mu \to e\gamma)$. The dependence on the Yukawa couplings agrees

with our simple estimate above. We will find in the next section that this leads to strong constraint throughout the entire model parameter space.

	$Y = 1$	$Y = 2$
B_{conv}	6.7 TeV	4.7 TeV
$BR(\mu \to e\gamma)$	8.0	15.8

Table 4.2: Constraints on the first KK mode mass, M_{KK}, coming from $\mu - e$ conversion and $BR(\mu \to e\gamma)$, for canonical mixing angles, $\nu = 0$, and for $Y = 1, 2$.

4.5 Monte-Carlo scan of the anarchic RS parameter space

In this section we present our Monte-Carlo scan of the RS parameter space, to determine in detail how well the RS geometric origin of flavor can be tested by current and future lepton flavor-violation experiments.

We first describe the ranges over which we scan the various RS parameters. The scenario introduced in the previous sections contains the following free parameters: Y_e, Y_μ, Y_τ, the overall Yukawa couplings for the electron, muon, and tau; $U_{ij}^{L,R}$, the elements of both the left and right-handed mixing matrices; the KK mass M_{KK}. We make the following assumptions in our scan.

- We restrict the Yukawa couplings to the range $Y_x \in [\frac{1}{2}, 4]$. As discussed before, the natural value is $Y_x \approx 2$. Values larger than 4 begin to invalidate the perturbative expansion, while values smaller than 1/2 introduce an unnatural hierarchy in the model. We explained in the previous section that flavor violation cannot be removed by making the Yukawa couplings either large or small, due to tension between tree-level and loop-induced processes.

- We implement the anarchy of 5-D couplings in our scan, which indicates that $U_{ii}^{L,R} \sim 1$, $U_{12}^{L,R} \sim \sqrt{m_e/m_\mu}$, $U_{13}^{L,R} \sim \sqrt{m_e/m_\tau}$, etc. We fix $U_{ii}^{L,R} = 1$, and

define the canonical values

$$U_{12}^c = \sqrt{\frac{m_e}{m_\mu}},\ U_{13}^c = \sqrt{\frac{m_e}{m_\tau}},\ U_{23}^c = \sqrt{\frac{m_\mu}{m_\tau}}. \tag{4.53}$$

We then vary $U_{12}^L = \beta_{12}^L U_{12}^c$, with $\beta_{12}^L \in [1/4, 4]$. We independently vary U_{12}^R, $U_{13}^{L,R}$, and $U_{23}^{L,R}$ in a similar fashion. Again, we restrict the values to these ranges to insure no unnatural hierarchies in model parameters. We generate phases for the six independent $U^{L,R}$ in the range $[0, 2\pi]$.

- We approximately implement unitarity of the mixing matrices by setting $U_{21}^{L,R} = -\left(U_{12}^{L,R}\right)^*$, etc. This assures that unitarity is maintained up to corrections of the level $\sqrt{m_e/m_\mu}$, $\sqrt{m_\mu/m_\tau}$, which is sufficient for the scan performed here.

We scan over the following fifteen independent parameters: the three Y_x, and the six complex mixing matrix elements $U_{12}^{L,R}$, $U_{13}^{L,R}$, and $U_{23}^{L,R}$. We generate 1000 sets of fifteen random numbers, and distribute them in the ranges indicated above for fixed M_{KK}. We perform two separate scans, one for a brane Higgs field and one for a bulk Higgs with $\nu = 0$. The ν dependence of the bulk Higgs field bounds is studied separately.

4.5.1 Scan for the brane Higgs field scenario

We first perform a Monte-Carlo scan of the parameter space of the brane Higgs scenario. As discussed in Section 4.4, dipole decays of the form $l \to l'\gamma$ are UV sensitive. We do not consider these decays in the brane Higgs case, which leaves us with $\mu - e$ conversion, $\mu \to 3e$, and $\tau \to l_1 \bar{l}_2 l_3$.

We first study the muonic processes $\mu \to 3e$ and $\mu - e$ conversion. We show in Fig. 4.4 scatter plots of the predictions for $BR(\mu \to 3e)$ and B_{conv} coming from our scan of the RS parameter space, for the KK scales $M_{KK} = 3, 5, 10$ TeV. The most sensitive probe is the SINDRUM II limit of $B_{conv} < 6.1 \times 10^{-13}$ [80]. This rules out a large fraction of the parameter space for $M_{KK} < 5$ TeV, and restricts the allowed parameters even at 10 TeV. The PDG limit of $BR(\mu \to 3e) < 10^{-12}$ is

less severe: although it rules out a large fraction of the $M_{KK} = 3$ TeV parameter space, most of the $M_{KK} = 5$ TeV space is still allowed. We note there is an almost perfect correlation between the RS predictions for the two processes. This is not surprising; it is clear from Eqs. 4.35 and 4.36 that they depend almost identically on the same mixing angles.

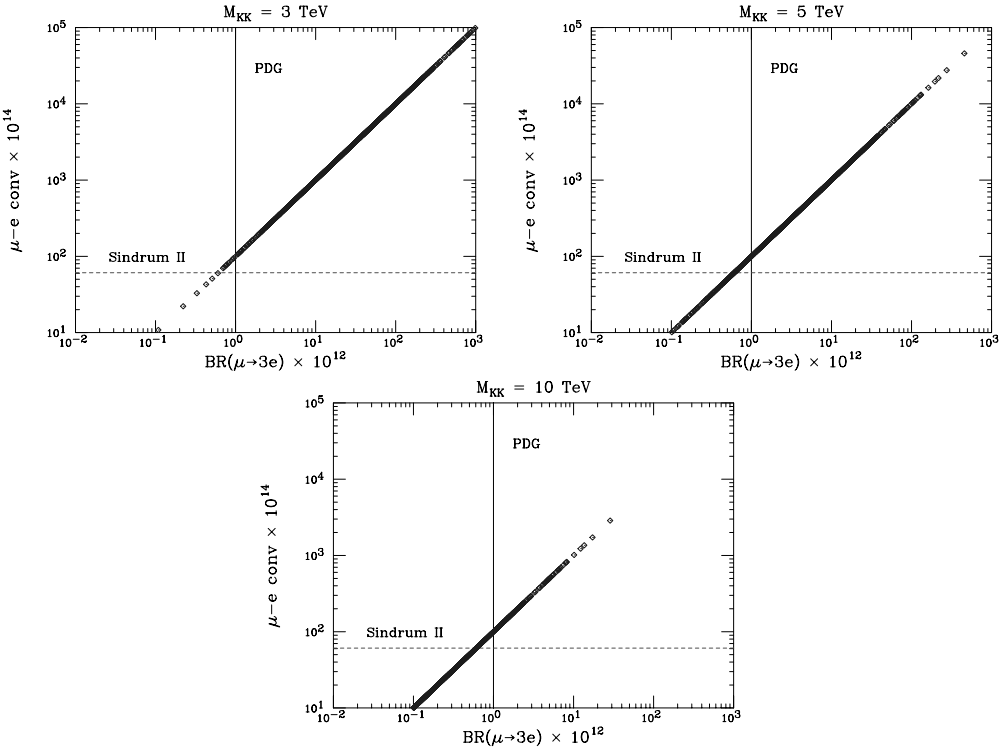

Figure 4.4: Scan of the $\mu \to 3e$ and $\mu - e$ conversion predictions for $M_{KK} = 3, 5, 10$ TeV. The solid and dashed lines are the PDG and SINDRUM II limits, respectively.

This result has implications for both the aesthetic appeal of the anarchic RS flavor picture, and the observation of this physics at the LHC. Although points with $M_{KK} \leq 3$ TeV are still allowed, it is clear from Fig. 4.4 that the model as formulated in our scan prefers KK masses of 5 TeV or larger. Increasing the KK scale to these higher values introduces a large fine-tuning in the electroweak symmetry breaking sector and is therefore not favored [71, 73]. With such large KK masses, many associated states will also be too heavy to observe at the LHC. The other method of avoiding these constraints, reducing the $U_{ij}^{L,R}$ matrix elements to the appropriate level, implies either some additional structure or fine-tuning in

the 5-D Yukawa matrix. We have studied the minimal model here, and it seems likely that more structure in the 5-D Yukawa matrix is needed for a completely natural description of the first and second generation flavor pattern in the brane Higgs case.

Another sector of the RS flavor picture to explore is that involving the third generation τ. This tests different model parameters than the muonic processes. We show in Fig. 4.5 a scatter plot of the RS predictions for $BR(\tau \to 3e)$ and $BR(\tau \to 3\mu)$ for $M_{KK} = 1$ TeV, together with the best limits coming from BABAR and BELLE. The lowest KK-scale allowed by electroweak precision tests in anarchic RS models is typically a few TeV. The B-factories are beginning to probe this region in the mode $\tau \to 3\mu$. There are plans to build a super-B factory with an integrated luminosity approaching 10 ab^{-1} [85]. The projected limits from this experiment are included in Fig. 4.5. Both the $\tau \to 3\mu$ and $\tau \to 3e$ modes at a super-B factory will constrain the anarchic RS parameter space. The LHC also has sensitivity to rare τ decays [86]; however, the projected sensitivities are slightly weaker than the current B-factory constraints, and have not been included. The expected sensitivities to rare τ decays at a future linear collider are also weaker than the limits set by the B-factories. Although the $M_{KK} \sim 1$ TeV scales probed with $\tau \to l_1 \bar{l}_2 l_3$ decays are lower than those constrained by $\mu - e$ conversion and $\mu \to 3e$, we stress that different model parameters are tested by each set of processes.

4.5.2 Scan for the bulk Higgs field scenario

We now present the results of our scan over the bulk Higgs parameter space. For the scan we set $\nu = 0$, which mimics the composite (or A_5) Higgs model of [73]; we present separately the ν dependence of the most important constraints.

We again begin by considering muon initiated processes. The constraints from $\mu \to 3e$ and $\mu - e$ conversion are highly correlated, as we saw in the previous subsection. Since the bounds from $\mu - e$ conversion are stronger, we focus on this and $\mu \to e\gamma$. We show in Fig. 4.6 scatter plots of the predictions for $BR(\mu \to e\gamma)$ and B_{conv} coming from our scan of the RS parameter space, for the KK scales

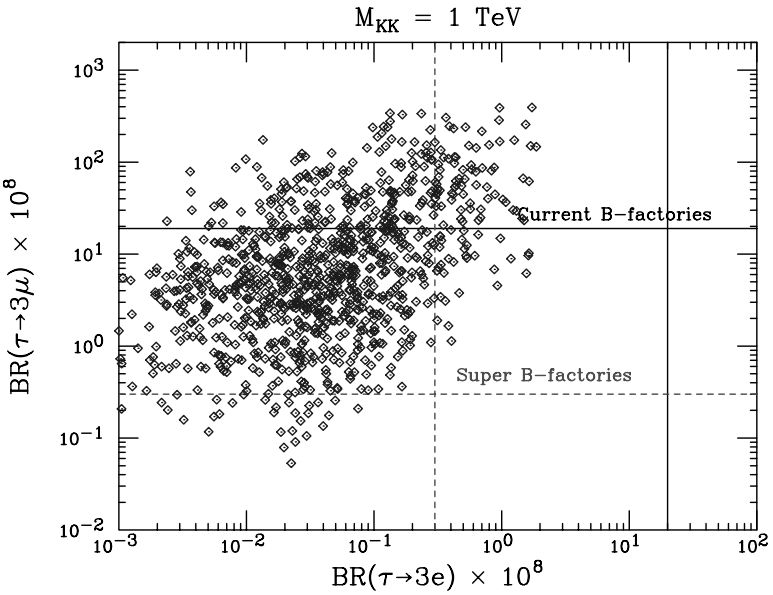

Figure 4.5: Scan of the $\tau \to 3e$ and $\tau \to 3\mu$ predictions for $M_{KK} = 1$ TeV. The solid and dashed lines are the current B-factory and projected super-B factory limits, respectively.

$M_{KK} = 3, 5, 10$ TeV. For $\mu \to e\gamma$ we include both the current constraint from the Particle Data Group [13] and the projected sensitivity of MEG [75]. The current bounds from $\mu \to e\gamma$ are quite strong; from the $M_{KK} = 3$ TeV plot in Fig. 4.6, we see that only one parameter choice satisfies the $BR(\mu \to e\gamma)$ bound. This point does not satisfy the $\mu - e$ conversion constraint. We can estimate that it would satisfy both bounds for $M_{KK} > 3.1$ TeV. In our scan over 1000 sets of model parameters the absolute lowest scale allowed is thus slightly larger than 3 TeV. Also, a large portion of the parameter set at both 5 and 10 TeV conflict with these bounds. We again find the need for a KK scale of $M_{KK} \geq 5$ TeV or additional structure in the mixing between the first and second generations to satisfy the experimental constraints for a significant fraction of model parameter space. In Fig. 4.7 we present the anarchic RS predictions for $\tau \to \mu\gamma$ and $\tau \to e\gamma$, together with current and future B-factory constraints, for $M_{KK} = 3$ TeV. The $\tau \to \mu\gamma$ mode is currently probing the few TeV range, while $\tau \to e\gamma$ will begin to test the anarchic RS scenario during the running of a super-B factory.

To study the sensitivity of the bulk Higgs field scenario to the location of the

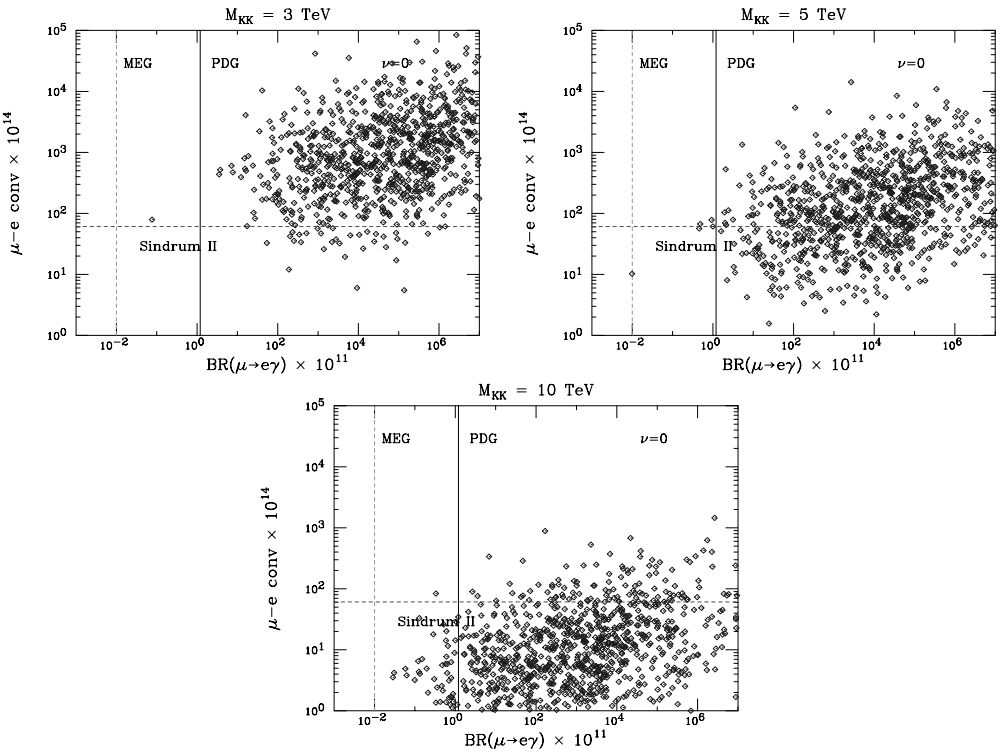

Figure 4.6: Scan of the $\mu \to e\gamma$ and $\mu - e$ conversion predictions for $M_{KK} = 3, 5, 10$ TeV and $\nu = 0$. The solid line denotes the PDG bound on $BR(\mu \to e\gamma)$, while the dashed lines indicate the SINDRUM II limit on $\mu - e$ conversion and the projected MEG sensitivity to $BR(\mu \to e\gamma)$.

Higgs boson in the fifth dimension, we show in Fig. 4.8 the dependence of the $\mu - e$ conversion rate and $BR(\mu \to e\gamma)$ on ν. We set the mixing angles to their canonical values, and show results for $Y_x = 1, 2$ and $M_{KK} = 5, 10$ TeV. The $\mu - e$ conversion results are weakest for $\nu = 0$, and quickly asymptote to the brane Higgs result as ν becomes large. The variation of $\mu \to e\gamma$ with ν is more intricate. The vanishing of the calculable component of this process as the Higgs boson is moved towards the TeV brane, discussed in Section 4.4, is clearly seen in Fig. 4.8. However, we expect cut-off effects to become more important for large ν. There is a strong dependence of the process on the position of the Higgs field for small ν, with the result varying by an order of magnitude for $0 \leq \nu \leq 5$. The $\nu = 0$ case is again the most favorable choice. Since UV sensitivity of the model is reduced for a bulk Higgs field, and since the experimental constraints are weakest for $\nu = 0$, we conclude that there

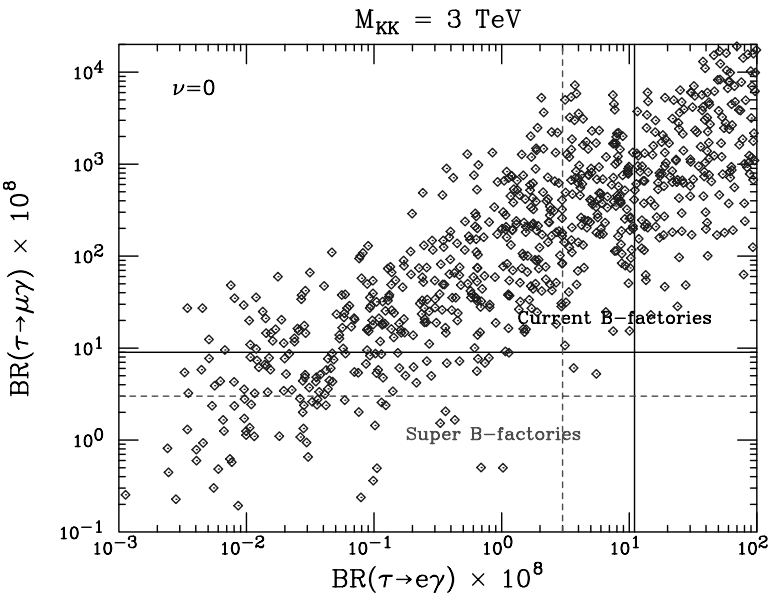

Figure 4.7: Scan of the $\tau \to \mu\gamma$ and $\tau \to e\gamma$ predictions for $M_{KK} = 3$ TeV and $\nu = 0$. The solid and dashed lines are the current B-factory and projected super-B factory limits, respectively.

is a preference for models of the type presented in [73].

4.5.3 Future sensitivities of MEG and PRIME

Finally, we emphasize here the importance of future searches for $\mu - e$ conversion by PRIME and $\mu \to e\gamma$ by MEG. Our analysis has shown that with some small tuning of parameters, particularly for those describing the mixing of the first and second generation, KK scales of 3 TeV are allowed by current measurements. Alternatively, KK scales of 5 TeV are permitted with completely natural parameters. Super-B factory searches for rare τ decays will not significantly constrain scales $M_{KK} \geq 5$ TeV. The LHC search reach for the new states predicted by the anarchic RS scenario is expected to be around 5-6 TeV. It is therefore difficult to definitively test the RS geometric origin of flavor using data from B-factories and the LHC.

Searches for $\mu - e$ conversion and $\mu \to e\gamma$ are already starting to require slight tunings of the model parameters. The limit on $BR(\mu \to e\gamma)$ is projected to improve from 1.2×10^{-11} to 10^{-13} after MEG, while the constraint on $\mu - e$ conversion

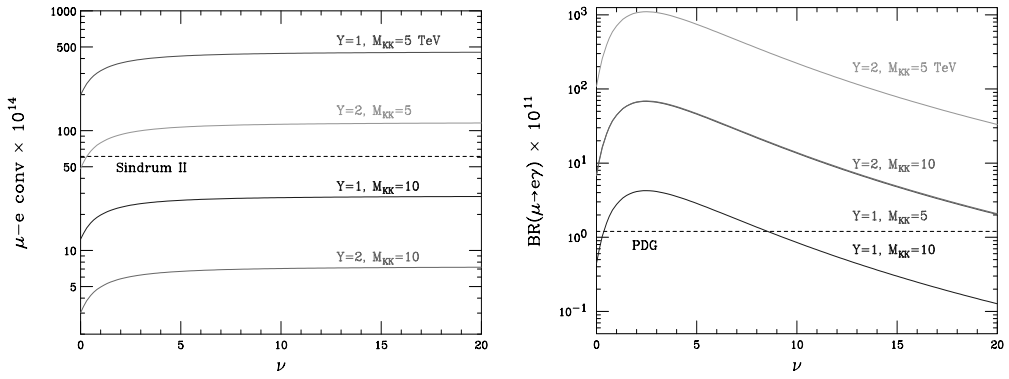

Figure 4.8: ν dependence of the RS predictions for $\mu - e$ conversion and $\mu \to e\gamma$ for canonical mixing angles and for several choices of Y_x and M_{KK}. In the right panel, the $Y = 1$, $M_{KK} = 5$ TeV and the $Y = 2$, $M_{KK} = 10$ TeV lines overlap.

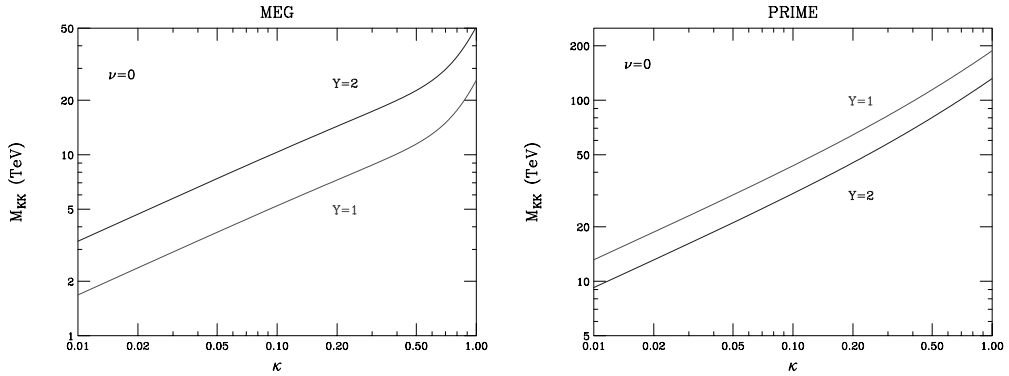

Figure 4.9: Projected bounds on M_{KK} coming from MEG (left) and PRIME (right) for $\nu = 0$. We have set the mixing angles to κ times their canonical values, and have varied κ in the range $[0.01, 1]$ for $Y_x = 1, 2$.

is projected to improve to 10^{-18} after PRIME. The bounds on M_{KK} that these constraints lead to are shown in Fig. 4.9. We have plotted the projected bounds as a function of the overall scale of the mixing angles; we have set $U_{12}^{L,R} = \kappa\sqrt{m_e/m_\mu}$, $U_{13}^{L,R} = \kappa\sqrt{m_e/m_\tau}$, etc., and have varied κ in the range [0.01,1]. This tests how far from the natural parameters these experiments will probe. We observe that MEG will probe $M_{KK} \leq 5$ TeV down to mixing angles 1/10 times their natural sizes. PRIME will test $M_{KK} \leq 20$ TeV down to mixing angles 1/10 times their natural sizes, and will probe $M_{KK} \leq 10$ TeV down to mixing angles 1/100 times their canonical values. Together, these experiments will definitively test the anarchic RS explanation of the flavor sector.

4.6 Summary and Conclusions

In this paper, we have studied lepton flavor violation with the SM propagating in a warped extra dimension. The principal motivation for this model is a solution to the Planck-electroweak hierarchy problem. Interestingly, there is also a solution to the flavor hierarchy of the SM. The large differences in the quark and lepton masses and mixing angles can be explained by differing profiles of SM fermions in the extra dimension, even though the $5D$ Yukawa coupling are of the same size without any structure. These profiles can vary substantially with small changes in the $5D$ fermion masses; no large hierarchies are required to account for the flavor hierarchy in the SM. Since the Higgs field is localized near the TeV brane, the small masses of the first and second generations are explained by their localization near the Planck brane.

The localization of fermion fields at different points in the extra dimension leads to flavor violation upon rotation to the fermion mass basis. The assumption of anarchic $5D$ Yukawa couplings implies that the mixing angles are related to the ratios of fermion masses. We can therefore estimate the leptonic mixing angles without a model of neutrino masses, unlike in the SM. The flavor violating couplings are proportional to the $4D$ Yukawa interactions. Therefore there is an analog of the GIM mechanism in the anarchic RS picture. However, the sensitivities of lepton flavor violating experiments are large, so we expect significant constraints. Bounds from electroweak precision measurements currently constrain the KK scale to be $M_{KK} \geq 3$ TeV, approximately.

To derive the implications of lepton flavor violating measurements for the anarchic RS scenario, we perform a Monte Carlo scan over the natural parameter space of this model: $O(1)$ Yukawa couplings and $O(1)$ variations of the mixing angles around their predicted size. We study both the case where the Higgs boson is localized in the TeV brane and when it is allowed to propagate in the full $5D$ spacetime. We study the processes $\mu \to 3e$, $\tau \to l_1 \bar{l}_2 l_3$, $\mu - e$ conversion, and dipole decays of the form $l \to l' \gamma$. In the brane Higgs case, cut-off effects render the dipole decays uncalculable in the $5D$ RS theory; this arises from the fact that

the $5D$ Yukawa couplings in this case have mass dimension $[-1]$, and cut-off scale effects are as large as those from KK modes. The bulk Higgs case does not suffer from this drawback.

We find strong constraints throughout the entire natural RS parameter space. The minimal allowed KK scale is 3 TeV, and this is permitted only for a very few points in our scan. In the bulk Higgs case, this occurs partially because of a tension between the tree-level mediated $\mu - e$ conversion process and the loop-induced decay $\mu \to e\gamma$. These processes have opposite dependences on the $5D$ Yukawa couplings, making it difficult to decouple the effects of flavor violation. There are a couple of possible ways to avoid these constraints. First, the KK scale can be raised slightly to 5 TeV, which allows large regions of the natural RS parameter space to be realized. However, this increases the fine-tuning in the electroweak sector, and will make it difficult to find the KK states present in this model at the LHC. Another possibility is to reduce the leptonic mixing angles slightly, implying some structure in the $5D$ Yukawa matrix and indicating that the observed flavor structure cannot be generated completely via geometry.

There are also several possible model-building possibilities to relax these constraints. Models with custodial isospin based on the gauge structure $SU(2)_L \times SU(2)_R \times U(1)_{B-L}$ contain an additional $Z^{'}$ and possibly additional fermions. The coupling of the $Z^{'}$ to the SM fermions is model-dependent [87], and can possibly be used to cancel some of the flavor-violating contributions we have studied. These models also contain an additional right-handed neutrino that contributes to loop-induced dipole decays. There is no zero-mode partner of this right-handed neutrino, and this contribution is therefore independent of the neutrino mixing parameters. Even an $O(1)$ suppression suffices to reduce the KK scale to the 3 TeV level, opening up more parameter space for study at the LHC.

The definitive test of whether the observed flavor structure can be explained by the anarchic RS scenario will come from future lepton flavor violating measurements. B-factories are currently probing mixing in the third generation using rare τ decays. These constraints will improve by an order of magnitude with data from a super-B factory, probing KK scales up to 5 TeV. These measurements probe dif-

ferent model parameters than $\mu - e$ conversion and rare μ decays, and are therefore complimentary to these other experiments. Improvements in the sensitivities of $\mu \to e\gamma$ and $\mu - e$ conversion of several orders of magnitude will be accomplished by the future experiments MEG and PRIME, respectively. They will definitively test the geometric origin of flavor structure; for example, PRIME will probe KK scales of $M_{KK} \geq 10$ TeV down to model parameters 1/100 of their natural size. These experiments will either confirm or completely invalidate this geometric origin of flavor.

In conclusion, the anarchic RS picture is an attractive solution to both the electroweak and flavor hierarchies in the SM. Measurements at the LHC, at future B-factories, and with the experiments MEG and PRIME will determine whether it is indeed realized in nature.

Appendix A

The Radion Modulus Field

The radion modulus field comes from the gravitational part of the action. To see how this comes about consider the usual Einstein-Hilbert action in five dimensions:

$$S_5 = \int d^5x\sqrt{-G}\left\{M_5^3\mathcal{R}_{(5)} + \mathcal{L}_{(5)M}\right\} \tag{A.1}$$

where M_5^3 is the five-dimensional Planck scale, G is the determinant of the five-dimensional metric, $\mathcal{R}_{(5)}$ is the five-dimensional Ricci scalar and $\mathcal{L}_{(5)M}$ contains any other fields. We can work in the gauge (coordinate system) where $G_{5\mu} \equiv 0$ so the differential line element is:

$$ds^2 = G_{MN}dx^M dx^N = g_{\mu\nu}(x,y)dx^\mu dx^\nu - r^2(x)dy^2 \tag{A.2}$$

Our convention is that the metric is mostly minus. $g_{\mu\nu}$ is the induced four-dimensional metric which is generally a function of the five-dimensional space-time, and $G_{55} \equiv -r^2$ is assumed to be independent of the extra dimension. Then $\sqrt{-G} = \sqrt{-g} \times r$ and upon carefully expanding the Ricci scalar, our action is:

$$S_5 = \int d^5x\sqrt{-g}\left\{rM_5^3(\tilde{\mathcal{R}}_{(4)} + \delta\mathcal{R}) + r\mathcal{L}_{(5)M}\right\} \tag{A.3}$$

where

$$\mathcal{R}_{(4)} \equiv \int dy\tilde{\mathcal{R}}_{(4)}$$

is the four-dimensional Ricci scalar and $\delta\mathcal{R}[g,r]$ are the terms in the five-dimensional Ricci scalar that depend on the fifth dimension explicitly.

In a flat extra dimension the four-dimensional background $g_{\mu\nu}$ is independent of y, so the y-dependence has been completely isolated and we can easily perform the integral over the fifth dimension[1]. However, the graviton kinetic term is no longer canonical. To fix this problem we can do a Weyl rescaling of the metric [55]:

$$\begin{aligned} g_{\mu\nu} &\longrightarrow \Omega^2 g_{\mu\nu} \\ g^{\mu\nu} &\longrightarrow \Omega^{-2} g^{\mu\nu} \end{aligned}$$

Under this transformation:

$$\sqrt{-g} \longrightarrow \Omega^4 \sqrt{-g} \tag{A.4}$$

$$\mathcal{R}_{(4)} \longrightarrow \Omega^{-2}\left\{\mathcal{R}_{(4)} + 6\left[(\partial(\log\Omega))^2 + \partial^2(\log\Omega)\right]\right\} \tag{A.5}$$

It is clear from these equations that in a flat extra dimension $S^1/\mathbb{Z}_2$ where $y \in [0,\pi]$:

$$\Omega^2 = \frac{M_4^2}{\pi r M_5^3} \tag{A.6}$$

will generate the canonical kinetic term for the four-dimensional graviton, where M_4 is the usual 4D Planck scale. In addition it will also generate a canonical kinetic term for the radion:

$$S_4 = \int d^4x\sqrt{-g}\left\{M_4^2\mathcal{R}_{(4)} + \frac{1}{2}(\partial\rho)^2 + \cdots\right\} \tag{A.7}$$

where I have defined the canonical radion field:

$$\rho \equiv \sqrt{12}M_4 \log\left(\frac{r}{r_0}\right) \tag{A.8}$$

[1]It is not this simple in general. For example, in the RS model there is also warp factor and more work needs to be done. However, it is not much harder to handle this case.

where r_0 is the classical radius, assumed to be stabilized. Notice that the canonical radion of flat space is the logarithm of R, as opposed to the exponential of R in the warped case [56].

By letting $r = r_0 + \delta r$ and expanding the logarithm the canonical radion field is related to the usual radion modulus by a constant:

$$\rho = \frac{\sqrt{12}M_4}{r_0}\delta r + \mathcal{O}\left((\delta r/r_0)^2\right) \tag{A.9}$$

So to compute the radion mass in Planck units ($M_4 \equiv 1$) we compute the radion potential at quadratic order: $V(r) = \frac{1}{2}\mu_r^2(\delta r)^2$. Then $M_{\text{radion}} = \mu_r r_0/\sqrt{12}$.

Using what we now know it is easy to see how the radion can be incorporated into the linearized supergravity action by extending into superspace. To see how this is done notice that the radion modulus appears in a $N = 1$ chiral superfield that contains the $\mathbb{Z}_2$-even fifth components of the fields that appear in the 5D supergravity multiplet. This field is called the "radion superfield":

$$T(x,\theta) = (r + iB_5) + \sqrt{2}\theta\Psi_R^5 + \theta^2 F_T \tag{A.10}$$

where B_5 is the fifth component of the graviphoton and Ψ_R^5 is the fifth component of the right-handed gravitino. This is derived in many places such as [57]. Now all we have to do is to include the radion superfield everywhere that it should appear so that we reproduce the correct action in terms of component fields. This was done in [45, 46] for a general class of theories [58]. It is important to notice that this matching must be done before the Weyl rescaling, as explained in [48].

Appendix B

KK Decomposition

In this appendix we will derive the KK decomposition for the model in Chapter 3. For simplicity the analysis will only be done for the Φ-sector. It is exactly the same for the Ψ-sector.

To perform the decomposition it is necessary to write out the Lagrangian for the scalar components by integrating out the auxiliary fields from Equation (3.2). This is given by[1]:

$$\begin{aligned}\mathcal{L} &= \phi^{c\dagger}\left[-\partial^2+\partial_5^2-m^2-\frac{2m}{R}\left(\delta(y)-\delta(y-\pi)\right)\right]\phi^c \\ &\quad +\phi^{\dagger}\left[-\partial^2+\partial_5^2-m^2+\frac{2m}{R}\left(\delta(y)-\delta(y-\pi)\right)\right]\phi \\ &\quad -\phi\left(-\partial_5+m\Theta(y)\right)S-\phi^{\dagger}\left(-\partial_5+m\Theta(y)\right)S \qquad \text{(B.1)}\end{aligned}$$

where $S = J\delta(y) - J'\delta(y-\pi)$. The extra delta functions in each bracket come from the fact that the mass term is an odd term. This yields the equations of motion:

$$\left[-\partial^2+\partial_5^2-m^2-\frac{2m}{R}\left(\delta(y)-\delta(y-\pi)\right)\right]\phi^c = 0 \qquad \text{(B.2)}$$

$$\left[-\partial^2+\partial_5^2-m^2+\frac{2m}{R}\left(\delta(y)-\delta(y-\pi)\right)\right]\phi = \left(-\partial_5+m\Theta(y)\right)S \qquad \text{(B.3)}$$

We wish to decompose the fifth dimension so we let:

[1]Recall: $\partial_5 \equiv \partial_y/R$

$$\phi(x,y) = -\frac{J}{2}\Theta(y)e^{-mR|y|} + \sum_\lambda \phi_\lambda(x)\xi_\lambda(y) \tag{B.4}$$

$$\phi^c(x,y) = -B(x)e^{+mR|y|} + \sum_\lambda \phi^c_\lambda(x)\xi^c_\lambda(y) \tag{B.5}$$

where the first term in ϕ is the particular solution to Equation (B.3); it plays the role of a y-dependent vev. This immediately takes care of the source terms for the ϕ field. Notice that this first term is not a zero mode; the coefficient is fixed by the inhomogeneous source terms on the right-hand side of Equation (B.3) which eliminate it as a degree of freedom. The even field however does contain a zero mode. We explicitly include a minus sign so that both ϕ and ϕ^c have the same sign in the physical region. This is done purely for convenience and does not change any results.

Now the equations of motion for the KK basis states are:

$$\left[\partial_5^2 - \frac{2m}{R}\left(\delta(y) - \delta(y-\pi)\right)\right]\xi^c_\lambda = -\lambda^2\xi^c_\lambda \tag{B.6}$$

$$\partial_5^2\xi_\lambda = -\lambda^2\xi_\lambda \tag{B.7}$$

where we have dropped the delta functions in the equation for ξ_λ since it is an odd field and therefore does not feel the delta functions on the boundary. Then $\phi_n(x), \phi^c_n(x)$ are the KK modes with masses $M^2_\lambda = m^2 + \lambda^2$.

The equation for $\xi(y)$ is a very easy equation to solve. Remembering that the odd fields must vanish at the boundaries:

$$\xi_\lambda(y) = \sqrt{\frac{2}{\pi}}\sin(ny) \qquad\qquad \lambda = \frac{n}{R} \tag{B.8}$$

The equation for ξ^c is not any more difficult. It is just the Schrodinger equation with delta function potentials and symmetric boundary conditions. We find that $\lambda^2 < 0$ cannot happen so there are no "bound states". The final solution is:

$$\xi^c_\lambda(y) = \sqrt{\frac{2}{\pi}}\sin\left[ny - \tan^{-1}\left(\frac{n}{mR}\right)\right] \qquad\qquad \lambda = \frac{n}{R} \tag{B.9}$$

These are the modes that appear in Equation (3.19-3.20). They have been normalized so that $\int_0^\pi dy\, \xi_\lambda \xi_{\lambda'} = \delta_{\lambda\lambda'}$. Also notice that the zero mode of ϕ^c is orthogonal to the higher modes, which is easily checked.

Appendix C

Supergravity Contributions

In this section, we present the masses and vevs of the hypermultiplets from Chapter 3 after the lowest-order supergravity effects are taken into account. We make the following definitions:

$$a = \frac{1}{2}m^3\pi^2 J'^2 \tag{C.1}$$

$$b = \tilde{\lambda}\pi\mu^2 K^2 (J'/J)^{2\mu/m}\left(\frac{2}{r_0}+\frac{1}{2}\mu\pi\tilde{\lambda}\right) \tag{C.2}$$

$$d = (m\mu)^{3/2} JK (J'/J)^{1+\mu/m}\left(\tilde{\lambda}+\frac{2\pi}{\mu r_0}\right) \tag{C.3}$$

$$f = \frac{6\pi}{r_0\sqrt{2}}m^{3/2}J' \tag{C.4}$$

$$g = \frac{6\pi}{r_0\sqrt{2}}\mu^{3/2}(J'/J)^{\mu/m}\tilde{\lambda}K \tag{C.5}$$

These parameters are defined up to terms with $R \neq r_0$. Then in terms of these parameters, the masses, vevs and mixing parameter in the paper are:

$$m^2_{\tilde{B}} = \frac{2R}{3M_5^3} X_{\tilde{B}} = \frac{r_0}{3M_5^3}\left((a+b) + \sqrt{(a-b)^2 - d^2}\right) \tag{C.6}$$

$$m^2_{\tilde{C}} = \frac{2R}{3M_5^3} X_{\tilde{C}} = \frac{r_0}{3M_5^3}\left((a+b) - \sqrt{(a-b)^2 - d^2}\right) \tag{C.7}$$

$$\langle \tilde{B} \rangle = \frac{\alpha}{\sqrt{1+\epsilon^2}} \cdot \frac{f + \epsilon g}{(a+b) + \sqrt{(a-b)^2 - d^2}} \tag{C.8}$$

$$\langle \tilde{C} \rangle = \frac{\alpha}{\sqrt{1+\epsilon^2}} \cdot \frac{g - \epsilon f}{(a+b) - \sqrt{(a-b)^2 - d^2}} \tag{C.9}$$

$$\epsilon = \frac{b-a}{d} + \sqrt{\left(\frac{b-a}{d}\right)^2 - 1} \tag{C.10}$$

where α is the superpotential parameter that cancels the cosmological constant as explained in the paper:

$$\alpha = \sqrt{\frac{1}{u_0} \cdot \frac{\mu K^2}{e^{2\mu\pi r_0} - 1}} \tag{C.11}$$

where $U_0 = u_0 \alpha^2$ is defined in the text below Equation (3.28)[1].

Notice that $m^2_{\tilde{B}}, m^2_{\tilde{C}} > 0$ for any value of the parameters, so the theory is stable.

[1] U_0 is quadratic in α, so u_0 is independent of α.

Appendix D

Explicit formlas for Overlap Integrals

In this Appendix, we present expressions for the various parameters that appear in the Yukawa matrix in Chapter 4. The case where the Higgs was confined to the TeV brane was considered in the text. Here, we will consider the case of a bulk Higgs.

Recall the most general expression for the mass matrix in the case of a bulk Higgs is given by

$$\mathcal{M} = \begin{pmatrix} M_D & \frac{v}{\sqrt{2}}\Delta_R & 0 \\ \frac{v}{\sqrt{2}}\Delta_L & \Delta_1 & M_{KK} \\ 0 & M_{KK} & \Delta_2 \end{pmatrix} \tag{D.1}$$

In this expression, M_D is the 3×3 diagonal matrix with the masses of the zero-mode leptons, and M_{KK} is the diagonal matrix with the KK masses to zeroth order in v (in our case, we are assuming that it is proportional to the identity matrix). The other entries can be expressed in terms of two matrices containing the overlap integrals:

$$F^{ij} = \frac{\int_{-\pi}^{\pi} d\phi \chi_H(\phi) f_L^0(\phi; c_i) f_L^1(\phi; c_j)}{\int_{-\pi}^{\pi} d\phi \chi_H(\phi) f_L^0(\phi; c_i) f_L^0(\phi; c_j)} \tag{D.2}$$

$$G_{L,R}^{ij} = \frac{\int_{-\pi}^{\pi} d\phi \chi_H(\phi) f_{L,R}^1(\phi; c_i) f_{L,R}^1(\phi; c_j)}{\int_{-\pi}^{\pi} d\phi \chi_H(\phi) f_L^0(\phi; c_i) f_L^0(\phi; c_j)} \tag{D.3}$$

where χ_H is given by Equation (4.16) and the $f^n(\phi; c_i)$ can be found in [64]. In terms of these matrices and the diagonal mass matrix M_D, we can express the other submatrices in Equation (D.1):

$$\frac{v}{\sqrt{2}}\Delta_R^{ij} = U_{Lik}(U_L^\dagger M_D U_R)^{kj} \times F^{kj} \tag{D.4}$$

$$\frac{v}{\sqrt{2}}\Delta_L^{ij} = (U_L^\dagger M_D U_R)^{ik} U_{Rkj}^\dagger \times F^{ki} \tag{D.5}$$

$$\Delta_1^{ij} = (U_L^\dagger M_D U_R)^{ij} \times G_L^{ij} \tag{D.6}$$

$$\Delta_2^{ij} = (U_L^\dagger M_D U_R)^{ij} \times G_R^{ij} \tag{D.7}$$

where there is no sum over the indices i, j. Notice that in the expression for $\Delta_{L,R}$, we cannot use $U_{ik}^\dagger U^{kj} = \delta_i^j$ because of the way the F matrix elements contribute.

To see how this reduces to the brane Higgs case, we replace the Higgs wavefunction with a delta function on the TeV brane. Immediately, this sets $G_R = 0$ due to the boundary conditions $f_R^1(\phi = \pi) = 0$; therefore $\Delta_2 = 0$ as it should. Also notice that $F^{ij} \equiv F^j$, since the i flavor cancels out of the ratio in Equation (D.2), and that $G_L^{ij} = F^i F^j$, again matching our results for the brane Higgs. Also notice that with the first index in F cancelling out, we can once again use the unitarity conditions on the $U_{L,R}$. These connections make it clear that the matrix multiplication presented in the text for the brane Higgs case match the results here.

Appendix E

Diagonalizing the Mass and Yukawa Matrices

The most general mass matrix for the lepton zero mode and first KK mode considered in Chapter 4 is given in Equation (D.1). The Yukawa matrix is the same as this matrix divided by $v/\sqrt{2}$ and $M_{KK} = 0$. We will diagonalize this matrix in stages. First we will diagonalize the lower 2×2 block containing the KK masses to leading order in v/M_{KK}; this compensates for mixing between the KK states. After that, we will diagonalize the entire 3×3 matrix to leading order in v/M_{KK}, which will compensate for mixing between the zero and KK modes. This later step is not necessary for a TeV brane Higgs, but turns out to be important for a bulk Higgs. In the mass insertion approximation, it corresponds to a mass insertion on the external fermion line; such contributions can be shown to be important.

As a warm-up, consider the simplified 2×2 matrix:

$$T = \begin{pmatrix} x & 1 \\ 1 & y \end{pmatrix} \tag{E.1}$$

where x, y are arbitrary, not equal to each other and smaller than unity. This matrix is diagonalized to leading order by the following unitary transformation, up to a phase:

$$\tilde{V} = \frac{1}{\sqrt{2}} \begin{pmatrix} 1+\frac{x-y}{4} & 1-\frac{x-y}{4} \\ 1-\frac{x-y}{4} & -(1+\frac{x-y}{4}) \end{pmatrix} \tag{E.2}$$

Then $\tilde{V}T\tilde{V}^\dagger$ is diagonal with eigenvalues $\pm(1 \pm \frac{1}{2}(x+y))$ to leading order in x and y. Note the difference in the sign of y in $\tilde{V}$ and the eigenvalue.

We now make this the lower 2×2 block of a diagonalization matrix V, identifying $X \equiv x - y = \frac{\Delta_1 - \Delta_2}{M_{KK}}$, and compute $V\mathcal{M}V^\dagger$:

$$\mathcal{M} = \begin{pmatrix} M_D & \frac{v}{\sqrt{2}}\Delta_R \frac{1}{\sqrt{2}}(1+\frac{X}{4}) & \frac{v}{\sqrt{2}}\Delta_R \frac{1}{\sqrt{2}}(1-\frac{X}{4}) \\ \frac{1}{\sqrt{2}}(1+\frac{X}{4})\frac{v}{\sqrt{2}}\Delta_L & M_{KK} + \frac{\Delta_1+\Delta_2}{2} & 0 \\ \frac{1}{\sqrt{2}}(1-\frac{X}{4})\frac{v}{\sqrt{2}}\Delta_L & 0 & -M_{KK} + \frac{\Delta_1+\Delta_2}{2} \end{pmatrix} \tag{E.3}$$

Now we may proceed to phase two: capturing the effects of zero-KK mode mixing. This is again accomplished with a unitary transformation:

$$Y = \begin{pmatrix} 1 & -\frac{v/\sqrt{2}}{M_{KK}}\Delta_R \frac{1}{\sqrt{2}}(1-\Gamma) & \frac{v/\sqrt{2}}{M_{KK}}\Delta_R \frac{1}{\sqrt{2}}(1+\Gamma) \\ \frac{1}{\sqrt{2}}(1-\Gamma)\frac{v/\sqrt{2}}{M_{KK}}\Delta_L & 1 & 0 \\ -\frac{1}{\sqrt{2}}(1+\Gamma)\frac{v/\sqrt{2}}{M_{KK}}\Delta_L & 0 & 1 \end{pmatrix} \tag{E.4}$$

where $\Gamma = \frac{\Delta_1 + 3\Delta_2 - 4M_0}{M_{KK}}$. The mass matrix loses its off-diagonal elements, which contribute to the eigenvalues at order in $(v/M_{KK})^2$, so we need not worry about them; although this will be important for the Yukawa matrix below.

The full diagonalization matrix is YV. It is a simple matter to apply this to determine the Yukawa couplings. It is also simple to multiply this with the appropriate phase matrix, which is $P = \mathrm{diag}(1, 1, -1)$.

At this point, we can immediately read off the masses of the KK fermions to leading order in v/M_{KK}:

$$M_{KK}^{(1)} = M_{KK} + \frac{\Delta_1 + \Delta_2}{2} \tag{E.5}$$

$$M_{KK}^{(2)} = M_{KK} - \frac{\Delta_1 + \Delta_2}{2} \tag{E.6}$$

These expressions for the KK masses are used when computing the amplitude for $\mu \to e\gamma$. The expression is valid for both the brane and bulk Higgs scenarios.

Let us get the Yukawa matrix in the diagonal basis. The Yukawa matrix Λ in the flavor basis is obtained by dividing by $\frac{v}{\sqrt{2}}$ and setting $M_{KK} = 0$ in Equation (D.1). Multiplying $YV\Lambda(YV)^\dagger P$, we obtain:

$$\Lambda = \begin{pmatrix} \lambda_{4D} & \frac{1}{\sqrt{2}}\Delta_R\left[1+\left(\frac{X}{4}-\frac{\Delta_2-M_0}{M_{KK}}\right)\right] & -\frac{1}{\sqrt{2}}\Delta_R\left[1-\left(\frac{X}{4}-\frac{\Delta_2-M_0}{M_{KK}}\right)\right] \\ \frac{1}{\sqrt{2}}\left[1+\left(\frac{X}{4}-\frac{\Delta_2-M_0}{M_{KK}}\right)\right]\Delta_L & \cdots & \cdots \\ \frac{1}{\sqrt{2}}\left[1-\left(\frac{X}{4}-\frac{\Delta_2-M_0}{M_{KK}}\right)\right]\Delta_L & \cdots & \cdots \end{pmatrix} \tag{E.7}$$

where we do not inlude the lower 2×2 block since we do not need it here. There are a couple of things to notice about this matrix. First of all, notice that $\Delta_2 \gg M_0$, so we can drop the dependence on the zero mode mass matrix in the off-diagonal terms. These correspond to subleading contributions of order M_0F^2. Secondly, if we had not included the zero-KK mixing (Y), we would have only gotten $(1\pm X/4)$ in these terms and would have therefore missed the important Δ_2 contribution. So it was important to take this mixing into account, as we expected from the mass-insertion calculation.

Bibliography

[1] A. E. Blechman, A. F. Falk, D. Pirjol, J. M. Yelton, *Phys. Rev.* **D71**, 085013 (2005).

[2] A. E. Blechman, *Phys. Rev.* **D67**, 074033 (2003).

[3] K. Agashe, A. E. Blechman, F. Petriello, submitted to *Phys. Rev.* **D**, arXiv:hep-ph/0606021.

[4] S. L. Glashow, *Nucl. Phys.* **22**, 579 (1961); S. Weinberg, Phys. Rev. Lett. **19** 1264 (1967); A. Salam, in *Proceedings of the Eighth Nodel Symposium*, N. Svartholm (Ed), Almqvist and Wiksell, Stockholm (1968).

[5] G. 'tHooft, unpublished; H. D. Politzer, *Phys. Rev. Lett.* **30**, 1346 (1973); D. J. Gross, F. Wilczek, *Phys. Rev. Lett.* **30**, 1343 (1973).

[6] P. Higgs, *Phys. Lett.* **12** 132 (1964), *Phys. Rev. Lett.* **13** 508 (1964); F. Englert, R. Brout, *Phys. Rev. Lett.* **13** 321 (1964); G. S. Guralnik, C. R. Hagen, T. W. B. Kibble, *Phys. Rev. Lett.* **13** 585 (1964).

[7] A. F. Falk and T. Mehen, *Phys. Rev.* **D53**, 231 (1996).

[8] S. P. Martin, *A Supersymmetry Primer*, arXiv:hep-ph/9709356.

[9] R. Barate, *et al.* [LEP Working Group for Higgs Boson Searches], *Phys. Lett.* **B565**, 61 (2003). [arXiv:hep-ex/0306033]

[10] I. Antoniadis, *Phys. Lett.* **B246**, 377 (1990); N. Arkani-Hamed, S. Dimopoulos, G. Dvali, *Phys. Lett.* **B429** 263 (1998). [arXiv:hep-ph/9803315]

[11] T. Kaluza, *Sitzungsber. Preuss. Akad. Wiss. Berlin (Math. Phys.)* 966 (1921); O. Klein, *Z. Phys.* **37** 895 (1926).

[12] L. Randall, R. Sundrum, *Phys. Rev. Lett.* 83, 3370 (1999) [hep-ph/9905221].

[13] S. Eidelman *et al.* [Particle Data Group], Phys. Lett. B **592**, 1 (2004). http://pdg.lbl.gov

[14] Z. Chacko, M. Luty, *JHEP* **0105**, 067 (2001). [hep-ph/0008103]

[15] D. E. Kaplan, G. D. Kribs, M. Schmaltz, *Phys. Rev.* **D62**, 035010 (2000). [hep-ph/9911293]; Z. Chacko, M. A. Luty, A. E. Nelson, E. Ponton, *JHEP* **0001**, 003 (2000). [hep-ph/911323]

[16] M. A. Luty, N. Okada, *JHEP* **0304**, 050 (2003). [hep-th/0209178]

[17] J. M. Yelton, UF-IHEPA-02-01, Talk given at Flavor Physics and CP Violation (FPCP), Philadelphia, 16-18 May 2002, hep-ex/0206068.

[18] N. Isgur and M. B. Wise, Phys. Rev. Lett. **66**, 1130 (1991).

[19] M. B. Wise, Phys. Rev. D **45**, 2188 (1992); G. Burdman and J. F. Donoghue, Phys. Lett. B **280**, 287 (1992); T. M. Yan, H. Y. Cheng, C. Y. Cheung, G. L. Lin, Y. C. Lin and H. L. Yu, Phys. Rev. D **46**, 1148 (1992) [Erratum-ibid. D **55**, 5851 (1997)].

[20] P. Cho, Phys. Lett. B **285**, 145 (1992).

[21] A. F. Falk, Nucl. Phys. B **378**, 79 (1992).

[22] H. Albrecht *et al.* [ARGUS Collaboration], Phys. Lett. B **317**, 227 (1993); Phys. Lett. B **402**, 207 (1997); P. L. Frabetti *et al.* [E687 Collaboration], Phys. Rev. Lett. **72**, 961 (1994); Phys. Lett. B **365**, 461 (1996); K. W. Edwards *et al.* [CLEO Collaboration], Phys. Rev. Lett. **74**, 3331 (1995).

[23] K. Hagiwara *et al.* [Particle Data Group Collaboration], Phys. Rev. D **66**, 010001 (2002).

[24] P. Cho, Phys. Rev. D **50**, 3295 (1994).

[25] L. A. Copley, N. Isgur and G. Karl, Phys. Rev. D **20**, 768 (1979) [Erratum-ibid. D **23**, 817 (1981)].

[26] S. Capstick and N. Isgur, Phys. Rev. D **34**, 2809 (1986).

[27] D. Pirjol and T. M. Yan, Phys. Rev. D **56**, 5483 (1997).

[28] G. Chiladze and A. F. Falk, Phys. Rev. D **56**, 6738 (1997).

[29] C. K. Chow, Phys. Rev. D **54**, 3374 (1996).

[30] J. P. Lee, C. Liu and H. S. Song, Phys. Rev. D **62**, 096001 (2000).

[31] C. K. Chow and T. D. Cohen, Phys. Rev. Lett. **84**, 5474 (2000); C. K. Chow and T. D. Cohen, Nucl. Phys. A **688**, 842 (2001); C. K. Chow, T. D. Cohen and B. Gelman, Nucl. Phys. A **692**, 521 (2001); Z. Aziza Baccouche, C. K. Chow, T. D. Cohen and B. A. Gelman, Nucl. Phys. A **696**, 638 (2001).

[32] S. E. Csorna *et al.* [CLEO Collaboration], Phys. Rev. Lett. **86**, 4243 (2001).

[33] J. P. Alexander *et al.* [CLEO Collaboration], Phys. Rev. Lett. **83**, 3390 (1999).

[34] F. Hussain, J. G. Körner and S. Tawfiq, Phys. Rev. D **61**, 114003 (2000); S. Tawfiq, J. G. Körner and P. J. O'Donnell, Phys. Rev. D **63**, 034005 (2001).

[35] M. Lu, M. B. Wise and N. Isgur, Phys. Rev. D **45**, 1553 (1992); A. F. Falk and M. E. Luke, Phys. Lett. B **292**, 119 (1992).

[36] J. M. Link *et al.* [FOCUS Collaboration], Phys. Lett. B **525**, 205 (2002).

[37] M. Artuso *et al.* [CLEO Collaboration], Phys. Rev. D **65**, 071101 (2002).

[38] Jiu Zheng, Studies of charmed baryons decaying to $\Lambda_c^+(n\pi)$, University of Florida PhD Dissertation, 1999.

[39] M. Artuso *et al.* [CLEO Collaboration], Phys. Rev. Lett. **86**, 4479 (2001).

[40] W. D. Goldberger, M. B. Wise, *Phys. Rev. Lett.* **83**, 4922 (1999). [hep-ph/9907447]

[41] N. Arkani-Hamed, L. Hall, D. Smith, N. Weiner, *Phys. Rev.* **D63**, 056003 (2001). [hep-ph/9911421]

[42] N. Arkani-Hamed, S. Dimopoulos, *Phys. Rev.* **D65**, 052003 (2002). [hep-ph/9811353]

[43] N. Maru, N. Okada, *Phys. Rev.* **D70**, 025002 (2004). [hep-th/0312148]

[44] L. Randall, R. Sundrum, *Nuc. Phys.* **B557**, 79 (1999). [hep-th/9810155]

[45] D. Marti, A. Pomarol, *Phys. Rev.* **D64**, 105025 (2001). [hep-th/0106256]

[46] N. Arkani-Hamed, T. Gregoire, J. Wacker, *JHEP* **0203**, 055 (2002). [hep-th/0101233]

[47] L. O'Raifeartaigh, *Nuc. Phys.* **B96**, 331 (1975).

[48] M. A. Luty, R. Sundrum, *Phys. Rev.* **D62**, 035008 (2000). [hep-th/9910202]

[49] R. N. Mohapatra, *Unification and Supersymmetry (2nd Ed)*, Springer-Verlag, New York (1992).

[50] M. Son, R. Sundrum, unpublished.

[51] J. Polonyi, Budapest Preprint No KFKI-1977-93 (1977); see [49] for details.

[52] The only problem with the Polonyi model is that it might conflict with cosmological constraints such as Big Bang Nucleosynthesis. For a nice description on how to fix such problems, see T. Moroi, *Prog. Theor. Phys. Suppl.* **123**, 457 (1996). [hep-ph/9510411]

[53] J. Bagger, T. Moroi, E. Poppitz, *JHEP* **0004**, 009 (2000). [hep-th/9911029]

[54] E. Cremmer, S. Ferrara, C. Kounnas, D.V. Nanopoulos, *Phys.Lett.* **B133**, 61 (1983); J. Bagger, E. Poppitz, L. Randall, *Nuc. Phys.* **B455**, 59 (1995). [hep-ph/9505244]

[55] R. M. Wald, *General Relativity*, University of Chicago Press, Chicago (1984).

[56] W. D. Goldberger, M. B. Wise, *Phys. Lett.* **B475**, 275 (2000). [hep-ph/9911457]

[57] W. D. Linch III, M. A. Luty, J. Phillips, *Phys. Rev.* **D68**, 025008 (2003). [hep-th/0209060]

[58] This actually only works if you ignore the gravitational dynamics. For instance, the action in Eq (3.2) includes the term $\phi\partial_\mu\phi\partial^\mu B_5$ + h.c., which is not 5D Lorentz invariant or gauge invariant. In this paper, however, we are only dealing with constant fields and therefore this error is not a problem. I thank M. Son and M. Luty for bringing this to my attention.

[59] W. D. Goldberger and M. B. Wise, Phys. Rev. Lett. **83**, 4922 (1999) [arXiv:hep-ph/9907447].

[60] H. Davoudiasl, J. L. Hewett and T. G. Rizzo, Phys. Lett. B **473**, 43 (2000) [arXiv:hep-ph/9911262]. A. Pomarol, Phys. Lett. B **486**, 153 (2000) [arXiv:hep-ph/9911294].

[61] Y. Grossman, M. Neubert, *Phys. Lett.* **B474**, 361 (2000). [hep-ph/9912408]

[62] T. Gherghetta, A. Pomarol, *Nuc. Phys.* **B586**, 141 (2000). [hep-ph/0003129]

[63] S. J. Huber and Q. Shafi, Phys. Lett. B **498**, 256 (2001) [arXiv:hep-ph/0010195];

[64] H. Davoudiasl, J. L. Hewett and T. G. Rizzo, Phys. Rev. D **63**, 075004 (2001) [arXiv:hep-ph/0006041].

[65] S. J. Huber, Nucl. Phys. B **666**, 269 (2003) [arXiv:hep-ph/0303183].

[66] G. Burdman, Phys. Lett. B **590**, 86 (2004) [arXiv:hep-ph/0310144].

[67] S. Khalil and R. Mohapatra, Nucl. Phys. B **695**, 313 (2004) [arXiv:hep-ph/0402225].

[68] K. Agashe, G. Perez and A. Soni, Phys. Rev. Lett. **93**, 201804 (2004) [arXiv:hep-ph/0406101]; Phys. Rev. D **71**, 016002 (2005) [arXiv:hep-ph/0408134].

[69] G. Moreau and J. I. Silva-Marcos, JHEP **0603**, 090 (2006) [arXiv:hep-ph/0602155].

[70] S. J. Huber and Q. Shafi, Phys. Rev. D **63**, 045010 (2001) [arXiv:hep-ph/0005286]; S. J. Huber, C. A. Lee and Q. Shafi, Phys. Lett. B **531**, 112 (2002) [arXiv:hep-ph/0111465]; C.Csaki, J. Erlich, J. Terning, *Phys. Rev.* **D66**, 064021 (2002) [hep-ph/0203034]; J. Hewett, F. Petriello, T. Rizzo, *JHEP* **0209**, 030 (2002) [hep-ph/0203091].

[71] K. Agashe, A. Delgado, M. May, R. Sundrum, *JHEP* **0308** 050 (2003). [hep-ph/0308036]

[72] H. Davoudiasl, J. L. Hewett and T. G. Rizzo, Phys. Rev. D **68**, 045002 (2003) [arXiv:hep-ph/0212279]; M. Carena, E. Ponton, T. M. P. Tait and C. E. M. Wagner, Phys. Rev. D **67**, 096006 (2003) [arXiv:hep-ph/0212307]; M. Carena, A. Delgado, E. Ponton, T. M. P. Tait and C. E. M. Wagner, Phys. Rev. D **71**, 015010 (2005) [arXiv:hep-ph/0410344].

[73] K. Agashe, R. Contino and A. Pomarol, Nucl. Phys. B **719**, 165 (2005) [arXiv:hep-ph/0412089].

[74] H. Davoudiasl, B. Lillie and T. G. Rizzo, arXiv:hep-ph/0508279.

[75] G. Signorelli, J. Phys. G **29**, 2027 (2003).

[76] A. Sato, talk given at 7th International Workshop on Neutrino Factories and Superbeams (NuFact 05), Frascati, Italy, 21-26 Jun 2005.

[77] R. Kitano, Phys. Lett. B **481**, 39 (2000) [arXiv:hep-ph/0002279].

[78] W. F. Chang and J. N. Ng, Phys. Rev. D **71**, 053003 (2005) [arXiv:hep-ph/0501161].

[79] Y. Kuno and Y. Okada, Rev. Mod. Phys. **73**, 151 (2001) [arXiv:hep-ph/9909265].

[80] P. Wintz, *Prepared for 29th International Conference on High-Energy Physics (ICHEP 98), Vancouver, Canada, 23-29 Jul 1998*

[81] Y. Yusa *et al.* [Belle Collaboration], Phys. Lett. B **589**, 103 (2004) [arXiv:hep-ex/0403039]; M. Hodgkinson [BaBar Collaboration], Nucl. Phys. Proc. Suppl. **144**, 167 (2005).

[82] H. Davoudiasl, J. L. Hewett and T. G. Rizzo, Phys. Lett. B **493**, 135 (2000) [arXiv:hep-ph/0006097].

[83] K. Abe *et al.* [Belle Collaboration], Phys. Rev. Lett. **92**, 171802 (2004) [arXiv:hep-ex/0310029]; J. M. Roney [BaBar Collaboration], Nucl. Phys. Proc. Suppl. **144**, 155 (2005) [arXiv:hep-ex/0412002].

[84] K. Hayasaka *et al.*, Phys. Lett. B **613**, 20 (2005) [arXiv:hep-ex/0501068]; B. Aubert *et al.* [BABAR Collaboration], Phys. Rev. Lett. **96**, 041801 (2006) [arXiv:hep-ex/0508012].

[85] J. Hewett (ed.), *et al.*, arXiv:hep-ph/0503261.

[86] N. G. Unel, arXiv:hep-ex/0505030.

[87] K. Agashe, R. Contino, L. Da Rold and A. Pomarol, arXiv:hep-ph/0605341.

Vita

Andrew Blechman was born on August 18, 1979. His degrees include a Bachelor of Science degree in Physics and a Bachelor of Arts degree in Mathematics, Magna cum Laude, from The University of Rochester in 2001, and a Master of Arts degree in Physics from The Johns Hopkins University in 2003. He is a member of The Phi Beta Kappa, Sigma Pi Sigma and Golden Key National Honors Societies. He will be taking up a position as a research associate at the University of Toronto beginning in the fall of 2006.